EXPERIMENTAL AND COMPUTATIONAL INVESTIGATIONS OF THE EFFECTS OF GEM-DIFLUORO-SUBSTITUENTS ON CYCLOPROPANE

By

FENG TIAN

A DISSERTATION PRESENTED TO THE GRADUATE SCHOOL
OF THE UNIVERSITY OF FLORIDA IN PARTIAL FULFILLMENT
OF THE REQUIREMENTS FOR THE DEGREE OF
DOCTOR OF PHILOSOPHY

UNIVERSITY OF FLORIDA

1999

TO

MOM, DAD, HONG-LIN, YU-HENG

HONG TIAN, KAI TIAN AND YANG TIAN

ACKNOWLEDGMENTS

I would like to thank my research advisor, Dr. William R. Dolbier, Jr, for all his guidance and encouragement. Based on his profound understanding of science, he has shown me a world of chemistry. His unique educational style has helped me unleash my imagination, and eventually find a new way of self-expression, that is, exploring the unknown in chemistry.

I thank Dr. Merle A. Battiste, a true scientist, for all his inspiring discussions, which were essential for the success of the cation project. I thank Dr. Kirk S. Schanze, for all his understanding, encouragement and helpful discussion.

It has been an unforgettable experience to work in Dolbier's group. I would like to thank all my colleagues and friends: Dr. Michael D. Bartberger for introducing me to computation chemistry, which has become an important tool in my research; John M. Baker, a great friend, for his help in English in writting this dissertation; Dr. Alex Roche and Dr. Maurice Médebielle for their stimulating discussion; Dr. Conrad Burkhoder, Dr. Michelle Fletcher, Yuelian Xu, LianHao Zhang, Li Zhang, Dr. Alexander B. Shtarev, Dr. Virgini Kruger, Dr. Rogelio Ocampo, Dr. Luz Amalia, Dr. Lian Luo, more recently Raphaele Fayolle, and Olivia Bautista for all their help and friendship. I also thank Dr. YiBing Shen and Kevin Ley from the neighboring lab for all their help and friendship.

My thank also goes to Dr. Jodie V. Johnson for his help in HPLC experiment.

I would like to give my special thanks to Dr. Zhaozhong Jia, a friend forever, for helping me to apply to UF, and his friendship that has lasted over the 18 years. Also, I thank Dr. XiaoXing Rong, for his help in the lab.

The love from my family is always essential. I thank my parents for all the love they have given me, for the man I was and the man I will be. Finally and most importantly, I would to thank my wife, HongLin, for her support, the love and all the years we have been together.

TABLE OF CONTENTS

ACKNOWLEDGMENTS....iii

ABSTRACT....vii

CHAPTER

1. GENERAL ASPECTS OF THE CYCLOPROPYL GROUP

Introduction....1
Structure and Strain Energy....2
Electronic Structure....4
Fluorine Substitution Effects on Cyclopropane....7
Conclusion....16

2. A NOVEL FACILE AND HIGHLY EFFICIENT SYNTHESIS OF GEM-DIFLUOROCYCLOPROPANES

Introduction....18
Results and Discussions....21
Conclusion....31

3. STEREOMUTATION OF 1-ETHYL-2, 2-DIFLUORO-3-METHYLCYCLOPROPANE

Introduction....32
Precursor Syntheses....38
Kinetic Studies of Stereomutation....43
Discussion....49
Conclusion....55

4. COMPUTATIONAL STUDIES OF FLUORINE SUBSTITUTION EFFECTS ON THE KINETICS OF CYCLOPROPYLCARBINYL AND OXRINYLCARBINYL RADICAL RING OPENING

Part1 Simple Cyclopropylcarbinyl Radical Ring Opening....57
Part 2 Fused Cyclopropylcarbinyl Radical Ring Opening....80
Part 3 Oxiranylcarbinyl Radical Ring Opening....84

5. KINETIC STUDIES OF 2,2-DIFLUOROCYCLOPROPYLCARBINYL RADICAL RING OPENING

Introduction..94
First Attempt to Measure the Radical Ring Opening Rate 96
Second and Successful Attempt at Measuring the Rate of Radical Ring Opening...99
Conclusion..108

6. REACTIVITY AND REGIOCHEMICAL BEHAIOR OF THE 2, 2-DIFLUOROCYCLOPROPYL CARBINYL CATION

Introduction.. 109
Computational Studies..114
Experimental Studies..118
Results and Discussion..120
Conclusion..126

7. EXPERIMENTAL

General Methods...127
Experimental of Chapter 2...129
Experimental of Chapter 3...133
Computational Data of Chapter 4...153
Experimental of Chapter 5...163
Experimental of Chapter 6...175

APPENDIX SELECTED ^{19}F NMR ^{1}H NMR AND GC SPECTRA.............................190

REFERENCES..205

BIOGRAPHICAL SKETCH...216

Abstract of Dissertation Presented to the Graduate School
of the University of Florida in Partial Fulfillment of the
Requirements for the Degree of Doctor of Philosophy

EXPERIMENTAL AND COMPUTATIONAL INVESTIGATIONS OF THE EFFECTS OF GEM-DIFLUORO-SUBSTITUENTS ON THE CYCLOPROPANE

By

Feng Tian

December 1999

Chairman: William R. Dolbier, Jr.
Major Department: Chemistry

Various aspects of chemistry involving gem-difluorocyclopropanes have been investigated in this dissertation, which include the synthesis, the thermal stereomutation of gem-difluorocyclopropanes, and also the gem-difluorocyclopropylcarbinyl radical as well as its cation rearrangements. Computational methods have been utilized as a powerful tool to predict, and as well as to explain the experimental results obtained in those investigations.

In the study of gem-difluorocyclopropane synthesis, a novel and highly effective difluorocyclopropanation methodology had been developed. Using this method, alkenes, even the highly electron deficient ones, such as butyl acrylate, were cyclopropanated in excellent, and sometimes, virtually *quantitative* yields under mild conditions.

In the second area, a kinetic study of the thermal stereomutations of optically active 1-ethyl-2, 2-difluoro-3-methylcyclopropanes, revealed that, the racemization of the cis compound was 102 times faster than its epimerization, whereas, for the trans

compound the difference was only 6.6 times. These results elucidated a disrotatory ring opening and closure preference in gem-difluorocylopropane stereomutation, which confirmed Borden's theoretical predication.

In the third area of study, density functional calculations were utilized to investigate the fluorine substitution effects on the cyclopropylcarbinyl as well as the oxiranyl carbinyl radical rearrangements. Stereoelectronic effects, instead of thermochemical effects, were found to contribute mostly to the kinetics of these processes. The standard activation enthalpy of gem-difluorocylopropylcarbinyl radical ring opening was calculated to be only 1.6 kcal/mol with the exclusive distal C-C bond to the CF_2 cleavage. Using conventional transition state theory, the rate constant was calculated to be $1.5 \times 10^{11} s^{-1}$ at room temperature. Several radical processes that have no barrier were found computationally.

The subsequent experimental study provided a rate constant of $1.0 \times 10^{11} s^{-1}$ at 99.3°C, utilizing the competition technique, in which TEMPO was used as competitive radical trapping reagent.

In the fourth area, gem-difluorocyclopropylcarbinyl cation was found not to be a stable intermediate computationally. It rearranges with the proximal C-C bond cleavage to give a α fluorinated cation, a regiochemistry that is different from that of gem-difluorocyclopropyl carbinyl radical rearrangement. The solvolysis study of its tosylate confirmed the prediction, and revealed a rate, which is similar to that of primary alkyl group.

These properties qualify gem-difluorocyclopropylcarbinyl group as an ideal mechanistic probe that can distinguish between radical and cation intermediates.

CHAPTER 1
GENERAL ASPECTS OF CYCLOPROPANE

Introduction

Cyclopropane was first synthesized by Freund[1] in 1881 by treatment of 1,3 dibromopropane with sodium, a process, which had earlier been unsuccessfully attempted by Reboul. [2] However, it was Perkin's work,[3] two years later, on what is now known as the 'classical' malonic ester synthesis (Figure 1.1), that attracted considerable attention and was to be considered the foundation of modern alicyclic chemistry.

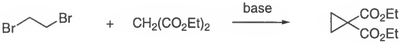

Figure 1.1 Perkin's cyclopropane synthesis

Since then, as the smallest cycloalkane, cyclopropane has attracted tremendous interest from both experimental and theoretical chemists and it is probably one of the most-investigated structural groups. Cyclopropane synthesis methodologies, span from the Freund's early discovery to the latest chiral syntheses, and the theoretical methodologies that had been utilized range from Extended Hückel to the more recent *ab initio* method. Those studies had been well reviewed.[4-7] The purpose of this chapter is not to provide a complete review of all aspects of cyclopropane chemistry or to create theoretical disputes, but to, introduce and clarify various concepts such as ring strain, bond strength, refined Walsh orbitals and fluorine substitution effect of cyclopropane, using literature work as well as our own speculations and results to assist our understanding and to help rationalize the results presented in this dissertation. More specific introductions to the subjects of cyclopropane stereomutation, cyclopropylcarbinyl radical ring opening, cyclopropylcarbinyl cation rearrangement and synthesis of *gem*-difluorocyclopropanes will be presented in the following individual chapters.

Structure and Ring Strain Energy

Since the first gas phase electron diffraction study of cyclopropane was published in 1946,[8,9] its three member ring structure with D_{3h} symmetry (Figure 1.2) has been redetermined by the methods of gas phase microwave spectroscopy and crystal X-ray diffraction. The agreement among different experimental methods is quite good.[10] Listed in Table 1 are the results of a recent gas phase electron diffraction study[11] and theoretical studies, utilizing different level of theories with medium basis sets which have been used to generate the equilibrium structure. The calculated structure at MP2/6-31G(d) level of theory is consistent with experimental data within experimental errors. HF/6-31G(d) gives a slightly shorter C-H bond and B3LYP/6-31G(d) yields a slightly longer C-C bond.

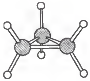

Figure 1.2 Structure of cyclopropane

Table 1.1 Structure parameters of cyclopropane

	C-C (Å)	C-H (Å)	H-C-H (deg)	Reference
Experimental (r_e)[a]	1.501(5)	1.083(5)	114.5(9)	11
HF/6-31G(d)	1.497	1.076	114.0	12
MP2/6-31G(d)	1.502	1.084	114.2	13
B3LYP/6-31G(d)	1.508	1.087	113.9	This study

a. The hypothetically motionless molecule.

Interestingly, the C-C bond is shorter in cyclopropane than in the other cycloalkanes, with the bond length having a maximum value in cyclobutane (Table 1.2). The C-C bond is shorter if one of the methylene groups in cyclopropane is replaced by an NH group (1.481 Å)[14] or by O (1.466Å)[15]. The C-H bonds are shorter in cyclopropane, in line with its higher s character, than in cyclobutane or in the CH_2 group of propane, and they are comparable to the $C(sp^2)$-H bond lengths in benzene and ethene (Table 1.3).

Table 1.2 C-C bond lengths in different cycloalkanes

	c-C_3H_6	c-C_4H_8	c-C_5H_{10}	c-C_6H_{12}
C-C (Å) r_g	1.5139(12)	1.554(1)	1.546(1)	1.535(2)
Reference	11	16	17	18

Table 1.3 C-H bond lengths

	c-C_3H_6	c-C_4H_8	C_3H_8	C_6H_6	C_2H_4
C-H (Å) r_z	1.084(2)	1.093(3)	1.096(2)	1.083(6)	1.0868(13)
Reference	11	16	19	20	21

The concept of ring strain was first introduced by Baeyer in 1885.[22] In the two page addendum to his polyacetylene publication, Baeyer, with the aid of planar models, proposed that the three and four member carbocycles would be less stable than their five and six membered homologues because of the necessary deviation in bond angles from the normal tetrahedral value of 109°28'. With the finding that non-planar models of cyclohexane can be formed without distorting the tetrahedral bond angle,[23] Baeyer's original idea was questioned and modified.[24] In organic chemistry, strain effects are now generally discussed in terms of bond angle and bond length distortions, as well as torsional effects and non-bonded interactions.[7]

The strain energy of a molecule is the addition of inbuilt energy of a system when compared with a suitable strain free model system. In general, cyclohexane is to be strain free. The molecule has a heat of formation (ΔH_f) of –29.5 kcal/mol,[25] which equates to –4.92 kcal/mol per methylene unit. The fact that a methylene unit in a straight chain alkane has a value of –4.926 kcal/mol[26] indicates that the presence of gauche interactions in cyclohexane is of minimal thermodynamic consequence. For cyclopropane, with three methylene units, the 'strain-free' energy is therefore 3 x (-4.92)= -14.76 kcal/mol and this compares with a heat of formation of +12.73.[27] The difference, 27.5 kcal/mol is considered to be the strain energy of the molecule. In a similar vein, the strain energies of the homologous cycloalkanes are 26.5, 6.2, 0.0 and 6.3 kcal/mol for cyclobutane to cycloheptane, respectively.

For compounds, whose heats of formation have not been determined, computational values can now provide a satisfactory alternative. Our own calculation performed at the B3LYP/6-31G(d) level of theory using geometry optimized at the HF/6-31G(d) level of theory with ZPE (Zero Point Energy) correction led to a calculated ring strain of 28.2 kcal/mol for cyclopropane.

Electronic Structure

Walsh proposed an orbital model for the bonding in a three-membered ring. [28] He chose sp^2 hybridization for the carbon, with one hybrid being used for each C-H bond and the third pointing directly into the center of the ring. The unhybridized p orbital lies in the plane of the ring. The three sp^2 hybrids pointing toward the ring center overlap and form three σ-molecular orbitals, one bonding and two antibonding. The three p orbitals interact through overlap that is intermediating between the end-on type characteristic of σ bonds and the side-on type characteristic of π bonds to form the three delocalized orbitals, two bonding and one antibonding.

Walsh orbitals have attracted tremendous interest, in particular among organic chemists, since they seem to be close to the canonical SCF MOs of cyclopropane and seem to explain: (a) the π character of its C-C bonds; (b) substituent effects on ring geometry and stability; (c) the ability of the cyclopropyl group to conjugate with other groups; (d) the relationship between cyclopropane complexes and π-complexes; and (e) delocalization of electrons in the plane of the ring. However, Walsh orbitals suffer from a number of deficiencies,[29] such that if one wants to use Walsh orbitals to properly discuss the properties of the cyclopropyl group, one needs to refine them.

The refined Walsh orbitals have been obtained by assuming a set of sp hybrid orbitals complemented by two p orbitals for each C atom. These orbitals are classified as radially oriented (with regard to the center of the ring) sp_{in} and sp_{out} orbitals and tangentially oriented (with regard to the perimeter of the ring) p_{ip}(in-plane)and p_{op}(out-plane) orbitals. The six Walsh orbitals are formed from the (radial) $sp_{in}$and (tangential) p_{ip} starting orbitals. The refined Walsh result from mixing between the original Walsh orbitals. The HOMOs (w_A and w_S), which can be classified as a 'π-bridged-π orbital' (π-orbital bridge at C1) and a 'σ- bridged-π-orbital' (σ-orbital bridged at C1),[30,31] are depicted in Figure 1.3.

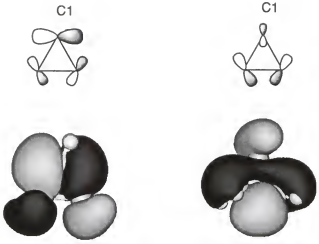

w_A ‘π-bridged-π orbital’ w_S ‘σ- bridged-π-orbital’

Figure 1.3 Two degenerated HOMO of refined Walsh Orbital and the calculated orbitals of cyclopropane at HF/6-31G(d) level.

A bent bond model of cyclopropane was first proposed by Förster[32] and was later refined by Coulson and Moffitt.[33] They determined sp^n (CC) and sp^m (CH) hybrid orbitals with optimal hybridization ratios n and m to describe bonding in cyclopropane. Caclulations showed that, for cyclopropane, the p-character of the CC hybrid orbitals had to be increased from sp^3 to sp^4 while the s-character of the CH hybrid orbitals increase from sp^3 to sp^2. The Förster-Coulson-Moffitt orbitals reveal that the CC hybrid orbitals are considerably bent in an attempt to avoid the geometrical angle (60°) and to come close to the strain-free tetrahedral angle. Bending of the hybrid orbitals can only be achieved by an increase in their p character. The corresponding orbital energies are increased, and the CC bond is weakened. Hence, the Förster-Coulson-Moffitt orbitals suggest weakening of the CC bonds and a strained three-membered ring as a result of this bond weakening.

Fluorine Substituent Effects on Cyclopropane

Fluorine substituent effects have aroused particular interest, because of fluorine's small size,[34] and hence its minimal steric impact when incorporated into organic molecules, and because of its unique intrinsic nature.[35,36] The van der Waals radius of fluorine, 1.47 Å (compare to chlorine, 1.73 Å; bromine 1.84 Å; carbon, 1.70 Å; oxygen 1.52 Å and hydrogen 1.20 Å) allow it to form a short C-F σ bond (1.39 Å relative to a C-Cl bond 1.781 Å in CH_3X).[37] The unusual properties of fluorine as a substituent derive largely from its high electronegativity and its three non-bonding electron pairs. The high electronegativity and effective orbital overlap combine to give rise to a very polar and strong C-F bond. The bond dissociation energy of C-F in CH_3F is 108.3 kcal/mol (compared to BDE of C-Cl 82.9 kcal/mol). Fluorine's non-bonding electron pairs can interact with a conjugated π system through conjugative interaction to either destabilize a filled πsystem (π bond) or stabilize a vacant π system (carbocation) (Figure 1.4).

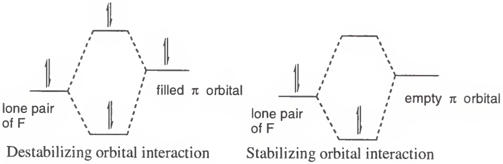
lone pair
of F
filled π orbital
Destabilizing orbital interaction
lone pair
of F
empty π orbital
Stabilizing orbital interaction

Figure 1.4 Diagram of destabilizing (left) and stabilizing (right) orbital interactions

Incorporation of fluorine substituents onto a cyclopropane ring changes the structure and reactivity of the cyclopropane system dramatically. The unusual kinetic fluorine substituent effect on cyclopropane was first reported by Mitsch and Neuvar, who observed the increasing ease of cleavage with the increasing fluorine substituents on cyclopropane.[38] Later in 1968, O'Neal and Benson pointed out that the kinetic behavior of fluorinated cyclopropanes were due to a ground state effect,[39] that is, fluorine substituents destabilize cyclopropanes and estimated that there is an increase of strain of 4.5~5 kcal/mol per fluorine substituent on a cyclopropane ring. In 1982, on the basis of relative heats of hydrogenation Roth reported that 1,1-difluorocyclopropanes are destabilized by 12-14 kcal/mol relative to their non-fluorine analogues.[40] Then in 1997, enthalpy of combustion data reported by Rüchardt for the first time provided reliable strain-free fluorinated group equivalents that allowed one to more confidently estimate the heats of formation of strain-free fluorinated hydrocarbon systems.[41] Using Rüchardt group equivalent values in combination with Roth's heats of hydrogenation allows one to place a value of 41.8 kcal/mol as the strain of a 1,1-difluorocyclopropane ring, which means that the incremental strain due to the geminal fluorine substituents is 14.2 kcal/mol.

Different computational studies have also been used to estimate the increase of ring strain upon fluorine substitution on cyclopropane. Greenberg and Liebman reported a ring strain increase of 11.7 kcal/mol of 1,1-difluorocyclopropane by comparing the heat of hydrogenation of the fluorinated cyclopropane with that of the parent cyclopropane at 4-31G level of theory.[42] Wiberg's isodesmic reaction energy calculations(Figure 1.5), which are essentially the same as Greenberg and Liegman's heat of hydrogenation model, provided similar results, 13.3 kcal/mol (MP2/6-31G(d)//MP2/6-31G(d)), 14.2 kcal/mol (MP2/6-311+G(d)//MP2/6-31G(d)) and 11.2 kcal/mol (B3LYP/6-311+G(d)//B3LYP/6-

31G(d)).[43] By assuming1,1,4,4-tetrafluorocyclohexane to be strain-free, our own calculation performed at B3LYP/6-31G(d)//HF/6-31G(d) level of theory revealed ring strains of 28.2 kcal/mol for cyclopropane and 37.2 kcal/mol for 1,1-difluorocyclopropane.

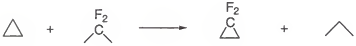

Figure 1.5 The hypothetic reaction used for calculation of cyclopropane ring strain caused by fluorine substituents.

Using the 'hydrogenation approach', propane and 2,2-difluoropropane were chosen as the reference states to deduce the respective ring strain. While in 'cyclohexane approach', cyclohexane and 1,1,4,4-tetrafluorocyclohexane were chosen as the respective reference state. The discrete heats of formations of CH_2 group in 2,2-difluoropropane and 1,1,4,4-tetrafluorocyclohexane will furnish the different increases of ring strain due to the fluorine substituents. However, even though there is no reliable way to put an accurate number on such strain energy, the increase of ring strain about 5~7 kcal/mol per fluorine on cyclopropane is widely accepted.

Structurally, a fluorine substituent shortens the adjacent C-C bonds and lengthens the opposite bonds of a cyclopropane ring (Table 4).[10] The F-C-F angle in gem-difluorocyclopropane is much smaller than the H-C-H angle in cyclopropane. The calculated equilibrium geometries of gem-difluorocyclopropane, which are generally compared to r_e data, reproduced these structural features and when electron correlation was incorporated, the agreement among different levels of theory was quite good (Table 1.5).

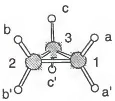

Table 1.4 Experimental bond lengths (Å) and bond angles (deg) in fluorine substituted cyclopropanes

F position	methods	C1-C2	C2-C3	C-F	F-C-F(H)
a, a'	MW r_0	1.464 (2)	1.553 (1)	1.355 (2)	108.4 (2)
a, b	MW	1.488 (3)	1.503 (4)	1.368 (6)	111.3 (4)
a, b'	MW	1.466 (4)	1.488 (5)	1.383 (3)	111.3 (4)
a, b, c	MW	1.507 (1)		1.354 (1)	112.3 (2)
a, b, c'	MW	1.500 (3)	1.478 (10)	1.367 (8)	109.4 (8)
				1.387 (8)	114.7 (15)
a, a',b, b'	MW	1.471 (3)	1.497 (10)	1.344 (4)	109.9 (4)
a, a',b, c	MW	1.481 (20)	1.533 (3)	1.355 (4)	110.1 (20)
a, a',b ,b', c, c'	ED, r_a	1.505 (3)		1.314 (1)	112.2 (10)

Table 1.5 Calculated bond lengths (Å) and bond angles (deg) in gem-difluorocyclopropane

methods	C1-C2	C2-C3	C-F	F-C-F(H)	reference
HF/6-31G(d)	1.465	1.535	1.330	109.4	This work
MP2/6-31G(d)	1.473	1.546	1.359	109.7	This work
B3LYP/6-31G(d)	1.480	1.547	1.355	109.7	This work
B3LYP/6-311+G(d)	1.472	1.545	1.359	109.7	43

The specific effects of geminal difluoro substitution on the thermal behavior of cyclopropane compounds were examined qualitatively Jefford,[44] who observed the rapid thermal interconversion of exo and endo isomers (Figure 1.6) at 60 °C, a result which is consistent with a weakening of the C2-C3 bond.[45]

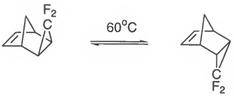

Figure 1.6 The rapid thermal interconversion of exo and endo isomers

Dolbier conducted systematic kinetic investigations on thermal rearrangements of gem-difluorocyclopropanes, which provided further evidence and great insight regarding fluorine substitution effects on cyclopropanes.[46] The geometrical isomerization of cis-1,1-difluoro-2,3-dimethylcyclopropane to its trans isomer (Figure 1.7) exhibited a significant diminution of activation energy (E_a= 49.7 kcal/mol)[47] compared to the analogous hydrocarbon rearrangement (E_a= 59.4 kcal/mol).[48] This result is consistent with O'Neal and Benson's approximation of the increase in strain that would be expected for two fluorine substituents. The thermal isomerization of 2,2-difluoro-2-vinylcyclopropane not only showed substantial lowering of the activation energy (E_a = 40.3 kcal/mol)[49] relative to hydrocarbon analog, but also provided evidence for the preferential cleavage of the C-C bond opposite to the CF_2 group. Accordingly, Dolbier concluded that the kinetic effects of the 9~10 kcal/mol of the incremental strain seem to derive largely from weakening of that C-C bond which is opposite the CF_2 group, while the strengths of the bonds adjacent to the CF_2 group are affected only minimally.[46]

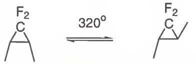

Figure 1.7 The epimerization of gemdifluorocyclopropane

Nevertheless, Dolbier's earlier conclusion was undermined later by the reported formation of significant amounts of rearrangement products that arise from the cleavage of a proximal C-C bond in 1,1-difluoro-2-vinylcyclopropanes.[50] Therefore, the preference for the distal C-C bond cleavage in 1,1-difluorocyclopropanes may not be as overwhelming as the results of earlier Dolbier's kinetic studies might suggest.[46]

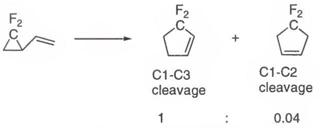

Figure 1.8 A substantial amount of product derived from C1-C2 cleavage was observed.

Dolbier's speculation about the regiochemistry of the thermolyses of fluorinated cyclopropanes is consistent with the general thermodynamic preference of electronegative atoms, such as fluorine, to be attached to the more substituted of the two carbon atoms,[51-54] and with Borden's *ab initio* calculation.[51] At the RHF/6-31G(d) level, 2,2-difluoropropane is computed to be 5.9 kcal/mol (7.2 kcal/mol at MP2/6-31G(d)) more stable than 1,1-difluoropropane. Using Rüchardt's recent group increments,[41] the heats of formation of 2,2-difluoropropane and 1,1-difluoropropane were calculated to be -129.8 kcal/mol and -126.0 respectively. Thus, 2,2-difluoropropane is estimated to be 3.8 kcal/mol more stable than the latter. At SDQ-CI/6-31G(d) level, the free energy of 1,1-difluorotrimethylene is calculated to be 4.8 kcal/mol higher than that of 2,2-difluorotrimethylene at 600 K.[51]

Both structural and theoretical studies seem to indicate that fluorine substituents on cyclopropane lengthen and *hence* weaken the distal C-C bond, and shorten and *hence* strengthen the proximal C-C bond. However, in cyclopropane compounds, bond length and bond strengths do not always correlate with each other. For examples, thermolysis of 1,2-dimethoxy-3-methylcyclopropanes involves the cleavage of the bond connecting the methoxy substituted carbon atoms.[55] And also, at 340 °C, while CF_2: extrusion is a major decomposition pathway, 1,1,2,2-tetrafluorospiropentane rearranges with a substantial fraction (40%) by cleaving the shorter CF_2-CF_2 bond to give the cyclobutane product shown in Figure 1.9.[56]

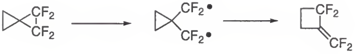

Figure 1.9 The cleavage of the shorter C-C bond on the cyclopropane ring

Bond strength in a molecule is defined by the energy associated with its homolytic cleavage. When all the major conditions are equal, the longer bond is weaker. Generally, the cleavage of a specific bond in a molecular will not cause significant change of the intrinsic characters of the other bonds, therefore, the bond strength correlates with the bond length quiet well. However, in cyclopropane, the cleavage of one C-C bond on the ring is associated with extensive alteration of the other two C-C bonds from bent to normal C-C bonds with the releasing of the ring strain. The longer and hence weaker bond releases more energy and vice verse in the normalization process, which will offset the energy, needed for the cleavage of the other bond on the ring. Thereby, there should be no intrinsic correlation between the bond strength and the thermal regiochemistry of cyclopropane thermolyses. For substituted cyclopropanes, their observed thermal regio-selectivities are largely derived from the stability of the resulting biradicals.

Because the C-C bonds on cyclopropane are all associated with each other, it is awkward to use the traditional bond strength concept to characterize the individual C-C bond on the ring. It seems necessary to split the traditional bond strength concept into 'thermal bond strength', which is associated with the bond dissociation energy and 'structural bond strength', which is related to the bond length, with all other thing being equal, the longer bond being weaker.

A variety of theoretical models have been put forth to explain the fluorine substitution effects on cyclopropane. In 1970, both Hoffmann[57] and especially Günther[58] argued that π-donors, by interacting with the vacant Walsh orbital of $1a_2'$ symmetry (Figure 1.10), should destabilize the ring but lengthen all the cyclopropane C-C bonds. The predicted destabilization of π-donors was confirmed experimentally, but this prediction on geometrical mutation was shown experimentally not to be correct for 1,1-difluorocycloporpane.

Based on *ab initio* SCF MO calculations after rejecting the significance of π donator and σ acceptor substitution effects, Durmaz and Kollmar,[59] adopted Bent[60] and Bernett's[61] discussion about the influence of changes in the hybridization of carbon atoms in fluoro-substituted hydrocarbons, invoked 'Local effects', which state lengthening of the opposite and shortening of the adjacent bonds can be due to an increase in ring strain caused by a change in hybridization of the carbon atom bonded to the substituent. They evaluated the HCH bond angle value, which changed from 109.5° in methane to 113.7° in CH_2F_2 and rationalized that fluoro-substitution in cyclopropane will increase the ring strain and the system will avoid the increased strain by simultaneously lengthening the opposite and shortening the adjacent bonds. In 1998, Wiberg[43] re-emphasized the change of hybridization on fluoro-substituted carbon. Since the electronegative atoms such as fluorine prefer to be bonded to orbitals that have high p character,[60] Wiberg rationalized that the destabilization of fluorine substituents on cyclopropane is due to the higher s character carbon orbitals (~sp^2).[33,62]

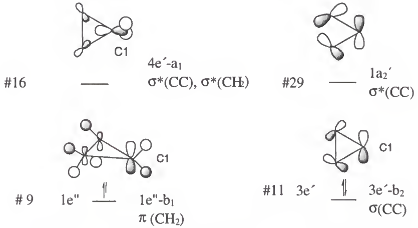

Figure 1.10 The MOs of a cyclopropane that interact with fluorine substituents

Clark, Schleyer and coworkers have distinguished four different classes of substituents, namely π-acceptor, π-donor, σ-acceptor and σ-donor.[63] This classification is based on possible 2-electron –2-orbital interactions involving substituent and cyclopropane MOs. Prerequisites for these interactions are comparable orbital energies for substituent and ring and a sufficiently large primary overlap between the orbitals involved. The latter requirement implies large amplitude of the interacting cyclopropane orbital at C1, which is the location of the substituent. This excludes all MOs of cyclopropane, but those in Figure 1.10.

Depopulation or population of MOs #9, #11 and #16, but not the $1a_2'$ MO #29, leads to opposing changes in proximal and distal bond lengths. Accordingly, one can expect characteristic changes in the geometry of cyclopropane upon substitution by a π/σ-acceptor/donor substituent (Table 6). Fluorine was classified as an σ-acceptor, which withdraws electron density from the $1e'$-b_1 of cyclopropane (# 9). This results in a lengthening of the distal and shortening of proximal CC bonds. The depopulation of the bonding orbital is the cause of the destabilization of fluorocyclopropanes.

Table 6. Substituent effect on the geometry of cyclopropane as a function of interactions between substituent and cyclopropane MOs.

Substituent type	MO of cyclopropane involved	Change in vicinal bonds C1C2	Change in distal bond C2C3
π-Acceptor	# 11	longer	shorter
π-Donor	# 16	longer	shorter
σ-Acceptor	# 9	shorter	longer
σ-Donor	#16	longer	shorter

Cremer and Kraka proposed a 'principal of avoidance of geminal and vicinal charge concentrations', which they derived form an analysis of the Laplace concentration in the valence shell of bonded atoms which classified fluorine as either σ-attractor or π-repeller.[64] In most cases, Cremer and Kraka's electron density model and Clark, Schleyer and coworker's model led to the similar predictions.

The two HOMO orbitals of gem-difluorocyclopropane calculated at HF/6-31G(d) level are shown in Figure 1.11, which is similar to the degenerated HOMO of cyclopropane except for the participation of the 2p orbitals of fluorine, which cause differentiation of the degenerate HOMOs in cyclopropane. As a result, ψ_{20} is slightly higher in energy than ψ_{19}. The components and coefficients of the two molecular orbitals are also depicted.

Conclusion

In this chapter, several concepts, such as structure, strain and molecular orbitals of cyclopropane, which are important to our understanding of the cyclopropane chemistry, were reviewed or stated briefly. The effects of fluorine substitution, which influence the properties of cyclopropane structurally and hence energetically, were introduced. The concept of bond strength was split into thermal bond strength and structural bond strength in order to explain the lack of correlation between the thermal regiochemistry and the bond length.

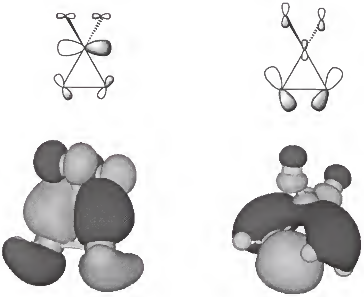

ψ_{20} −11.82 ev ψ_{19} −12.50 ev

Figure 1.11

Calculated molecular orbital of *gem*-difluorocyclopropane (HF/6-31G(d))

CHAPTER 2
A NOVEL FACILE AND HIGHLY EFFICIENT SYNTHESIS OF GEM-DIFLUOROCYCLOPROPANES

Introduction

There has been an unceasing effort among organic chemists over nearly four decades to try to find good practical methods to synthesize gem-difluorocyclopropanes.[65-68] Based on those efforts, fluorinated cyclopropanes have been the focus of abundant theoretical and experimental studies. Numerous pesticides,[69] fungicides and antibacterial agents,[70] were developed, which have as an integral component of their structure a difluorocyclopropane unit (Figure 2.1.).

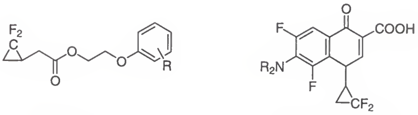

Pesticide

Antibacterial Reagent

Figure 2.1 Examples of a pesticide and an antibacterial reagent that have gem-difluorocyclopropane unit

The major method for synthesis of *gem*-difluorocyclopropanes moiety is cyclopropanation reactions of alkenes using electrophilic difluorocarbene or carbenoid reagents. However, difluorocarbene, because of the interaction of the long pairs of the two fluorine substituents with the carbene center, is a highly stabilized carbene and therefore, it is less reactive than other dihalocarbenes. Therefore, although electron rich alkenes react readily with difluorocarbene under mild conditions, this is not the case for less nucleophilic alkenes. In practice, there are only few difluorocarbene reagents that have been found to react with electron deficient alkenes to give reasonable yields of difluorocyclopropanes, and these reagents all suffer from various limitations as far as their general synthetic applications are concerned.

The first difluorocarbene reagent, which was developed to transfer difluorocarbene to alkenes, and perhaps the most commonly used commercial source of difluorocarbene, is sodium chlorodifluoroacetate.[71] For example, at 190 °C, the sodium salt decarboxylates in the presence of (Z)-4-(benzyloxy)-2-butenyl acetate, resulting in an 83 % yield of [3-Benzyloxymethyl-2,2-difluorocyclopropyl]-methyl acetate (Figure 2.2.).[72] However, the use of a large excess of the acetate salt (11 equivalents) combined with the required high reaction temperature comprise significant disadvantages of this method.

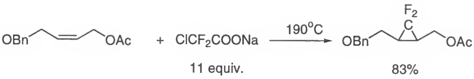

Figure 2.2 A large excess of $ClCF_2COONa$ is needed for cyclopropanation

Another difluorocarbene reagent, Seyferth's phenyl(trifluoromethyl)mercury is probably the most efficient difluorocarbene reagent so far developed. When treated with sodium iodide at 80°C in benzene, this reagent transferred difluorocarbene to1-heptene to form 1,1-difluoro-2-pentylcyclopropane in a 70% yield (Figure 2.3).[73] Nevertheless, the absolute anhydrous condition required by this reaction and the use of mercury in the difluorocarbene precursor inhibit the potentially extensive and especially large-scale application of this method.

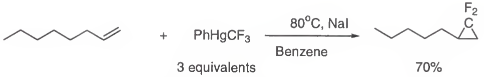

Figure 2.3 Seyferth reagent for difluorocyclopropanation

Difluorodiazirine is not only a photochemical source of difluorocarbene but also a thermal source of difluorocarbene.[74] Above 165°C, reactions with alkenes give good yield of difluorocyclopropanes. However, the drawbacks include its potentially explosive nature[75] and the required use of elemental fluorine during its preparation.

In a non-carbene process, reaction of gem-dichlorocyclopropanes with excess of tetra-n-butylammonium fluoride trihydrate (TBAF) in DMF can provide *gem*-difluorocyclopropanes in moderate yields (Figure 2.4).[76] However, requiring a rather strong electron withdrawing group and a hydrogen atom α to this group in the *gem*-dichlorocyclopropane precursors for the success in the transformation limits its extensive application.

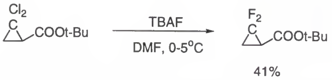

Figure 2.4 A non-carbene process of making gem-difluorocyclopropane

In viewing all the methods mentioned above suffering from various significant limitations, insofar as their general synthetic application is concerned, there was until our current work, no practically applicable method available to synthesize *gem*-

difluorocyclopropanes from relative electron deficient alkenes, such as mono alkyl substituted alkenes.

Fluorosulfonyldifluoroacetic acid FSO_2CF_2COOH, which can be obtained from the readily available FSO_2COF, was found by Chen to be a suitable carbene precursor.[77] In the presence of Na_2SO_4, the acid reacted with 2,3-dimethyl-2-butene, an electron rich alkene, to give 1,1-difluoro-2,2,3,3-tetramethylcyclopropane in a 53% yield (Figure 2.5). It was presumed that the intermediate anion, $FSO_2CF_2COO_2^-$, generates difluorocarbene by elimination of SO_2, CO_2 and F^-.

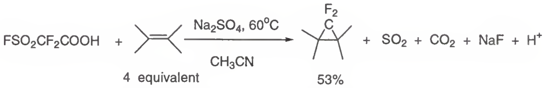

Figure 2.5 FSO_2CF_2COOH was used as a difluorocyclopropanation reagent

By alternating the pathway of anion generation, we have found that the trimethylsilyl derivative of the acid, $FSO_2CF_2COOTMS$, is much improved difluorocarbene precursor, which in the presence of catalytic amount of NaF, cyclopropanated mono-alkyl substituted alkenes and more remarkably highly electron deficient alkenes such as butyl acrylate, bearing an electron withdrawing substituent on the double bond, to afford gem-difluorocyclopropanes in excellent and in some cases virtually quantitative yields under mild conditions.

Results and Discussion

Trimethylsilyl fluorosulfonyldifluoroacetate, **21**, can be easily synthesized from the reaction of fluorosulfonyldifluoroacetic acid with TMS chloride with a yield of 78%

after vacuum distillation (Figure 2.6). The reagent is a colorless liquid, and is stable at room temperature with no decomposition being observed after stored in a plastic bottle for a month. Without solvent, the reagent exhibited no obvious decomposition at ambient temperature in the presence of CsF and at 105°C, without fluoride anion being present, no notable decomposition was observed.

$$\mathrm{FSO_2CF_2COOH} + \underset{\text{4 equivalents}}{\mathrm{TMSCl}} \longrightarrow \underset{\substack{\mathbf{21}\\ \text{78\% yield}}}{\mathrm{FSO_2CF_2COOTMS}} + \mathrm{HCl}$$

Figure 2.6 Making of $FSO_2CF_2COOTMS$

In the presence of a catalytic amount of NaF, under an N_2 and under appropriate conditions such as at elevated temperature in specific solvents, trimethylsilyl fluorosulfonyldifluoroacetate was added slowly into the reactant alkenes using a syringe pump with a Teflon® needle. The emission of gas indicated that the carbene precursor underwent decomposition, probably via a chain process depicted in Figure 2.7.

The well-known deprotecting nucleophilic attack of F^- on the TMS group gives TMSF and an anion $FSO_2CF_2COO^-$, which readily decomposes to generate CF_2: with the elimination of SO_2, CO_2 and F^- to achieve the propagation by fluoride ion. The difluorocarbene reacts with the olefinic substrate to provide difluorocyclopropane products. All of the by-products in this chain process are gaseous which constitutes part of the advantage of this methodology: easy isolation and a potential one-pot reaction for a multistep process.

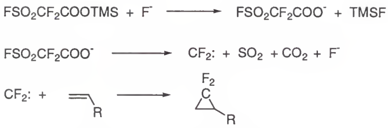

Figure 2.7 Proposed chain decomposition process of $FSO_2CF_2COOTMS$

The reactivity of this difluorocarbene reagent towards different alkenes was investigated using a specific identical condition (105°C, 1.5 equivalent of carbene reagent), and the results are given in Table 2.1. The ^{19}F NMR yields of seven relatively electron deficient alkenes were obtained by comparing the ^{19}F single integration of products with that of the internal standard, α,α,α-trifluorotoluene which was added afterwards. Reaction 1~ 4 are neat reactions, in reaction 5~7, methyl benzoate was used as a solvent.

Table 2.1 Non-optimized ^{19}F NMR yields[a] of *gem*-difluorocyclopropanation reactions[b].

reaction	olefins	Yields(%)
1	Allyl benzoate[c]	78
2	3-butenyl benzoate[c]	89
3	4-pentenyl benzoate[c]	97
4	2-Cyclohexenyl benzoate[c]	65(trans:cis=5:1)
5	1-Octene [d]	74
6	Allyl acetate[e]	56
7	Butyl acrylate[e]	73

a. The yields were calculate using internal standard α,α,α-trifluorotoluene.
b. Reaction temperature is 105 °C. NaF is used as initiator. 1.6mmol scale.
c. Neat reaction
d. 0.5 equivalent of methyl benzoate as solvent
e. 2.0 equivalent of methyl benzoate as solvent

With only 1.5 equivalent of difluorocarbene reagent, the exceptional cyclopropanation ability of this reagent is demonstrated by these results. In reaction 3, an unprecedented 97% yield in the synthesis of mono-alkyl substituted gem-difluorocyclopropane was achieved. From reaction 1 to 3, the yields ascended with the nucleophilicity of the alkenes, which is determined by the distance between the double bond and the electron withdrawing oxygen substituent. Those three reactions as well as reaction 7 were very clean. There were no significant amounts of side products observed by either ^{19}F or ^{1}H NMR. The proton NMR of the reaction mixture of reaction 2 upon complete conversion was almost identical to that of the pure product except for some little TMS peaks. This indicates that the pre-isolation yield of this reaction is virtually *quantitative.*

For reaction 5, in the post-reaction mixture, there was only about 3% starting material left with a yield of 74% difluorocyclopropane. The escaping of the relatively volatile alkene reactant from the open system probably is responsible for the less than excellent yield for 1-octene in such a small-scale reaction (180 mg). Indeed, at lower temperature (85°C), the yield decreased to 49%, but with 44% of the starting material left in the reaction mixture. Therefore, a larger scale reaction and a better condensing apparatus would probably overcome this problem and afford a better yield.

The reaction with 2-cyclohexenyl benzoate seemed to provide a "low end" yield in this series. But considering the 15% yield provided by the 6 folds excess difluorocarbene precursor using Schlosser's method (Figure 2.8),[78] our 65% yield with only 1.5 equivalent of difluorocarbene should be considered to be a tremendous improvement.

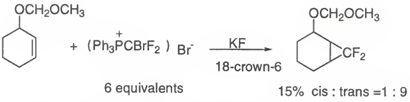

Figure 2.8 Schlosser's difluorocyclopropanation method

It is noteworthy that even though already striking, the yields listed in Table 2.1 are not optimized yields. With a larger excess of difluorocarbene reagent, higher conversions, and thus higher yields should be obtained. This has been demonstrated clearly by the experimental results in Table 2.2, *e.g.* by varying the difluorocarbene reagent from 1 to 2 equivalents, the yield of allyl benzoate cyclopropanation increased from 63% to 89%.

Table 2.2 Variation of yields with the amount of difluorocarbene precursor added[a]

Reactant	Equivalent of CF_2: precursor		
	1.0	1.5	2.0
Allyl benzoate[b]	63 %	78%	89%
3-butenyl benzoate[b]		89	92%
4-pentenyl benzoate[b]	75%	97%	

a. Reaction temperature is 105 °C. NaF is used as initiator. 1.6mmol scale.
b. Neat reaction

Several other factors including temperature, solvent, initiator and the addition speed of the carbene reagent that may alter the efficiency of this difluorocarbene precursor and eventually influence the yield were also investigated.

The temperature dependence of reactivity of difluorocarbene has long been recognized, because of the special stability of this carbene. This led to the development of several high-temperature thermal carbene sources.[65] In our current study, using 1.0 equivalent of difluorocarbene precursor, when the reaction temperature was increased from 85°C to 125°C, the yield of difluorocyclopropanation of allyl benzoate increased from 27% to 75%. A further increase in the reaction temperature to 145°C, did not result in a better yield.

Table 2.3 Temperature Dependence of the Yields of difluorocyclopropanation of Allyl Benzoate[a]

T (°C)	85	105	125	145
Yields(%)	27	63	75	75

a. Neat reaction at 1.6mmol scale, NaF as initiator, 1 equivalent of carbene reagent.

Among the different fluoride initiators tested, NaF gave the best result (Table 2.4). This may be caused by the lower solubility of NaF than KF and CsF in organic solvents, which provides benefit by reducing the number of chains initiated, thus maintaining a constant low concentration of reactive species, difluorocarbene. As a consequence, the possibility of carbene self-coupling is minimized and thus, the yield of cyclopropanation was increased. The different stabilities of FSO_2CF_2COOM (M = Cs, K, Na) may also play a role here.

By maintaining a low concentration of fluoride ion, another potential competition process, that is the formation of trifluoromethyl anion,[79] by the capture of F^- by difluorocarbene to give CF_3^-, is not likely to occur. This would consume the fluoride ion initiator, and eventually shut down the reaction. On the contrary, the difluorocarbene precursor decomposes completely in all the reactions listed in Table 2.4 in the presence of only a catalytic amount of NaF.

At low temperatures such as below 65°C, the initiation using NaF might be too slow to get the reaction started. In this case, KF or even CsF might be a better choice.

Table 2.4 Effect of Different Initiator on the Yields of Difluorocyclopropanation of Allyl Benzoate[a]

Initiator	Equivalent of Carbene	Yields (%)
CsF	3.0	61
KF	2.0	78
NaF	2.0	89

a. Neat reaction at 1.6mmol scale, 105 °C reaction temperature

Without solvent, the benzoates reacted well, but 1-octene and especially, allyl acetate performed poorly (Table 2.5). When methyl benzoate was added as a solvent, the yields of these reactions were elevated. Interestingly, when toluene was used as solvent only the reaction of allyl acetate exhibited an increase in yield, it having no effect on the yield of the reaction of 1-octene. It seems that both the existence of a benzene ring, either in the reagent or as an added solvent, and the polarity of the solvent system are beneficial for the cyclopropanation process.

Table 2.5 Solvent effect on the Difluorocyclopropanation Yields[a]

Solvents	Methyl Benzoate		Toluene		No Solvent
	Yields	E.S.[b]	Yields	E. S.[b]	Yields
1-Octene	78%	1.0	34%	1.0	35%
Allyl Acetate	21%	1.0	51%	1.0	~5%
	57%	3.0	60%	4.0	

a. 1.6mmol reaction scale, CsF as initiator, 3 equivalent of carbene precursor, 105 °C.
b. E. S.= equivalent of solvent

It has been recognized that carbene could interact with π electrons to form a carbene-alkene[80], carbene-carbonyl and carbene-benzene π complexes.[81] The complexes may lower the concentration of free carbene, and as a consequence the cyclopropanation is kinetically more favored. The competition experiment between allyl acetate and allyl benzoate showed that allyl benzoate is 1.6 times more reactive than allyl acetate, an indication of possible weak intra-complex carbene shift.

The beneficial effect of the polarity of the solvent system might be rationalized by the polar transition state of the carbene cyclopropanation, where a substantial amount of charge transfer from alkene to carbene was found.[80] A polar solvent can stabilize a polar transition state more than a non-polar complex, and thus lower the activation barrier.

Table 2.6 The variation of yields with the hours of addition in allyl benzoate cyclopropanation[a]

reactions	Hours for addition	Yields (%)
1	1.5	58%
2	2.6	83%
3	4.5	86%

a. 1.6mmol reaction scale, NaF as initiator, 2 equivalent of carbene precursor, at 105 °C.

Based on our observations, we deduced that a low concentration of free carbene leads to better yields. Besides manipulating the initiator and the solvent, we could also adjust the speed of addition of the carbene reagent in order to control the relative concentration of free carbene to alkene reactant. On the other hand, under the reaction conditions, using a larger excess of the reactant alkene can also serve the same purpose. Indeed, in the case of the allyl benzoate cyclopropanation, a longer time for the addition of the carbene precursor, led to a better yield we got (Table 2.6). However, within the error limits of NMR integration, the yields of runs 2 and 3 can be considered the same. Therefore, in this case, an addition speed of 0.8 equivalents per hour appears to be good enough.

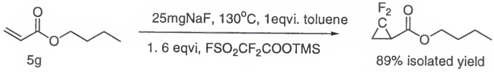

Figure 2.9 Demonstration of preparation scale synthesis of difluorocyclopropane

It is not the purpose in this discussion to provide a "standard" reaction procedure, but rather to describe how the key factors (temperature, initiator and solvent) influence the reaction efficiencies, in order to help people to develop their own reaction procedures accordingly. As an example and also to substantiate all the reported NMR yields mentioned above, we cyclopropanated butyl acrylate, possibly the most electron deficient olefin investigated, in a 5g (39mmol) scale (Figure 2.9). Using a 130°C oil bath, 25mg of NaF as initiator, and 3.6g (1 equivalent) toluene as solvent, the difluorocarbene precursor was added slowly to avoid the formation of foam. About 28 hours later, after 16g (1.6 equivalent) of precursor was added complete conversion was achieved. Vacuum distillation of the reaction mixture provided 6.08 g of product, which is equivalent to an 89% isolated yield.

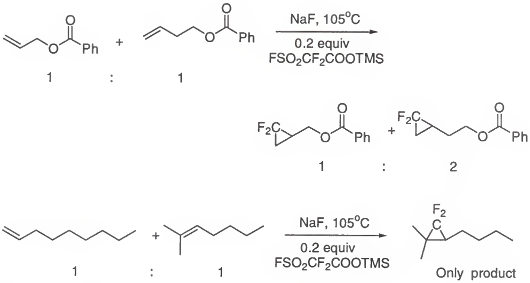

Figure 2. 10 Competition reactions

The exceptional reactivity, towards electron deficient alkenes, of the presumed difluorocarbene intermediate generated from the decomposition of $FSO_2CF_2COOTMS$, may lead people to suspect its electrophilicity, the trait of a normal carbene. However, in addition to the early indication (Table 2.1), a competition study did show the preference of this reagent for electron-rich alkenes (Figure 2.10). Whereas allyl benzoate is only 2 times less reactive than 3-butenyl benzoate, 1-octene is routed in the competition with 2,3-dimethyl-2-hexene.

The NMR spectra of the *gem*-difluorocyclopropane products are very interesting. The chemical shifts and coupling profile on the ring of butyl 2',2'-difluorocyclopropanacetate, which is resolved by a decoupling experiment, is depicted in Figure 2.11. The F-H coupling constants are around 12 Hz for the cis-proton and 6 Hz for the trans proton. The H-H coupling constants are around 11 Hz between the cis protons and 7 Hz between trans protons. In comparing with 2,2-difluorocyclopropylcarbinyl benzoate, the cyclopropanation product of allyl benzoate, all the chemical shifts including both F and H on the ring are shifted shift down field, an indication of losing electron density on the ring to the neighboring potent electron withdrawing carbonyl group.

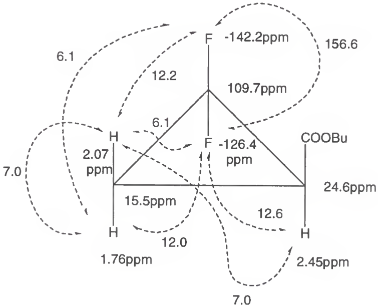

Figure 2.11 Chemical shift and coupling constants (Hz) of F and H on the cyclopropane ring of butyl 2',2'-difluorocyclopropanacetate

Finally and arguably, an open question that may never will be answered is whether the final "active gradient" of this reagent $FSO_2CF_2COOTMS$ is a free difluorocarbene which is the same as many other reagent in literature, and if so why the difluorocarbene generated in this study is more efficient in its alkene addition reactions?

Conclusion

A novel highly difluorocarbene reagent was found, which can react with alkenes including highly electron deficient alkenes to give difluorocyclopropanes in good to excellent yield under mild conditions. Various effects, which may influence the reaction yields, were evaluated.

CHAPTER 3
STEREOMUTATION OF 1-ETHYL-2, 2-DIFLUORO-3-METHYLCYCLOPROPANE

Introduction

Pyrolysis of cyclopropane or its substituted derivatives causes two major reactions: hydrogen shift to an olefin (e.g. cyclopropane to propene)[82] and stereomutation (e.g. trans- to cis-cyclopropane-1,2-d_2) (Figure 3.1). The thermal stereomutation reactions have attracted extensive experimental and theoretical efforts over the last 30 years directed toward understanding the mechanistic detail and this work has been extensively reviewed.[83-87]

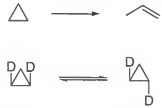

Figure 3.1 Two major reactions of cyclopropanes

Three extreme mechanisms have been proposed for the stereomutation of cyclopropane. The Smith mechanism[88] involves rotation of one of the substituted carbons through 180°, converting trans cyclopropane to cis, a process that plausibly might occur in an "expanded ring".[89,90] By this mechanism, conversion of a substituted trans cyclopropane to its enantiomeric trans compound requires two alternating, consecutive rotations with an obligatory pause at the cis compound (Figure 3.2).

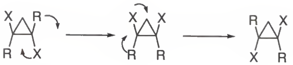

Figure 3.2 Smith mechanism

Based on the activation parameters for the thermal isomerization of cyclopropane and the calculated differences of heats of formation between the trimethylene diradical and cyclopropane, O'Neal and Benson[39] first derived a reaction coordinate diagram for cyclopropane isomerization. In this diagram, the trimethylene biradical is an intermediate sitting in a potential energy well around 10 kcal/mol deep. Thus, Benson proposed that bond rotations in the trimethylene diradical are very fast relative to recyclization. The ring opening would thus be followed by random ring closure to form racemic trans and cis cyclopropane (Figure 3.3).

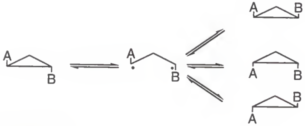

Figure 3.3 Benson mechanism

Hoffmann, in1968, conducted extended Hückel calculations, and located two biradicals as intermediates.[91] The anti-symmetric trimethylene biradical (0,0) (defined by the angle between the plane of HCH on two radical and the plane of CCC), which results from conrotatory ring opening, is about 10 kcal/mol more stable than the trimethylene biradical (0, 90), which is formed from single rotatory ring opening (Figure 3.4). Accordingly, Hoffmann predicted that synchronous conrotatory motions are preferred for cyclopropanes. If only one specific bond breaks, this mechanism would not allow the inter-conversion between cis and trans isomers.

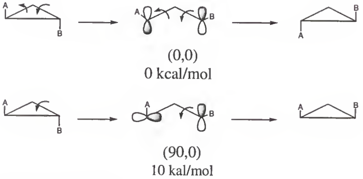

Figure 3.4 Hoffmann prediction

However, numerous experiments with substituted cyclopropanes[83-87] have failed to confirm Hoffmann's 1968 prediction,[91]. Elegant experiments on cyclopropanes, containing deuterium as the only substituent, have led to conflicting results, as discussed below.

Berson and coworkers found a strong preference for coupled rotation of two methylene groups in their study of the stereomutation of cyclopropane-1,2-d_2 (Figure 3.5.a.).[92,93] Experimental results on the stereomutation of cyclopropane-d_2, in a very similar system to that of Berson and coworkers, have also been reported.[94] In contrast, Baldwin and coworkers reported nearly equal rate constants for single and double methylene rotations in cyclopropane-^{13}C-1,2,3-d_3(Figure 3.5.b).[95] More recently, however, a statistical analysis has led Baldwin to conclude that one of the rate constants, measured by him and his coworkers, contains too large an uncertainty to warrant any definitive conclusion being drawn about the ratio of double to single methylene rotations in the stereomutation of cyclopropane-d_2.[83] Recent *ab initio* calculations of the potential surface for stereomutation of cyclopropane and vibrational analyses, performed at the stationary points on this surface, found that the computed isotope effects are incapable of reconciling the results of these two studies.[96,97]

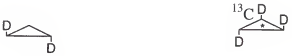

a b

Figure 3.5 Systems Berson (a) and Baldwin (b) investigated

On the potential energy surfaces that were computed there is only ca. 1 kcal/mol difference between the energies of the transition state for conrotation and the transition states for both single methylene rotation and disrotation.[96,97] Moreover, the calculations indicated that alkyl substituents significantly reduce the already small preference predicted for conrotatory ring opening and ring closure.[96] These computational findings explain the failure of the large number of experiments on substituted cyclopropanes to detect any significant preference for stereomutation via coupled conrotation.

Transition-state theory, when applied to the potential surfaces computed for stereomutation of unsubstituted cyclopropane, predicts that disrotatory ring opening should be followed, preferentially, by conrotatory ring closure. Transition-state theory makes this prediction because the conrotatory transition state is the lower energy of the two transition states for ring closure. Since disrotatory ring opening, followed by conrotatory ring closure, has the same net effect as passage across the transition state for rotation of a single methylene group,[96,98] transition-state theory, when applied to the potential surfaces computed for stereomutation of cyclopropane, predicts nearly equal rate constants for double rotation and net single rotation.[97]

In contrast to transition state theory, very recent reaction dynamics calculations on similar potential energy surfaces for cyclopropane stereomutation predict a three- to five-fold preference for double rotation.[99,100] The physical reason for the difference between the predictions made by transition state theory and by reaction dynamics is that in the dynamical calculations, conservation of angular momentum tends to result in disrotatory ring opening being followed by disrotatory, rather than conrotatory, ring closure.[100] Thus, the dynamical calculations predict that disrotation makes a significant contribution to the coupled rotation that appears to dominate the stereomutation of cyclopropane-1,2-d_2.[83,92-94]

Unfortunately, with deuterium as the only substituent, there is no way to distinguish experimentally between the contributions of con- and disrotation to the double rotation found in cyclopropane-1,2-d_2.[83,92-94] The results of the reaction dynamics calculations caution against assuming that the observation of coupled rotation in this cyclopropane implies that the mode of coupling is necessarily the conrotation that was predicted by Hoffmann.[91]

Inspired by Dolbier's pyrolyses work on fluoro-substituted cyclopropane, which showed that geminal difluoro-substituents accelerate the rate of cyclopropane stereomutation and the distal C-C bond to the CF_2 group on the ring is probably preferred to cleave,[46] Borden performed *Ab initio* calculations and found that the geminal fluorine substituents in 1,1-difluorocyclopropane made the stereomutation very different from that of cyclopropane.[101,102] Unlike the hydrocarbon, 1,1-difluorocyclopropane is predicted to show a *large* preference for stereomutation by *disrotation* of C(2) and C(3). At the GVB and SD-CI level, disrotation is calculated to be preferred to conrotation by 2.4 kcal/mol and 3.7 kcal/mol, respectively. The preference for disrotation over conrotation and over all the possible pathways that effect net rotation of just one of these carbons is predicted to be *enhanced*, not diminished,[96] by alkyl substituents. A pair of methyl groups increase the preference for (0,0) over (0,90) from 3.4 kcal/mol in 2,2-difluorotrimethylene to 4.0 in 3,3-difluoropentane-2,4-diyl at GVB/6-31G* level (Figure 3.6). Finally, since the s-*trans*,s-*trans*-(0,0) conformation of 3,3-difluoropentane-2,4-diyl is computed to be 3 - 4 kcal/mol lower in energy than the s-*cis*,s-*trans*-(0,0) conformation (Figure 3.6),[102,103] the relative rates of coupled rotation in *cis*- and *trans*-1,1-difluoro-2,3-dialkylcyclopropanes via these two possible transition states are predicted to be useful for differentiating experimentally between con- and disrotation.

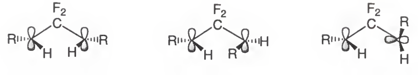

	s-trans,s-trans-(0,0)	s-trans, s-cis-(0,0)	s-trans-(0,90)
R=H	0		3.4
R=Me	0	3.6	4.0

Figure 3.6 Relative GVB/6-31G* energies (kcal/mol)

More specifically, an optically active *cis*-1,1-difluoro-2,3-dialkylcyclopropane is predicted to racemize much more rapidly than its *trans* stereoisomer. As shown in Figure 3.7, the *cis*-cyclopropane can undergo disrotatory ring opening to the preferred s-*trans,*s-*trans* transition state for racemization; whereas, disrotatory ring opening of the *trans*-cyclopropane gives the higher energy s-*cis,*s-*trans* conformation of the diradical. On the other hand, if conrotation were, in fact, preferred to disrotation, racemization of an optically active *trans*-1,1-difluoro-2,3-dialkyl-cyclopropane should be significantly faster than racemization of its *cis* stereoisomer.

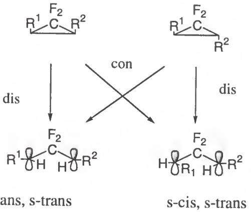

Figure 3.7 Diagram of the concenquences of the disrotatory and conrotatory ring opening of substituted gem-difluorocyclopropane

Precursor Syntheses

To accomplish both experimental simplicity along with minimum deviation from the calculated model system, optically active cis and trans-1,1-difluoro-2-ethyl-3-methylcyclopropane were chosen as the target substrates. Scott[104] and Bartberger conducted some preliminary work and demonstrated that the four enantiomers of the *cis* and *trans* compounds could be resolved by GC using a capillary chiral column provided by professor V. Schurig and H. Grosenick from Institut für Organische Chemie, Universität Tübingen. However, unfortunately no preparative column was available. Bergman synthesized a similar optically active hydrocarbon system with an 8-step synthesis after three recrystallization resolutions.[105] However, due to the limitations regarding *geminal* difluorocyclopropane synthesis at the time this work was conducted, we did not have the luxury to follow Bergman's trails. Instead, encouraged by Grandjean and Chuche's work,[106] an enzymatic resolution centered synthetic strategy was designed, even though it had failed when acetate instead of butyrate was used.[104] The first approach to the synthesis of optically active cis compound is outlined in Figure 3.8.

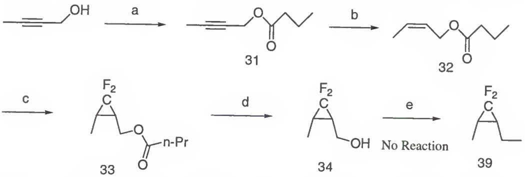

Figure 3.8 First approach of synthesis of optically active cis-1,1-difluoro-2-ethyl-3-methyl. a. n-PrCOCl, DMAP b. H_2 1atm,Pd/$BaSO_4$ (unreduced) c. $PhHgCF_3$, NaI d. PPL, H_2O, pH=6.5 e. CH_3Li, CuI, [Ph_3PNCH_3Ph]I, $LiCH_3$

In the exploratory study, the ester **31** was synthesized following the literature procedure with high yield and, and was then reduced to cis-2-butenyl butyrate **32** by hydrogenation with 1 atm H_2, catalytic amount of $Pd/BaSO_4$(unreduced) and quinoline.[107] Difluorocyclopropanation using the Seyferth reagent $PhHgCF_3$, which is not commercially available anymore, provided difluorocyclopropane product **33** in 27% yield. The subsequent enzymatic hydrolysis using PPL (lipase type II, crude, from porcine pancreas) yielded alcohol **34** with a d.e.% of about 70% upon 50% conversion of the reaction. The ^{19}F NMR of the diasteromeric R-(O)-Acetylmandelic acid esters of alcohol **34** is used to estimate the d.e.%. However, the last step, methylation, which worked well for cyclopropyl carbinol in a test run, gave no sign of conversion from alcohol **34** to product **39**.[108] The inertness of the cis alcohol probably is due to steric hindrance from the *cis* methyl group, which is right in the path of nucleophilic attack of methyl anion to displace the carbinyl oxygen. This approach was thus abandoned.

$$HgO + CF_3COOH \longrightarrow Hg(OOCCF_3)_2 \xrightarrow{230^oC} CF_3HgOOCCF_3$$

$$PhBr + Na_2Hg \longrightarrow PhHgPh$$

$$PhHgPh + CF_3HgCO_2CF_3 \xrightarrow[\text{reflux}]{PhH} PhHgCF_3$$

Figure 3.9 Making of Seyferth reagent

The synthesis of Seyferth reagent was depicted in Figure 3.9 using literature procedure.[109] One of the starting materials diphenylmercury, was made from bromobenzene and sodium amalgam.[110] The methylation reagent, N, N-

Methylphenylaminotriphenylphosphonium Iodide, was synthesized by following Murahashi's procedure.[111]

A second approach (Figure 3.10) was designed to overcome the difficulty encountered in the first approach by building the carbon skeleton first. This would ensure the success of the last step, radical deoxygenation, but may reduce the efficiency of the enzymatic resolution because the reaction center is one more carbon away from the chiral center. Fortunately, this was demonstrated to be a successful approach.

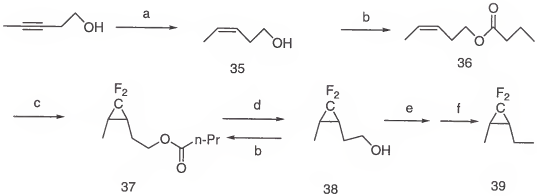

Figure 3.10. Second approach of synthesis of optically active cis-1,1-difluoro-2-ethyl-3-methyl. a. H_2 1 atm, Pd/$CaCO_3$, Pb poisoned, MeOH b. n-PrCOCl, Pyridine c. $PhHgCF_3$, NaI, PhH d. PPL, H_2O, pH=6.5 e. 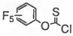, Pyridine f. Bu_3SnH

The same strategy as in the first approach was tried initially here to synthesize the butyrate ester **36.** Typical esterification process produced 3-pentynyl butyrate in excellent yield, and it was hydrogenated under the same conditions as in the synthesis of **32.** However, unlike the earlier reaction, in which the hydrogenation stopped after the total conversion of alkyne to alkene, over-hydrogenated product was obtained. In this case, even though the volume control of hydrogen is an obvious choice, we decided to utilize Lindlar catalyst[112] in order to gain better control over the reaction. As shown in Figure

3.10, the sequence of the synthesis was adjusted to start with hydrogenation of 3-pentyn-1-ol. The hydrogenation reaction produced cis-3-penten-1-ol **35** in 98% yield. The following esterification provided cis-pentenyl butyrate **36** in good yield with no surprises. Using the Seyferth reagent, the ester **36** was then converted to cis-2-(2', 2'-difluoro-3'-methylcyclopropyl) ethyl butyrate **37** in 28% yield.

Two enzymatic hydrolysis kinetic resolutions were carried out at around 3°C using PPL(Lipase type II, crude, from porcine pancreas, Sigma). The pH of the reaction solution was maintained around 6.5 by adding 1.0N NaOH/H_2O solution to neutralize the acid generated in the reaction. The volume of NaOH/H_2O solution consumed indicated the reaction progress. Upon 40% completion, the first enzymatic resolution was quenched and the isolated optically active alcohol **38** was converted back to butyrate ester for further resolution. A d.e. of 13.6%, as determined by ^{19}FNMR analysis of its R-(O)-acetylmandelic acid esters, was achieved from the first resolution. The consecutive second kinetic resolution, quenched upon 30% completion, elevated the d.e. to 28.5%, which we considered to be adequate for our kinetic study of racemization.

Finally, the first required target substrate, optically active cis-1,1-difluoro-2-ethyl-3-methylcyclopropane **39**, was prepared using a two-step-one-pot radical deoxygenation process developed by Barton.[113] The optically active alcohol **38** was first converted to penta-fluoro phenylthioformate in the presence of pyridine and a catalytic amount of N-hydroxy succinimide, and after filtering away the precipitate generated in the reaction, the intermediate product was subsequently reduced under radical condition by Bu_3SnH initiated by AIBN. The product was distilled out of the reaction mixture by a slow N_2 flow, collected in a cool trap and purified by preparative GC. The ^{19}F NMR, ^{1}HNMR, GCMS data all matched those of the non-optically active authentic sample. The d.e. determined by GC with the chiral column was 30.2%, which is very close to the value determined earlier by ^{19}FNMR.

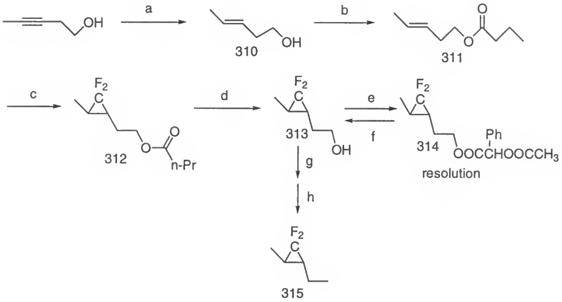

Figure 3.11. Synthesis of optically active trans-1,1-difluoro-2-ethyl-3-methyl. a. Na, NH_3 b. n-PrCOCl, Pyridine c. $PhHgCF_3$, NaI, PhH d. PPL, H_2O, pH=6.5 e. R-(O)-Acetylmandelic acid, DCC. f. NaOH, H_2O g. 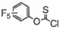, pyridine h. Bu_3SnH, AIBN

With the success attained for the *cis* compound, we applied the same methodologies to synthesize the *trans* compound, hoping that the PPL would resolve the *trans* butyrate ester as well as it did the *cis* compound. The *trans*-3-penten-1-ol **310** was synthesized by reduction of 3-pentyn-1-ol with sodium in liquid ammonium in 87% yield. Esterification of the trans alcohol provided trans-3-pentenyl butyrate **311**, which was then difluorocyclopropanated using the Seyferth reagent to produce trans-2-(2', 2'-difluoro-3'-methylcyclopropyl) ethyl butyrate **312**. Unfortunately the subsequent enzymatic hydrolysis of **312** to trans-alcohol **313**, gave no sign of any resolution.

Disappointed by the enzymatic resolution, we examined the temperature dependence of the diasteromeric resolution of ester **314** on TLC. It was found that, at around -70°C, the two diasteromers of **314** was completely separable on silica gel TLC using 10%ether/hexanes as elute. All trans alcohol **313** was converted to R-(O)-acetylmandelate ester **314**, which was resolved at -70°C on a flash chromatography column. Early fractions with d.e.% of at least 50% of the same diasteromer were combined and then hydrolyzed to give optically active trans alcohol **313**. Radical deoxygenation of the optically active **313** provided the second target product optically active trans-1,1-difluoro-2-ethyl-3-methylcyclopropane. The ^{19}F NMR, ^{1}HNMR, GCMS data all matched those of the non-optically active authentic sample and the d.e. as determined by GC with the chiral column was 66.1%.

Kinetic Studies of Stereomutation

Derivation of Kinetic Equations

The racemization and epimerization reaction diagram of cis and trans 1,1-difluoro2-ethyl-3-methylcyclopropane is shown in Figure 3.12. In the system, four isomers, Ta (trans diasteromer a), Tb, Ca (cis diasteromer a) and Cb can convert to each others through either single rotation ring opening and closure or coupled rotation ring opening and closure with the cleavage of any C-C bond on the ring. Assuming all the reactions are primary, the racemization rate constants for trans compound and cis compounds are k_{tr} and k_{cr}, respectively, which correspond to the coupled rotation with the cleavage of the distal C-C bond to the CF_2 group. The epimerization rate constants for trans and cis compound are $k_{tc}=(k_{tc1} + k_{tc2})$ and $k_{ct}= (k_{ct1} + k_{ct2})$, respectively, which correspond to the sum of three possible processes. (1) The single rotatory ring opening and closure of either radical with the distal C-C bond cleavage to the CF_2 group. (2) The single rotatory ring opening and closure of the CH radicals with the proximal C-C bond cleavages to the CF_2 group. (3) The coupled rotatory ring opening and closure with the proximal C-C bond cleavages to the CF_2 group. Even though the disrotatory ring opening followed by the conrotatory ring closure and *vice versa*, will also result in epimerization product, this process was dismissed because of the conservation of angular momentum required during physical transformation.[100] The kinetic equations are derived below.

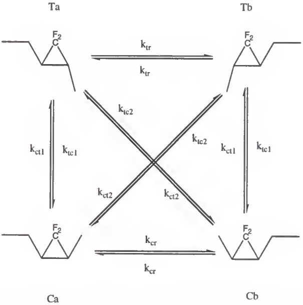

Figure 3.12 Reaction diagram of the pyrolysis of gem-difluorocyclocyclopropane

Racemization

When the kinetic study starts from trans compound,

$$-\frac{d[Ta]}{dt} = k_{tr}[Ta] - k_{tr}[Tb] + k_{tc1}[Ta] - k_{ct1}[Ca] + k_{tc2}[Ta] - k_{ct2}[Cb] \qquad (1)$$

$$-\frac{d[Tb]}{dt} = k_{tr}[Tb] - k_{tr}[Ta] + k_{tc1}[Tb] - k_{ct1}[Cb] + k_{tc2}[Tb] - k_{ct2}[Ca] \qquad (2)$$

(1)-(2)

$$-\frac{d\{[Ta]-[Tb]\}}{dt}=(2k_{tr}+k_{tc1}+k_{tc2})([Ta]-[Tb])-(k_{ct1}+k_{ct2})([Ca]-[Cb]) \qquad (3)$$

(1)+(2)

$$-\frac{d\{[Ta]+[Tb]\}}{dt}=(\mathrm{ktc1}+\mathrm{ktc2})([Ta]+[Tb])-(\mathrm{kct1}+\mathrm{kct2})([Ca]+[Cb]) \qquad (4)$$

Meanwhile

$$\begin{aligned} -\frac{d(d.e.)}{dt} &= \frac{\mathrm{d}\dfrac{[Ta]-[Tb]}{[Ta]+[Tb]}}{\mathrm{dt}} \\ &= -\frac{1}{[Ta]+[Tb]}\cdot\frac{d\{[Ta]-[Tb]\}}{dt}+\frac{[Ta]-[Tb]}{\{[Ta]+[Tb]\}^2}\cdot\frac{d\{[Ta]+[Tb]\}}{dt} \end{aligned} \qquad (5)$$

Substitute (3) and (4) in (5), we will have:

$$-\frac{d(d.e.)}{dt}=\frac{1}{[Ta]+[Tb]}\{(2k_{tr}+k_{tc1}+k_{tc2})([Ta]-[Tb])-(k_{ct1}-k_{ct2})([Ca]-[Cb])\}-$$

$$\frac{[Ta]-[Tb]}{([Ta]+[Tb])^2}\{(k_{tc1}+k_{tc2})([Ta]+[Tb])-(k_{ct1}+k_{ct2})([Ca]+[Cb])\}$$

$$\begin{aligned} &=\frac{2k_{tr}([Ta]^2-[Tb]^2)}{([Ta]+[Tb])^2}+ \\ &\frac{1}{([Ta]+[Tb])^2}\{2k_{ct2}([Ca][Ta]-[Cb][Tb])+2k_{ct1}([Cb][Ta]-[Ca][Tb]\} \end{aligned} \qquad (6)$$

Because $k_{tr} > k_{ct}$, and in the early reaction period, and starting from trans compound,

$$[Ca]\approx 0,[Cb]\approx 0$$

(6) is reduced to:

$$-\frac{d(d.e.)}{dt}=2k_{tr}\frac{[Ta]-[Tb]}{[Ta]+[Tb]}=2k_{tr}(d.e.)$$

After integration, we get the trans compound racemisation equation:

$$\ln(d.e._0/d.e.) = 2k_{tr}\, t \qquad (7)$$

Similarly, for cis compound,

$$\ln(d.e._0/d.e.) = 2k_{cr}\, t \qquad (8)$$

Epimerization is a simple first order reversible system.If we start from cis compound, we will have:

$$\ln[(Xe-X_0)/(Xe-X)] = (k_{tc}+k_{ct})\, t$$

Here $X=[trans]/\{[trans]+[cis]\}$

And when the equilibrium is established between trans and cis compounds:

$$X = Xe = k_{ct}/(k_{tc} + k_{ct})$$

when $t=0$, $X_0=0$:

$$\ln[Xe/(Xe-X)] = (k_{tc}+k_{ct})\, t \qquad (9)$$

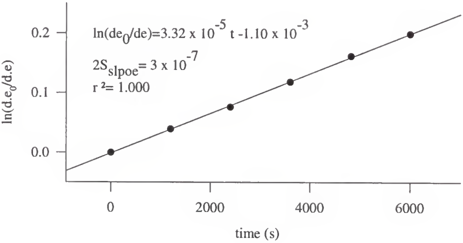

Figure 3.13 Plot of ln(d.e.$_0$/d.e.) *vs.* time of Racemization of trans-1,1-difluoro-2-ethyl-3-methylcyclopropane at 274.5°C.

Kinetics Results

The kinetic studies of optically active cis and trans compounds were carried out in toluene solution, using sealed capillary glass tubes. Analyses were performed by GC on a chiral polysiloxane cyclodextrin capillary column, which gave four well-resolved peaks for diasteromeric mixtures of the cis and trans compounds (see Appendix). Ideally, all four rate constants would be able to be obtained at one temperature for direct comparison. However, a preliminary study indicated that the epimerizations of both the cis and trans compounds are so slow compared to the fast racemization of cis compound that there is no such temperature at which all the rates fall within a the comfortable range for kinetic study. At 274.5 °C, both the racemization and the epimerization of the trans compound were measured (Figure 3.13 and 3.14), and the rate of the fast racemization of the cis compound at this temperature was calculated from activation parameters (Figure 3.15) obtained in a lower temperature range study (201.1~240.7 °C). Least squares method was

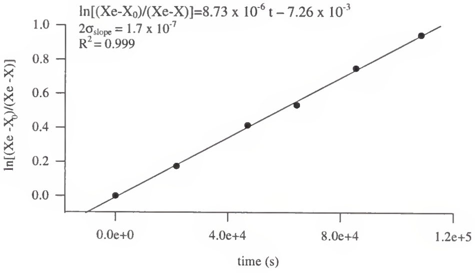

Figure 3.14 Plot of $\ln[(Xe-X_0)/(Xe-X_0)]$ *vs.* time of epimerization at 274.5°C

employed for those kinetic plots, and the excellent correlation and good mass balance (92%) that was found at 274.5 °C after 62 hours using n-hexane as internal standard indicated that the reactions were well-behaved first order reactions.

According to equation (7), with a slope of $(3.32 \pm 0.03) \times 10^{-5}$ (Figure 3.13.), the rate constant of racemization for trans compound k_{tr} is $(1.66 \pm 0.02) \times 10^{-5}\ s^{-1}$. Racemic cis-samples were used for the epimerization study since this procedure yields greater precision than does the determination of $(k_{tc}+k_{ct})$ starting with trans compound. The equilibrium constant for the epimerization was obtained after heating the sample at 298.1°C for 48 hours, and then at 274.5 °C for 48 hours (K_{eq} = [trans]/[cis] = 2.43), 60 hours (Keq=2.44). In conjunction with the slope of the plot in Figure 3.14 and equation (9), the rate constants of epimerization for cis (k_{ct}) and trans (k_{tc}) compounds are $(6.20 \pm 0.12) \times 10^{-6}\ s^{-1}$ and $(2.53 \pm 0.05) \times 10^{-6}\ s^{-1}$, respectively.

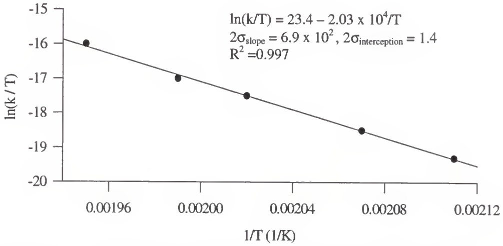

Figure 3.15 Eyring plot ln(k/T) vs. 1/T of cis compound racemization

An Arrhenius plot ($R^2 = 0.988$) of the cis compound racemization data provided the following activation parameters: log A =13.3 ± 0.9 and E_a= 41.3 ± 2.0 kcal/mol. However, it was the Eyring plot that was used to extrapolate the rate constant at 274.5 °C, k_{cr} = 6.35 x 10^{-4} s^{-1} because of its better correlation. The Eyring plot also provided activation activation enthalpy $\Delta H^{\neq}$= 40.4 ± 1.4 kcal/mol, which give Ea= 41.5 ± 1.4 kcal/mol at 274.5 °C.

Table 3.1. Rate constant ($x10^5$) (s^{-1}) for racemization and epimerization of cis- and trans-1,1-difluoro-2-ethyl-3-methylcyclopropane at 274.5 °C.

	Racemization (k_{cr})	Epimerization
Cis compound	63.5	0.620
Trans compound	1.66	0.253

Discussions

Solvent Effect in the Kinetic Study

When doing kinetic studies in solution, the solvent effect is always a concern, especially when the experimental result is subject to comparison with a gas phase theoretical prediction. In order to estimate the effect exerted by toluene solvent on this kinetic system, we carried out a preliminary study in toluene to measure the rate of epimerization starting from the cis compound and compared to that of 1,1-difluoro-2,3-dimethylcyclopropane in gas phase.[47]

At 298.1 °C, in toluene solution, the total epimerization rate constant (k_{tc} + k_{ct}) is (5.32±0.08) $x10^{-5}$ s^{-1}, with equilibrium constant $K_{eq}=k_{ct}/k_{tc}=2.50$, give k_{tc}=(1.52±0.02) $x10^{-5}$ s^{-1} and k_{ct}=(3.80±0.06) $x10^{-5}$ s^{-1}. At this temperature, in gas phase, the epimerization of 1,1-difluoro-2,3-dimethylcyclopropane (Figure 3.16) is extrapolated (k_{tc} + k_{ct}) = 4.89 x

10^{-5} s^{-1} ,K_{eq}=1.92.[47] Within experimental error, the almost identical k_{tc} (1.67 x$10^{-5}s^{-1}$) and the slightly slower k_{ct} (3.22 x $10^{-5}s^{-1}$) of 1,1-difluoro-2,3-dimethylcyclopropane compare to that of 1,1-difluoro-2-ethyl-3-methylcyclopropane are consistent with the facts that the steric interaction of cis-methyl-methyl is weaker than that of cis methyl-ethyl interaction on cyclopropane ring, whereas, such differentiation vanishes in trans compounds. More importantly, this result suggested that toluene solvent effect on the kinetics of cyclopropane stereomutation could be ignored.

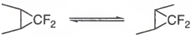

Figure 3.16 The gas phase kinetics of the epimerizations of gem-difluorocyclopropanes was investigated by Dolbier

Preference for Disrotation over Conrotation

The kinetic analysis indicates a lower transition state energy for *cis* racemization than for *trans* racemization, which is depicted schematically in Figure 3.17. At 274.5 °C, the racemization of cis-1,1-difluoro-2-ethyl-3-methylcyclopropane is k_{cr}/k_{tr} = 38.2 times faster than that of the trans compound which corresponds to a $\Delta\Delta G^{\neq}$= 4.0 kcal/mol. In comparison the free energy difference between ground state cis and trans compound $\Delta G°_{t\text{-}c}$ can be calculated form the K_{eq} (0.41) to be –1.0 kcal/mol. Thus, after the ground state energy correction, the difference between the free energies of cis and trans racemization transition state is 3.0 kcal/mol.

The experimental result strongly indicates that the racemization of *cis* and *trans* compounds pass through two different transition states. Utilizing the analysis depicted in Figure 3.7., we can rationalize that a coupled rotation, either conrotation or disrotation, is preferred, because if different compounds had different coupled rotation nature, the same transition state would be passed through in both processes, which conflicts with the experimental result.

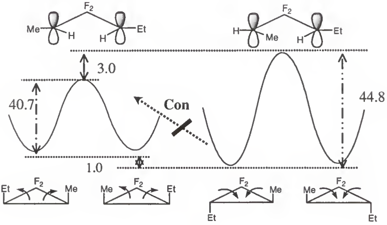

Figure 3.17 Free energy (kcal/mol) diagram of 1,1-difluoro-2-ethyl-3-methylcyclopropane coupled rotation

However, solely on the basis of the experimental data, we can not distinguish which of the two coupled rotation is preferred, unless we assume that the *s-trans, s-cis* transition state is less stable than s-trans, s-trans transition state. This is consistent with our chemical intuition that an *s-trans, s-cis* transition state is sterochemically more "crowded" than an *s-trans, s-trans* transition state, as supported by *ab initio* calculation.[102,103] Under this assumption, it is reasoned that the disrotation is preferred to conrotation in the racemization processes of both the *cis* and the *trans* compounds. The observed 3.0 kcal/mol free energy gap is similar to the energy difference between the *s-trans, s-trans* and *s-cis, s-trans* transition states (Figure 3.6) based on the results of *ab initio* calculations.[102]

In hydrocarbon system,[114] the racemization of cis-1-ethyl-2-methyl-cyclopropanes between 337.2~438.7 °C provided activation parameters of logA=16.4, E_a= 63.8 kcal/mol. The rate constant at 274.5 °C can be calculated from this data to be k_{cr}= 9.3 x $10^{-10}s^{-1}$. This amounts to a $\Delta\Delta G^{\neq}$=14.6 kcal/mol, with the *cis* fluorinated system racemizing 6.82 x 10^5 times faster than its hydrocarbon counter part system. For the *trans* system, the activation parameters of the hydrocarbon: logA=14.9, E_a= 60.4 kcal/mol give a racemization constant k_{tr}= 6.0 x $10^{-10}s^{-1}$, which is 2.8 x10^4 slower than its fluorinated analogue corresponding to a $\Delta\Delta G^{\neq}$= 11.1 kcal/mol.

This 3.5 kcal/mol difference in free energy of racemization between *cis* and *trans* compounds difference due to fluorine substituents is very close to the free energy difference of *s-trans, s-trans and s-trans, s-cis* transition states in the fluorinated system (3.0 kcal/mol), thus revealing the distinct coupled rotation profile in both system. For the hydrocarbon system, at 404.3 °C, the cis compound racemizes only 2.64 times faster than trans compound, which amounts to a $\Delta\Delta G^{\neq}$= 1.3 kcal. The difference of activation free energies is offset by the ground state effect. Given K_{eq}= 2.83, the free energy difference of the two transition states is only 0.1 kcal/mol. Within experimental error, the two transition states are considered to be the same.

Adopting the rational used in fluorinated system, we can see that unlike its fluorinated analogue, 1-ethyl-2-methyl-cyclopropane does not have the observable preference between coupled disrotation and conrotation. In all likelihood, the *cis* compound racemizes by disrotatory ring opening, whereas the *trans* compound racemizes by conrotatory ring opening.

It is worth mentioning that the 14.6 kcal/mol fluorine substitution effect in free energy at 274.5 °C is obtained the by the direct comparison of the same single chemical process--coupled disrotatory ring opening with the cleavage of the distal C-C bonds on the cyclopropane ring to CF_2 (CH_2) group. This result is consistent with general expectation of the increase in strain for two fluorine substituents and is very close to the recent experimental data obtained by using Rüchardt group equivalent values in combination with Roth's heats of hydrogenation.[40,41]

Preference for Coupled Disrotation over Single Rotation

At 274.5 °C, the epimerization, which is the sum of all the processes that result in net single rotation, is k_{cr}/k_{ct} = 102 times slower than the racemization for cis compound. Meanwhile for trans compound, the ratio of rate constant is k_{tr}/k_{tc} = 6.6. Considering the statistic factor that "degenerated" monorotation of either radical CH group is as probable as coupled rotation, the coupled rotation is *at least* 204 and 13.2 time faster than single rotation for cis and trans compound respectively.

If we presume that, among epimerization processes, single rotation with distal C-C cleavage prevails, the difference of activation free energy between racemization and epimerization for the *cis* compound, which refers to the free energy difference between *s-trans, s-trans* (0,0)and (0,90) transition states is calculated to be 5.8 kcal/mol. For the *trans* compound, the 2.8 kcal/mol difference represents the free energy difference between the *s-trans, s-cis* (0,0) and the (0,90) transition states. This is consistent with the calculated result at the CASPT2 level when the effects of dynamic electron correlation are included (Figure 3.18).[115]

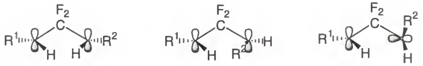

	s-trans, s-trans (0,0)	s-trans, s-cis (0,0)	(0,90)
Experiment	0	3.0	5.8
Calculation	0	4.4	6.6

Figure 3.18 Experimental and calculated relative energies (kcal/mol) of three conformations of substituted trimethylene. In experiment, (R^1,R^2)=(Et,Me), in calculation $R^1=R^2$=Me.

The strong preference for the coupled rotation over the sum of the all epimerization processes, including any motions with the cleavage of the proximal C-C bond to CF_2 group, in 1,1-difluoro-2-ethyl-3-methylcyclopropane, which was not observed in 2-ethyl-3-methylcycloporpane, *unambiguously* disclose the significant preference for C-C bond cleavage distal to CF_2 group on the ring, and thus, provide strong evidence for Dolbier's early claim that the distal C-C bond is preferred to cleave.[46]

Why Do Gem-difluorocyclopropanes Prefer Disrotation?

The preference for disrotatory, rather than conrotatory, opening and closure of gem-difluorocyclopropane which is different from that of cyclopropane can be traced to the wavefunction for the (0,0) geometry of 2,2-difluorotrimethylene, but there is a simple, useful physical interpretation.[102] In (0,0) the trimethylene part of the hyperconjugative stabilization that is provided by the σ and σ^* orbitals of the C-H bonds at the central carbon involves some net election donation form the central CH_2 to the terminal methylene groups. In contrast, at the same geometry of 2,2-difluorotrimethylene the low-lying C-F antibonding orbitals cause the CF_2 group to act as a net π-electron acceptor.

This difference between the central CH_2 group in trimethylene and the CF_2 group in 2,2-diflorotrimethylene can be represented in terms of the resonance structure in Figure 3. 19.

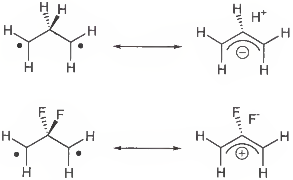

Figure 3.19 Contributing resonance structures for trimethylene and 2,2-difluoromethylene

To the extent that each of the hyperconjugated, ionic structure contributes, the electronic structure of trimethylene should resemble that of the allyl anion and 2,2-difluoromethylene should, resemble the allyl cation. Orbital symmetry causes the allyl anion to prefer conrotatory closure and the allyl cation to favor closure by a disrotatory pathway (Figure 3.20).[116]

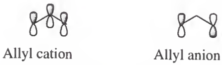

Allyl cation

Allyl anion

Figure 3.20 Homo of allyl cation and allyl anion

Conclusion

1,1-difluoro2-ethyl-3-methylcyclopropane is the first cyclopropane for which a very large preference for coupled rotation has been found. The mode of the coupled rotation has been identified as disrotation. The experimental results amply confirm the theoretical predications that disrotation is strongly favored over both conrotation and monorotation in the stereomutation of 1,1-difluorocyclopropane and that this preference survives the presence of alkyl groups at C2 and C3.

Such strong preference for coupled rotation over the sum of the other entire modes in cyclopropane stereomutation provided unambiguous evidence for the favored distal C-C bond cleavage to the CF_2 group in gem-difluorocyclopropanes.

CHAPTER 4
COMPUTATIONAL STUDIES OF FLUORINE SUBSTITUTION EFFECTS ON THE KINETICS OF CYCLOPROPYLCARBINYL AND OXRINYLCARBINYL RADICAL RING OPENING

Part 1. Simple Cyclopropylcarbinyl Radical Ring Opening

Introduction

Knowledge of the kinetics of radical reactions is of critical importance with respect to the design of synthetic and physical organic experiments that utilize such processes.[117] A radical reaction that has attracted particular interest over the years is the cyclopropylcarbinyl – allylcarbinyl rearrangement (Figure 4.1), which, because of its speed, has found considerable use as a mechanistic probe of radical intermediacy as well as a clock for competitive, very fast radical reactions.[118] A number of cyclopropylcarbinyl radical clocks have been calibrated generally by kinetic studies utilizing a competitive, very fast bimolecular hydrogen transfer process from benzeneselenol, but also by direct measurement using a "reporter group" approach.[119,120]

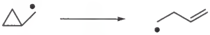

2

Figure 4.1 Cyclopropanylcarbinyl radical ring opening rearrangement

In particular, Newcomb's kinetic studies of the effect of alkyl, aryl, and alkoxy substituents appear to indicate that in these systems thermochemical, that is radical stabilizing, influences prevail in determining the rates of cyclopropylcarbinyl ring opening processes.[121-123] Polar influences appear to be relatively unimportant in such cases.

Newcomb's experimental results and the above conclusions have been corroborated very nicely by recent ab initio molecular orbital calculations. In their computational work, Martinez, Schlegel and Newcomb found good agreement between experiment and theory at the PMP2/6-31G(d) level.[124,125]

In this chapter, we wish to report at this time our own calculations, carried out at the B3LYP level of theory, which provide insight into the remarkable effect of fluorine substituents on the barrier height of cyclopropylcarbinyl radical ring openings. Preliminary experimental studies have indicated an extraordinarily fast ring opening for the 2,2-difluorocyclopropylcarbinyl radical, **2**, which has yet to be trapped bimolecularly (see Chapter 5).[49,126,127] Very fast radical rearrangements are required to act as probes and radical clocks in studies of mechanisms of reactions, including those catalyzed by enzymes, which are believed to involve radical intermediates.

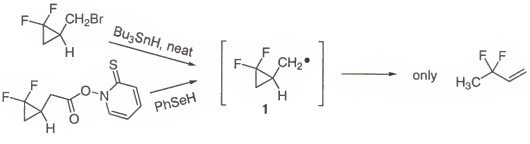

Figure 4.2 Earlier experimental studies of measuring the rate of ring opening of radical **1**

The effect of geminal fluorine substituents on cyclopropane structure, bonding and reactivity has been explored both experimentally and theoretically.[46,51,102,128,129] Our intent in carrying out the present calculations was to determine (a) whether such demonstrated thermochemical influences are the source of the reactivity of 2,2-difluorocyclopropylcarbinyl radical, (b) whether polar influences play a role, and (c) what the individual and collective effects of fluorine substitution at the various positions of the cyclopropylcarbinyl radical will be on the barrier height for its rearrangement.

Results and Discussion

Computational methods

Density Functional Theory calculations were performed using the Gaussian 94[130] and Gaussian 98[131] program package. Radical reactants, products and transition structures were optimized at unrestricted Hartree-Fock (UHF),[132] and then unrestricted Becke-style 3-Parameter (UB3LYP)[133] Density Functional Theory (DFT) level of theory using the 6-31G(d)[134] basis set. At the same level of theory, vibrational frequencies were calculated respectively to identify transition states and ground states, and zero-point energies (ZPE) were obtained. Single point energy calculations were performed at the B3LYP level of theory using the 6-311+G(2df,2p)[135] basis set (UB3LYP/6-311+G(2df,2p)//UB3LYP/6-31G(d)). Some calculation methods not mentioned here will be pointed out specifically. This methodology will be utilized in all the three parts of the computational studies in this chapter.

The reported values here as depicted in Figure 4.3, E_0 refers to the activation barriers, which is the difference between the zero point corrected electronic energies of transition state and reactant. The reaction energy (E_{rxn}) refers to the zero point corrected electronic energy difference between product and reactant. $\Delta^{\neq}H^{o}$, the standard enthalpy of activation, is obtained after the thermal correction of E_0 to 298.15 °C, 1 atm. The Arrhenius activation energy E_a can be obtained by $E_a=RT+\Delta^{\neq}H^{o}$. The heat of reaction ($\Delta H^{o}$) refers to the difference of enthalpies between the reactant and product of a reaction at 298.15 °C, 1 atm, which is obtained after the thermal correction of E_{rxn}.

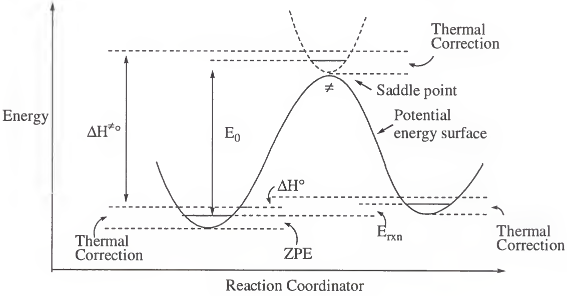

Figure 4.3 Energy diagram

Preliminary evaluation of methodology

Schlegel and Newcomb sought to establish an adequate level of *ab initio* theory to estimate the activation barriers for ring opening reactions of cyclopropylcarbinyl radicals.[124,125] In the present study, we have repeated part of their work, performing UHF/6-31G(d) and second-order Møller-Plesset perturbation (UMP2/6-31G(d)//UHF/6-31G(d)) with spin projection[136,137] (PMP2/6-31G(d)//UHF/6-31G(d)) calculations on the parent cyclopropyl-carbinyl radical **2** ring opening reaction. As a comparison, DFT calculations (UB3LYP/6-31G(d)//UHF/6-31G(d)) were added to the list. The same calculations were performed for the 2, 2-difluorocyclopropylcarbinyl radical **1** ring opening reaction, with the reaction barriers for both the parent and the fluorinated system being given in Table 4.1, and the computed heats of reaction in Table 4.2.

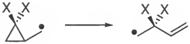

Table 4.1 Calculated Barriers (E_0) and Standard Enthalpies of Activation ($\Delta^{\neq}H^o$) for the Ring opening of the Parent Cyclopropyl-carbinyl Radical and for the 2, 2-Difluorocyclopropylcarbinyl Radical.[a]

Radicals	X	UHF		UMP2		PMP2		B3LYP		Exptl
		E_0	$\Delta^{\neq}H^o$	E_0	$\Delta^{\neq}H^o$	E_0	$\Delta^{\neq}H^o$	E_0	$\Delta^{\neq}H^o$	E_a
2	H	10.5	10.2	15.3	15.0	8.1	7.8	6.7	6.4	7.0[b]
1	F	5.2	4.9	9.1	8.8	2.9	2.6	2.2	1.8	
Differences		5.3	5.3	6.2	6.2	5.2	5.2	4.5	4.6	

[a] In kcal/mol, Using the geometry optimized at the UHF/6-31G(d) level with ZPE calculated at UHF/6-31G(d) and scaled by factor 0. 8929; [b] References 26 and 27. $\Delta^{\neq}H^o =$ 6.4 kcal/mol

Table 4.2 Calculated Heats of Reaction (ΔH^o) of the Ring opening of the Parent Cyclopropylcarbinyl Radical and for the 2, 2-Difluorocyclopropyl-carbinyl Radical.[a]

Radical	X	UHF	UMP2	PMP2	UB3LYP	Exptl
2	H	-5.2	-0.9	-0.0	-2.8	-5.4[b]
1	F	-12.8	-5.1	-7.9	-9.1	
Difference		7.6	4.1	7.9	6.3	

[a] In kcal/mol, Using the geometry optimized at the UHF/6-31G(d) level with ZPE calculated at UHF/6-31G(d) and scaled by factor 0. 8929; [b] Reference 124.

Our computed barriers (E_0) for the parent system are very similar to Schlegel, Newcomb and Radom's.[124,125,138] Although the barriers calculated at different levels can be seen to vary by as much as 10 kcal/mol, the barrier *differences* between reaction 1 and reaction 2 only vary over a range of about 2 kcal/mol. A similar situation is seen for the computed heats of reaction. Such results indicate that the calculated results at different levels of theory are self-consistent.

Comparing with Martinez, Schlegel and Newcomb's work,[124,125] a slightly more stable geometry of cyclopropylcarbinyl radical was obtained at UHF/6-31G(d) level of theory. At the same level of theory, same geometry of transition state and ring-opening product were obtained, but the single point energies of product at both MP2/6-31gG(d) and PMP2/6-31G(d) levels of theory are different from the data in that paper. Our data is more consistent with the data in Radom's work.[138]

In that paper, Radom reported that B3LYP provides a reliable level of theory for examining cyclopropylcarbinyl radical system.[138] Among the levels of theory utilized here, UB3LYP gave the best results.[139] From its $\Delta^{\neq}H^{o}$ of 6.4 kcal/mol, the Ea can be extrapolated to be 7.0 kcal/mol which is the same as the experimental results.[124,140]

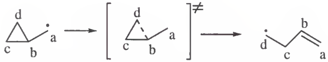

Table 4.3 Calculated reaction heats, barriers for ring opening of fluorinated cyclopropylcarbinyl radicals.[a]

Radical	Position of CF_2	E_0	$\Delta^{\neq}H^{o}$	E_{rxn}	ΔH^{o}
1	c	1.9	1.6	-10.4	-10.1
3	c and d	3.8	3.2	-18.4	-18.5
5	a and c	4.9	5.0	-9.2	-8.6
2	None	6.5	6.2	-4.5	-4.1
4	a; b; c; d	6.5	6.6	-19.3	-19.1
1	d	9.0	8.7	-9.8	-9.7
6	a	10.2	10.3	-2.6	-1.9
5	a and d	10.5	10.6	-11.2	-10.9

[a] calculated at UB3LYP/6-311+G(2df,2p)//UB3LYP/6-31G(d) level of theory with ZPE calculated at UB3LP/6-31G(d) and scaled by factor 0.9804. In kcal/mol.

System calculations

The barriers and heats of reaction for the ring opening of the cyclopropylcarbinyl radical with a CF_2 group at all possible positions and with all possible combinations have been computed (Table 4.3). With the labeling of the carbon skeletons of the computed molecules given below, the positions of fluorine substitution are indicated in the Table. For example, radical **4** is the perfluorocyclopropylcarbinyl radical. The geometry of some reactant radicals and ring opening transition state of **1** are depicted in Figure 4.4.

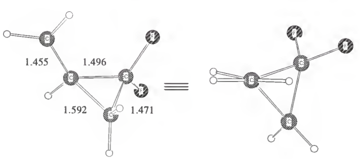

1

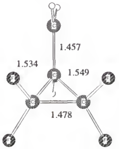

3

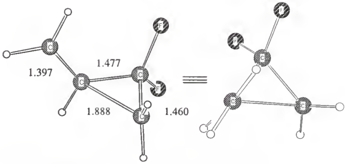

Ring opening transition state structure of **1**

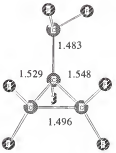

4

Figure 4.4 B3LYP/6-31G(d) optimized structures of radical **1**, **3**, **4** and ring opening transition state of **1**. C-C bond lengths are in Å.

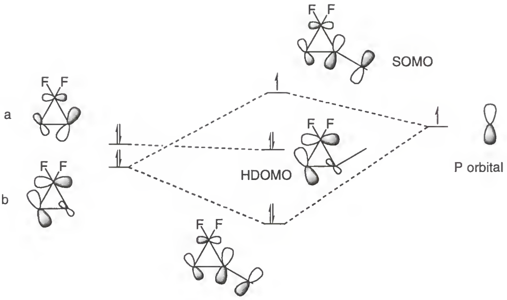

Figure 4.5 Diagram of orbital interaction

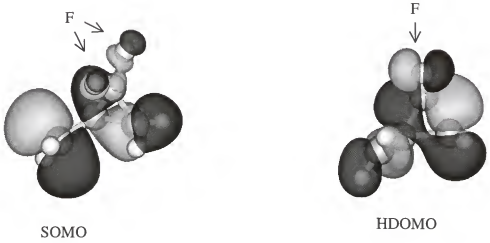

SOMO HDOMO

Figure 4.6 The calculated (UHF/6-31G(d)) SOMO and HDOMO of radical **1.**

Figure 4.4 shows the lowest energy conformations of radical **1,3,4** and the ring opening transition state of radical **1** distal to the CF_2 group on the ring. All those radicals are in "bisected" conformation, which means a bond on the radical center is dividing the adjacent ring. This conformation allows the best orbital interaction between the radical and the Walsh orbital of the cyclopropane ring, which is depicted in Figure 4.5. The calculated SOMO (Single Double occupied Molecular Orbital) and HDOMO (Highest Double Occupied Molecular Orbital) at UHF/6-31G(d) level of theory is depicted in Figure 4.6.

The interaction between the carbinyl radical and the Walsh orbital b will depopulate electron of orbital b. And as a result, the C1-C2 and C2-C3 bonds, which have bonding character, will lengthen. One the other hand, the C1-C3 bond, which has anti-bonding character, will shorten. This rational is consistent with the structural difference between gem-1,1-difluoro-2-methylcyclopropane and the gem-difluorocyclopropyl carbinyl radical (Figure4.7).

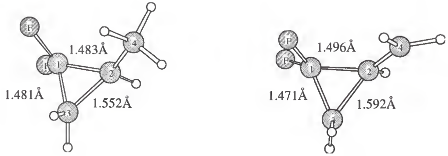

Figure 4.7 Calculated structure of between gem-1,1-difluoro-2-methylcyclopropane and radical **1**. (B3LYP/6-31G(d))

The radical centers of **1** and **3** are planar. Radical **4** gives a pyramidal radical center. The *geminal* fluorine substitutes on the ring are intended to shorten the proximal C-C bonds and lengthen the distal C-C bonds. Our calculation predicts a length for the breaking C-C (distal to CF_2 group) bond of 1.888 Å for radical **1** in its ring opening transition state structure, which indicates an early transition state.

The calculated activation barriers for rearrangements of radicals **1-6** are most definitely an interesting challenge to understand. They can be seen to vary widely, from a value of 1.9 kcal/mol for distal bond cleavage of **1** to a value of 10.5 kcal/mol for proximate bond cleavage of radical **5**, with there being absolutely *no* obvious correlation between such values and their respective heats of reaction!

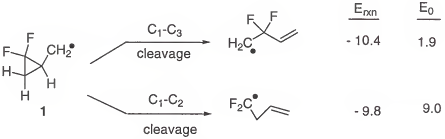

Figure 4.8 The lack of correlation between activation barriers and the reaction energies

In an result that is certainly related, when the cyclopropane ring bears but one CF_2 group, as in the case of radical **1**, the ring opening of the cyclopropylcarbinyl radical can take place with *two* possible regiochemistries, cleaving either the distal, C_1-C_3 bond, or the proximal, C_1-C_2 bond. Considering the fact that the reaction energies for these two competitive processes differ, for **1**, by < 1 kcal/mol, the huge difference in activation barrier for the two processes of radical **1** (7.1 kcal/mol) is quite remarkable (Figure 4.8).

The substantially lower predicted activation barriers for distal C-C bond cleavages in radicals **1**, **3** and **5**, and the regioselectivities exhibited by radicals **1** and **5** are consistent with an abundance of experimental results that indicate a kinetic preference for homolytic cleavage of the cyclopropane bond that is distal to the *geminal* fluorine substituents. These phenomena are also consistent with Hoffmann's original hypothesis that fluorine substituents on cyclopropane would weaken the distal C-C bond,[129] results which have been corroborated by Borden's *ab initio* calculations indicating a 3.9 kcal/mol difference in energy between the most stable geometries of the 2,2-difluoro- and 1,1-difluorotrimethylene diradicals which would be obtained by C_2-C_3 and C_1-C_2 bond homolysis, respectively, of 1,1-difluorocyclopropane.[101] Fluorine substitution has long been recognized to stabilize saturated hydrocarbon structures, because of the impact of fluorine's electronegativity on C-C and C-H bonding.[101,141,142] The overall thermodynamic influence of a CF_2 group is greater when it is bound to two carbons, rather than one carbon and a hydrogen. This effect is reflected by the 3.9 kcal/mol greater heat of hydrogenation of 1,1-difluorocyclopropane to 2,2-difluoropropane than to 1,1-difluoropropane (calculated using Rüchardt's group equivalent values).[41]

The fact remains that there is little underlying thermodynamic driving force that can be used to rationalize the above kinetic predictions.

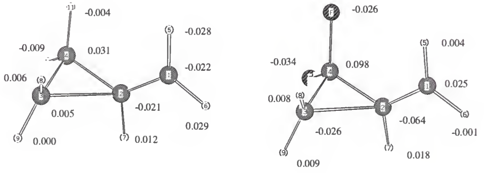

TS of 2

TS of 1

Figure 4.9 Charge developed in the ring opening transition state of radical **1** and **2** relative to their radical reactants (CHelpG scheme). C2-C3 bond is breaking.

Rates of radical processes are recognized to be influenced by four factors: thermodynamics, steric effects, polar effects, and stereoelectronic effects.[143,144] With thermodynamics and steric effects not playing a role in this series of reactions, it is tempting to try to invoke "polar" effects as the determining factor, since they've been suggested in the past as being important in cyclopropylcarbinyl rearrangements.[145] It's been suggested that the major orbital interaction in the transition state for the hydrocarbon cyclopropylcarbinyl radical rearrangement involves that between the semi-occupied orbital (at the slightly nucleophilic $CH_2\bullet$ site) and the vacant σ^* orbital of the cyclopropane C-C bond undergoing cleavage.[145] Thus, it is proposed that a fractional positive charge would be generated at the initial radical center along with a fractional negative charge at the incipient radical center, to give the transition state dipolar character.

However in our charge distribution calculations employing CHelpG scheme (Figure 4.9),[146] at the ring opening transition state of radical **2**, a partial negative charge (-0.022) is generated at the initial radical center, and a small fraction of positive charge is generated at the incipient radical center, which gave an opposite "electron flow" direction to the proposed "polar" effect.[147] In the case of radical **1**, a normal "polar" effect seems to have been observed. In both cases, relatively larger fractions of negative charge are generated at C2s, and relatively larger fractions of positive charge are generated at C4s, which were ignored by proponents of the proposed "polar" effect. Therefore, a more detailed study is needed to evaluate the importance of "polar" effects.

Further calculations indicate that when one adds a methyl substituent to the carbinyl position, as in radical **7** (Figure 4.10), the activation barrier will decrease to 1.6

kcal/mol, a result that is consistent with the carbinyl radical site of **7** being more nucleophilic than that of **1**, and also consistent with the charge distribution calculation of **1**.

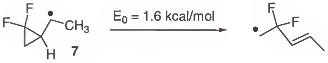

Figure 4.10 The methyl substituents at the radical lower the activation barrier.

Nevertheless, although such effects may play some role for radicals such as **1** and **7**, we believe that it is unlikely that polar factors are the main reason for the broad range of activation barriers found in the overall series. For example, the disparate computed barriers for the three radicals bearing fluorine substituents (i.e., **4**, **5**, and **6**) at the carbinyl position are difficult to rationalize only in terms of polar effects (Figure 4.11).

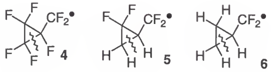

	4	5	6	
activation barriers	6.5	4.9	10.2	(kcal/mol)
reaction energies	-19.3	-9.2	-2.6	

Figure 4.11 Using polar effects can not explain the disparate activation barriers.

From the orbital perturbation point of view, at this stage, it can be rationalized that the differences in activation barriers for radicals **1-7** can be best understood in terms of stereoelectronic effects, that is the *effectiveness of transition state overlap* between the carbinyl radical SOMO and the appropriate cyclopropane σ^* orbital.

Table 4.5 Bond lengths versus activation barriers for radicals **1-6**

Radical	1	2	3	1	6	4	5
C_1-C_3	-	1.533	1.549	1.592	1.529	1.547	1.571
C_2-C_3	1.496	-	-	-	-	-	-
barrier	9.0	6.5	3.8	1.9	10.2	6.5	4.9

It can be seen in Table 4.5 that, if one looks separately at those radical systems that have a *CH_2* carbinyl group (i.e., **1**, **2**, and **3**) and those that have a *CF_2* carbinyl group (i.e., **4**, **5** and **6**), for each group there is an excellent correlation between the activation barriers and the ground state bond lengths of the σ bonds which are being cleaved. What this means is that, all other things being equal, longer, weaker cyclopropane bonds will have lower σ* orbital energies, which should lead to more effective interaction/overlap with their respective carbinyl SOMO's.

The disparity between the CH_2 and the CF_2 carbinyl systems can be simply attributed to the fact that whereas RCH_2• radicals are planar, π-radicals, RCF_2• radicals are pyramidal, σ-radicals,[148] which, in transforming to product, must become planar. The relative cost for conversion of a CF_2 carbinyl site versus a CH_2 carbinyl site to an olefinic site is demonstrated via the enthalpy computation of the hypothetical process depicted in the equation below. This computed 3.3 kcal/mol reaction energy is consistent with the observed incremental differences in activation barrier for otherwise analogous systems **6** vs. **2** (3.7 kcal/mol) and **5** vs. **1** (3.0 kcal/mol) (Figure 4.12).[66]

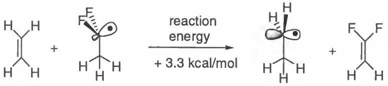

Figure 4.12 The hypothetic reaction used to calculated the difference of fluorine substituent effect on alkenes and radicals

Thus, we would conclude that stereoelectronic factors probably contribute most to the activation barrier differences computed for radicals **1-6**.

In the only kinetic study, which allows a direct comparison of distal versus proximal C-C bond cleavage, Roth found a difference of 3.6 kcal/mol for the two competitive vinylcyclopropane rearrangements of 2,2-difluorovinylcyclopropane (**8**) depicted below (Figure 4.13).[40] The smaller difference observed by Roth for distal versus proximal cleavage of **8** than that predicted for cyclopropylcarbinyl cleavage (7.1 kcal/mol) can be understood simply by the fact that the cleavage process of **1** *is exothermic*, whereas the homolysis process of **8** is highly *endothermic*. Thus it is reasonable that stereoelectronics should play a much larger role in the early transition state of **1**, whereas thermodynamics should play a more important role in the late transition state of **8**.

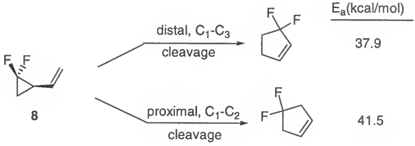

Figure 4.13 The distal cleavage is preferred in the 2,2-difluorovinylcyclopropane thermal rearrangement

A single fluorine substituent on the cyclopropane ring appears to have about half the effect of *gem*-fluorine substituents with respect to cleavage of the distal, C_1-C_3 bond. Thus, the activation barrier of such ring opening of the *cis*-2-fluorocyclopropylcarbinyl radical (**9**) is 4.4 kcal/mol, which is 2.1 kcal/mol lower than that of the hydrocarbon system (**2**) and 2.5 kcal/mol higher than that of the gem-difluoro system (**1**) (Figure 4.14). Likewise, the heat of reaction for distal cleavage of **9** (7.6 kcal/mol) is 3.1 kcal/mol greater than that of **2** and 2.8 kcal/mol less than that of **1**. Values for the *trans*-isomer are very similar: barriers, 4.2 kcal/mol (distal) and 6.8 kcal/mol (proximal); heat of reaction, -6.7 kcal/mol for both.

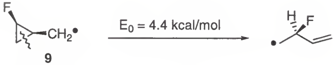

Figure 4.14 The effect of mono-fluorosubstituent on the cyclopropane ring is about the half the effect of gem-difluorosubstituents

The activation barrier for proximal, C_1-C_2 cleavage of **9** was calculated to be 6.7 kcal/mol, which is very close to the value for the hydrocarbon (**2**). This is consistent with the fact that, unlike the situation for multiple fluorine substitution, a single fluorine substituent is known to stabilize a radical.[148-151]

The regiochemical preference for distal cleavage of **9** can again be rationalized on the basis of stereoelectronics, which are reflected by bond length differences. For **9**, the distal C-C bond length is 1.558 Å, and the proximal C-C bond length is 1.514Å.

Interestingly, in the only kinetic study which will allow such a comparison, the $\Delta H^{\ddagger}$ for the thermal homo-1,5-hydrogen shift rearrangement of *cis,cis*-2-fluoro-3-methylvinylcyclopropane (**10**) was also approximately half way between those of the *gem*-difluoro and hydrocarbon analogues (Figure 4.15).[152-154]

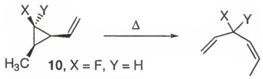

10, X = F, Y = H

X = Y = F, $\Delta H^{\ddagger}$ = 22.7 kcal/mol[46]
10, X = F, Y = H, $\Delta H^{\ddagger}$ = 26.7[44]
X = Y = H, $\Delta H^{\ddagger}$ = 29.9[45]

Figure 4.15 The fluorine substitution effects on the thermal rearrangement of vinylcyclopropane

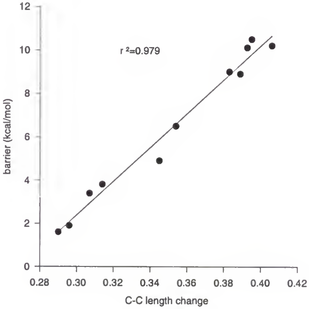

Figure 4.16 Plot of reaction barriers (kcal/mol) vs. C-C bond length changes (Å) between ground state and transition. Include all the reactions with CF$_2$ groups studied in the present work.

Furthermore, even though the lack of correlation between activation barrier and reaction energy (Figure 4.16) is inconsistent with the Hammond postulate, the correlation between the reaction barrier and the differences of the breaking C-C bond length between the starting radical and transition structure is consistent with the general structure and energy relationship, which states that for two molecules the more similar the structure the closer the energy.[155] This unique situation is attributed to the very early transition state of the radical rearrangement and the fact that the release of the ring strain is associated with the substantial rearrangement of the cyclopropane skeleton.

When a radical stabilizing substituent, such as phenyl group that can stabilize radical without obvious skeleton distortion, is introduced into radical **1**, the thermal chemistry which is similar to the hydrocarbon system, exerts substantial impact no the activation barrier. With a phenyl group on the starting radical carbon, the heats of reaction of the radical ring openings of **11** which are diminished by the stabilizing energy of the phenyl group, are reduced to -1.2 kcal/mol and -0.1 kcal/mol and the activation barriers for the cleavages of proximal and distal C-C bonds are increased to 6.2 kcal/mol and 14.1 kcal/mol, respectively (Figure 4.17).

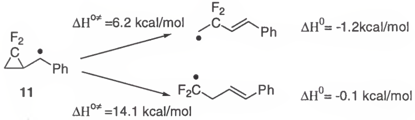

Figure 4.17 With a phenyl substituent at the initial radical position the barrier was increased by about 4 kcal/mol for both rearrangements

When a phenyl substituent is attached to the 3 position on the ring of radical **1**, the activation barrier of the radical ring opening with the cleavage of the distal C-C bond on the ring, which is already very small, is further reduced to, based on the scan of the potential energy, *zero*. What this means is that radical **12** on the potential energy surface is not a minimum and experimentally, in the process of the formation of radical **12**, the rupture of the distal C-C bond to CF_2 group on the cyclopropane ring to some extent will be simultaneous. To our best knowledge, this is the first example of a radical rearrangement that has no barrier. As a result, the bond dissociation energy of the C-X bond will be decreased to, according to the PES (Potential Energy Surface) scan, about 20 kcal/mol without considering the radical stabilization energy of cyclopropyl group in the initial “radical **12**” (Figure 4.18).

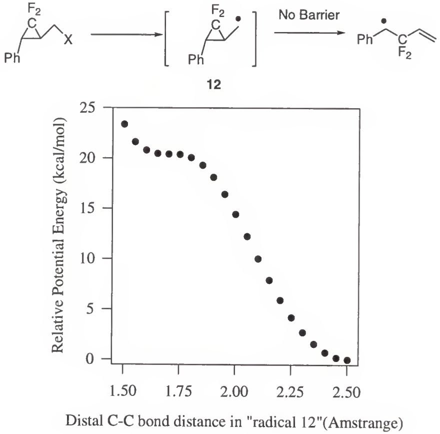

Figure 4.18 B3LYP/6-31G(d) potential energy surface scan of “radical **12**”

It is noteworthy to say that, the radical stabilizing effect of “radical **12**” is unique because of the association the thermal chemistry contribution of “radical **12**” in the future radical processes with the substantial rupture of the cyclopropane ring (*vide supra*), which further leads to the phenyl group participation that increases with the advance of the ring rupture. The earlier the transition state in a radical formation process, the less influence the "radical **12**" exerts and vice verse.

For example, the cyclopropyl carbinyl radical rearrangement, which has a very early transition state, may "sensed" very slightly the existence of the phenyl group (Figure 4.19). However, on the other hand, homolytic dissociation of C-X bond, a process that has a very late transition state, will be effected extensively by the "radical **12**". Thus, molecules with substituent X which have relatively weak C-X bonds such as iodide, bromide, chloride or "radical **12**" itself, might rupture to form radicals easily under very mild conditions. The C-C bond in **13** will be weakened substantially by two radical stabilization groups to nearly 40 kcal/mol! The decarboxylation and hydrogen abstraction process will also be influenced accordingly.

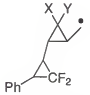

X, Y =H, F etc.

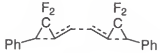

13

Figure 4.19 The interesting systems that have a zero-barrier radical rearrangement unit

The importance of rotational barriers in cyclopropylcarbinyl radical systems having very low activation barriers.

The rotation barriers of cyclopropylcarbinyl radicals have never been considered to be large enough to affect the kinetics or regiochemistry of their ring opening processes. However, when the barriers of radical ring opening become very small, such as in the cases of radicals **1** and **7**, they can be seen to actually be lower than those expected for rotation of the carbinyl group. A potential surface scan (Figure 4.20) indicated that the

CH_2• group of radical **1** has a rotation barrier of 3.1 kcal/mol. No doubt, radical **7** will have an even larger rotational barrier. It is therefore likely that the rates of ring-opening of radicals **1** and **7** will be faster than the rate of rotation of the of rotation of the carbinyl radical group. Assuming that a newly born cyclopropylcarbinyl radical will need to rotate to obtain the stereoelectronic orbital overlap required to ring open, we would predict that,

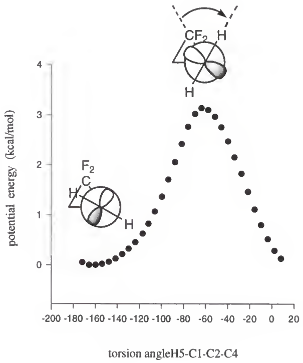

Figure 4.20 Methylene radical rotation barrier of radical (**1**) (UB3LYP/6-31G(d) without zero point energy correction).carbinyl radical group.

for radicals such at **1** and **7**, conformational equilibration of the radical will *not* be attained prior to ring opening, and rotation will be rate determining and product determining. That is, one could well envisage the diasteromeric radical precursors **14a** and **b**, giving rise to diastereomeric cyclopropylcarbinyl radical conformers **15a** and **b** that would, lacking conformational equilibration, lead to different ratios of isomeric products (Figure 4.21). The bigger bias in energy in transition state of radical formation and the lower barrier of the radical ring opening, the bigger difference in ratio of the isomeric products. Thus, an enlarged differentiation will be observed with a phenyl group at the 3 position on the ring.

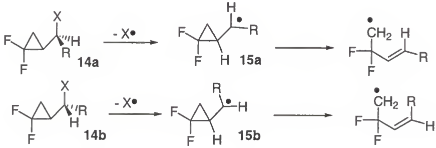

Figure 4.21 The predicated low-barrier radical rearrangements

Rearrangement of 1,1-difluorocyclopropyl-2-vinyl radical cation

A structural optimization starting from the ring closed 1,1-difluorocyclopropyl-2-vinyl radical cation, ended up with the ring opened radical cation (Figure 4.22) with the cleavage of C-C bond proximal CF_2 group, a regiochemistry the same as that of 2,2-difluorocyclopropylcarbinyl cation ring opening (Chapter 6).[156] Radical cation **16** is not a minimum on the potential energy surface of UB3LYP/6-31G(d). The Mulliken charge distribution revealed that the positive charge mainly locates on the CF_2 group (0.43 e), the terminal CH_2 group bearing 0.20 e. The radical, which is indicated by the spin density, is mainly located on C5 and C3. The distance of C2-C3 is 2.057Å, slightly shorter than that of cation, indicates that these two carbons may have more contact.

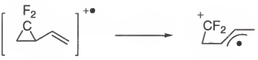

16 **17**

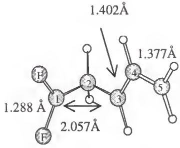

Figure 4.22 Calculated geometry of radical cation **16** (UB3LYP/6-31G(d)).

Thus, we predicate that experimentally radical cation **16,** upon its formation, will ring open to give radical cation **17**, which will then be attacked by a nucleophile mainly at the CF_2 position. The consequent quenching of the radical would form two possible products (Figure 4.23).

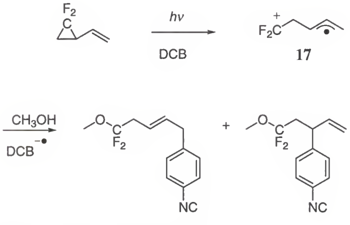

Figure 4.23 Predicated radical cation reaction

With a methyl substituent on the double bond, which can stabilize partial positive charge, the C2-C3 distance (1.923 Å) is longer that of radical cation **18**, and thus the ring opening character is not as clear as that of cation **18** Figure 4.24. Therefore, more nucleophilic attack would likely take place at C5 comparing with that of radical cation **17**.

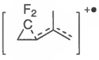

18

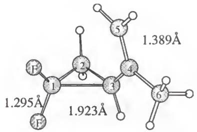

Figure 4.24 Calculated geometry of radical cation **18** (UB3LYP/6-31G(d))

Part 2. Fused Cyclopropylcarbinyl Radical Ring Opening

Introduction

Although cyclopropylcarbinyl radical ring opening reactions are well understood in monocyclic systems, the incorporation of this nucleus into a fused bicyclo [n.1.0] framework introduces additional factors of increased conformational rigidity, ring strain, and differing rate of reversible ring opening and reclosure.[157-159] The experimental results of rearrangement of bicyclo[3.1.0]hex-2-yl radical, **19**, and bicyclo[4.1.0]hept-2-yl, **20**, radicals were rationalized as follows. Kinetically the exo-ring openings are preferred due to stereoelectronics being that the outer C-C bond overlaps most efficiently with the SOMO.[160] Thermodynamically, the endo-ring opening product of radical **19** is more exothermic, whereas for radial **20** the exo-ring opening product is thermodynamically preferred.[161,162] However, more recently, the endo-ring opening product of radical **20** was found to have a greater thermodynamic stability which was also supported by semi-empirical calculations.[163] Semi-empirical calculations gave lower barriers for endo-ring openings for both radical **19** and **20**.[161,163] Therefore, there is no plausible kinetic rationale for the radical ring openings because of those contradictory results.

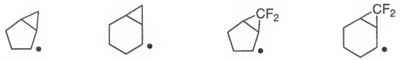

19 **20** **21** **22**

Figure 4.25 Systems investigated in this study

In this study, we employ density functional theory, which was proved to be adequate for the cyclopropylcarbinyl radical rearrangement reactions,[138,156] to provide some insight for the rearrangements of radical **19** and **20**, and the fluorine substitution effect on such radical reactions is examined.

Results and Discussion

The optimized structures are depicted in Figure 4.26. Interestingly, in radical **19**, C1-C6 are 1.540 Å which is longer than either C1-C5 (1.526 Å) or C5-C6 (1.499 Å). This bond length pattern on the cyclopropane ring in radical is the result of SOMO-HOMO interaction (Figure 4.5), which is further constrained by the five-member ring to give a better lineup between the radical and the external C1-C6 bond. Thus, for the hydrocarbon system, the external C-C bonds are weaker than the internal bonds.

For fluorinated system, although the breaking external C-C bonds of **21** (1.508 Å) and **22** (1.507 Å) are shorter than their internal C-C bond, 1.571 Å and 1.569 Å, respectively, compared with the fluorinated non-bicyclic system, radical **1** (proximal C-C bond 1.496 Å and distal C-C bond 1.596 Å on the ring), the same pattern of bond length change, which was observed in radical **19**, is still conserved in fluorinated radical **21** and **22**. Therefore, for fluorinated systems like radical **21** and radical **22**, the internal bonds are the weaker bonds.

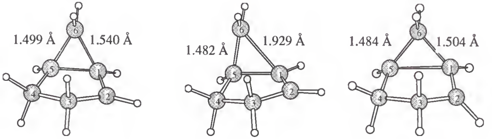

19
C1-C5=1.526Å

External TS of **19**
C1-C5=1.505 Å

Internal TS of **19**
C1-C5=1.922Å

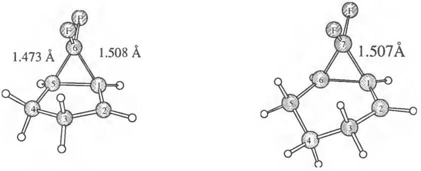

21
C1-C5= 1.571 Å

22
C1-C6=1.569Å

Figure 4.26 Calculated structure of radical **19**, transition state structures of external and internal ring opening and radical **21** and **22**.

The computed standard activation enthalpies ($\Delta H^{o\neq}$) and standard heat of reactions (ΔH^{o}) of the radical rearrangements of **19** and **20** and fluorinated radical **21** and **22** are listed in Table 4.6. Like the opening chain system, there are no obvious correlation between the activation enthalpies and the reaction energies. In all the cases we examined here, the activation enthalpies for the external ring opening are nearly the same as these for the none-bicyclic parent systems, whereas these for the internal ring opening are about 1~2 kcal/mol higher. This is largely due to the extra strain created by the distortion of the ring with the radical in order to reach the transition state conformation for the internal ring opening.

Table 4.6 Calculated standard activation enthalpies and standard heat of reaction of radical rearrangements. (kcal/mol)

	External ring opening		Internal ring opening	
	$\Delta H^{o\neq}$	ΔH^{o}	$\Delta H^{o\neq}$	ΔH^{o}
19	6.6	-3.5	8.1	-10.3
20	6.2	-4.9	8.0	-4.1
21	9.2	-9.1	3.1	-18.2
22	9.1	-10.3	3.6	-10.8

For radical **19** and **20**, the external ring openings are preferred over internal ring opening by 1.5 kcal/mol in standard activation enthalpy. Thermodynamically, the external ring opened product for radical **20** is preferred only by 0.8 kcal/mol, while the internal ring opened product for radical **19** is favored by 6.8 kcal/mol. This is consistent with the experimental results[161,162] which had not been corroborated with semi-empirical calculations.[161,163]

For the fluorinated system, the internal ring opening for both **21**and **22** are preferred for about 6 kcal/mol over external ring opening in activation enthalpy. Even though the external rupture of the cyclopropane ring is favored conformationally, which is observed in the non-fluorinated system, due to the stereoelectronic effect we invoked earlier—effectiveness of orbital overlap, the radical rearrangements of the internal ring opening are the preferred processes kinetically, the same regiochemistry observed in the open chain system. Thermodynamically internal ring opening of radical **21**and **22** are also favored.

Part 3. Oxiranylcarbinyl Radical Ring Opening

Introduction

As an extension of this research, the fluorine substitution effects on the kinetics of oxiranylcarbinyl radical ring opening were studied. Computationally, Radom[138] and Pasto[164] investigated the oxiranyl carbinyl radical ring opening parallel with their cyclopropylcarbinyl radical ring opening studies, and found that radical **19** regio-specifically ring open by cleaving the C-O bond with an activation barrier of about 3 kcal/mol, which is around 4 kcal/mol lower than that of the cyclopropylcarbinyl radical ring opening, to form the thermodynamically disfavored product.

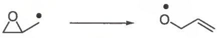

23

Figure 4.27 The rearrangement of oxiranyl radical

This results are consistent with the product analysis experiments[118] and also the fact that oxiranylcarbinyl radical **23** itself has never been spectroscopically observed.[165,166] Gleicher has assigned a lower limit for the rate of radical **23** ring opening at 1 x $10^{10}s^{-1}$ at 70°C, using competitive reactions of a cyclopropyloxiranylmethyl radical.[167] More recently, Rawal reported the rate constant of 3.2 x $10^{10}s^{-1}$ at 25-30°C for a cyclohexylsubstituted oxiranylcarbinyl radical.[168] The polar effect (*vide supra*) was used to rationalized the regiochemistry and kinetics of the ring opening process of radical **23**.[118]

Substitution effects at 3 position on the ring were investigated experimentally. It is observed that for alkyl and acyl substituted radicals, exclusive C-O scission takes place, though if the rearranged radical has a radical stabilizing substituent, such as phenyl or vinyl group, then C-C bond cleavage occurs.[169-171]

The fluorine substitution effect on cyclopropane has been well studied (see chapter 1), however such effect on its oxirane analog have not been reported yet. In the previous study, we demonstrated that fluorine substituents on the cyclopropyl ring can accelerate the distal C-C bond cleavage, while inhibiting the proximal C-C bond cleavage in the cyclopropylcarbinyl radical rearrangement. Here we are going to present the computational results of the fluorine substitution effect on oxirane itself and the oxiranylcarbinyl radical rearrangement.

Results and Discussion

The calculated structural parameters of oxirane and its derivatives with fluorine substituents are listed in Table 4.7. The calculated structure of oxirane, which is very similar to the experimental structure[15] reveals a C-C bond length of 1.469 Å which is shorter than the C-C bond in cyclopropane (1.508 Å)(Chapter 1) and normal C-C bond. However, the C-O bond length (1.430Å), on the other hand, is longer than the normal C-O bond (1.410 Å) in an open chain system such as dimethyl ether. Even though there is no way to make a direct comparison because of the difference in bonding characters, the opposite trends in the change of bond length of C-C and C-O bond in oxirane indicates the approaching of their structural bond strengths to each other. To some extent the sequence of bond strength might reverse, that is, the C-C bond become stronger than C-O bond in oxirane.

A detailed comparison of fluorine substitution effects on oxirane and cyclopropane reveals that, gem-difluoro substituents lengthen the distal bond and enlarge the C-C-C (O-C-C in oxirane) bond angle of the substituted carbon in cyclopropane by 0.039 Å and 3.0°, however in oxirane, by 0.058 Å and 4.7° respectively, an indication of a weaker C-O bond in oxirane (Table 4.7). The distal C-O is nearly equal to the C-C bond with one fluorine substituent in bond length, and longer than the C-C bond with gem-difluoro-substituents.

Consistent with this speculation, the C-O ring opening of the oxirane is preferred kinetically according to theoretical studies.[172] Alkyl substituted oxiranes favor C-O rupture in both photochemically and thermally induced reactions.[172]

Therefore, the C-O bond in oxirane is likely to have a weaker 'structural bond strength' than the C-C bond on the ring.

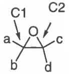

Table 4.7 Calculated (B3LYP/6-31G(d)) and Measured Structural Parameters of Oxiranes

substrates	C-C bond	O-C1 bond	O-C2 bond	OC1C2 angle
a=b=c=d=H[a]	1.472	1.436	1.436	59.5
a=b=c=d=H	1.469	1.430	1.430	59.1
a=F, b=c=d=H	1.460	1.387	1.457	61.5
a=b=F, c=d=H	1.452	1.358	1.488	63.8
a=b=c=d=F	1.451	1.406	1.406	58.9

a. experimental structure from reference [173]

Energetically, the structural distortion of oxirane caused by fluorine substituents is correlated with the increase of the ring strain. As shown in the hypothetical reaction, the incorporation of gem-difluoro-substituents in oxirane increases the ring strain by 12.5 kcal/mol, which is similar to the hydrocarbon system in which the ring strain increase by 5~7 kcal/mol per fluorine substituent (Figure 4.28).

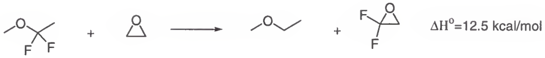

Figure 4.28 Hypothetic reaction used to calculated the fluorine substitution effect on ring strain of oxirane.

A systematic calculation was carried out to locate the geometry of the initial radicals, transition states and products of the oxiranylcarbinyl radical ring opening rearrangements with fluorine substituents at all the possible positions and the structures of mono-fluorinated oxiranylcarbinyl radical, **25**, and its two ring opening transition states are depicted in Figure 4.29.

The initial radical adopts a bisected conformation. The bond length of C-C bond and the adjacent C-O bond increase from 1.460 Å and 1.457Å in fluorooxirane to 1.481 Å and 1.507 Å in trans-fluorooxiranylcarbinyl radical, respectively. The 0.05 Å lengthening of the C-O bond compared with the 0.021 Å lengthening of the C-C bond indicate the further weakening of the C-O bond relative to the C-C bond. In the transition state of C-O cleavage, the C-O bond was lengthened from 1.507 Å to only 1.724 Å, while in the transition state of C-C bond cleavage, the C-C bond is 1.861 Å.

The structure analysis of the mono-fluorinated radical, **25**, reveals that the C-O bond is longer, thus likely weaker than the C-C bond on the ring in oxiranylcarbinyl radical. To reach its ring opening transition state, the breaking C-O bond only need to lengthen 0.22 Å. Such a very early transition state indicates that this reaction will have a very low activation barrier according to the structure-energy relationship.

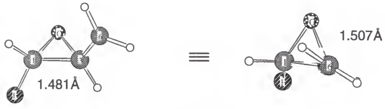

Radical **25**

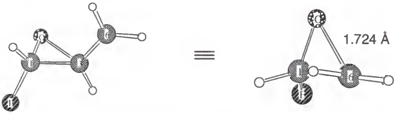

TS of C-O bond cleavage

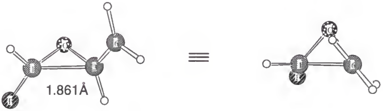

TS of C-C bond cleavage

Figure 4.29 Calculated structure of radical **25**, transition states for C-O and C-C bond cleavage.

The computed activation barrier activation enthalpies and the reaction heat of the oxiranylcarbinyl radical rearrangements and the results are listed in Table 4.8. In all the cases we encountered here, those processes involving C-O bond scission were found to be favored kinetically over C-C bond scission.

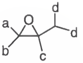

Table 4.8 Calculated reaction barriers (E_o), standard activation enthalpies, bond length and standard heat of reactions.

	reactants	E_o C-O ($\Delta H^{o\neq}$)	BL C-O	$\Delta H^{o}_{C\text{-}O}$	E_o C-C ($\Delta H^{o\neq}$)	$BL_{C\text{-}C}$	$\Delta H^{o}_{C\text{-}C}$
23	No F	3.2 (2.9)	1.462	-5.1	10.9 (10.8)	1.489	-6.5
24	c=F	6.9 (6.6)	1.413	-1.4	12.9 (12.7)	1.478	-4.7
25	b=F	0.7 (0.4)	1.526	-7.0	11.6 (11.4)	1.478	-3.3
26	a=F	0.1(-)					
27	a=b=F	no			no		
28	a~c=F	0.5 (0.2)	1.506	-3.9	13.7 (13.4)	1.468	-1.9
29	All F	1.8 (1.9)	1.467	-3.1	17.3 (17.3)	1.458	3.7
30	d=F	3.6 (3.6)	1.450	-5.7	15.8 (15.9)	1.470	-5.9

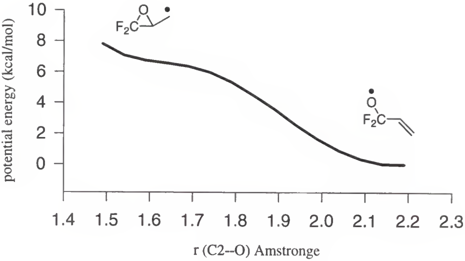

Figure 4.30 Potential energy surface scan of 2,2-difluorooxiranyl carbinyl radical (UB3LYP/6-31G(d))

Fluorine substituents accelerate ring opening with distal bond cleavage, while they hinder proximal bond cleavage. With one fluorine substituent at c position in radical

24, the reaction barriers for both C-C and C-O bond cleavage are elevated. With one fluorine substituent at a or b position, the reaction barriers to C-O cleavage decrease to 0.1 and 0.7 kcal/mol respectively. After the thermal correction, at 25 °C, the barrier in cis system diminishes.

For the system with gem-difluoro substituent on the ring, in radical **27**, the barrier of radical rearrangement with C-O cleavage is further reduced to *zero*, what this means is that, "radical **27**" is not a minimum on the potential energy surface (Figure 4.24). During the formation of "radical **27**", the oxiranyl ring starts to rupture simultaneously.

A polar transition state was proposed to rationalize the regiochemistry of radical **23** rearrangement.[118] However, logically, it is awkward to rationalize this regiochemistry on the basis of polar effects. In the charge distribution analysis for the hydrocarbon system, we found there is no negative charge developed at the incipient radical center on the ring, and there is no experimental evidence to support the proposed polar transition state in the parent system. Therefore, there is no basis for the argument saying that the oxygen on the ring in the oxiranyl system further stabilizes the negative charge on the ring at the transition state.

In all the systems we encountered in this chapter, the structurally weaker bonds were always the bonds that are going to break in the radical rearrangements regardless the polarity of the transition states. Thus, we believe, according to our calculation, that the regiochemistry of cyclopropylcarbinyl radical analogs are determined mainly by the stereoelectronic effect—the effectiveness of the radical interaction (*vide supra*). The transient polarity of the transition state can be attributed to the electron flow in the radical rearrangement and to some extent, it may correlate with the relative electrophilicity of the reacting center on the three member ring respect to the radical center,[156] but is not the ultimate factor that governs the kinetics and regiochemistry of cyclopropylcarbinyl radical analog rearrangements.

Therefore, the transition state of oxiranylcarbinyl radical ring opening may generate, for C-O cleavage, a partial negative charge on the oxygen atom, a partial positive charge on the original radical center. An opposite polarity between the reaction center for C-C bond cleavage may be observed.

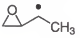

31

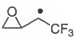

32

Table 4.9 Calculated standard activation enthalpies (kcal/mol)

radicals	$\Delta H^{o\neq}_{C\text{-}O}$	$\Delta H^{o\neq}_{C\text{-}C}$
31	1.9	10.9
32	3.7	10.2

Consistent with the predication, when a trifluoromethyl group, an electron withdrawing substituent is positioned at the original radical carbon, **32**, the standard activation enthalpies are elevated for C-O cleavage, whilst lowered for C-C cleavage compared to the situation with a methyl group (Table 4.9).

It is a challenge to understand the heat of reaction. They are not correlated with the reaction barrier, which is similar to result for the hydrocarbon system, nor, remarkably, is there a correlation with the number of fluorine substituents on the ring, which will increase the ring strain by about 6 kcal/mol per fluorine. Contradictory results have been reported on the reaction heats of the unsubstituted oxiranylcarbinyl radical ring opening.[138] [164] Between B3LYP/6-311+G(3df,2p) and CBS-RAD levels, although the calculated values of reaction barriers are very close, nearly 3 kcal/mol of deviations for the reaction energies were reported.[138] Therefore, the absolute values of the reaction heat at UB3LYP/6-31G(2df,2p)//UB3LYP/6-31G(d) level may be in question, however, the relative values, in which the system error will be cancelled to some extant, should reflect the trend of the fluorine substitution effects. The scattered heats of reactions could be understood when the following fluorine substitution effects are considered: (a) Highly electron negative substituents prefer to cumulate on the same carbon (b) Fluorination thermodynamically destabilizes double bonds.[37] (c) Fluorine substitution destabilizes the α oxygen and highly substituted carbon radicals (Figure 4.31).

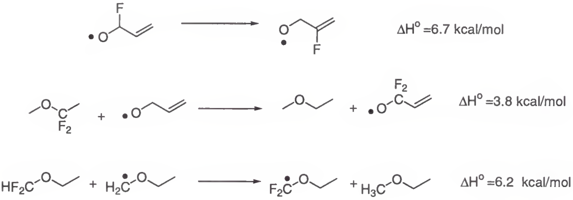

Figure 4.31 The fluorine substitution effects

Fluorine substituents at the carbinyl radical raise the reaction barrier by 0.4 kcal/mol for C-O bond cleavage, but 4.9 kcal/mol for C-C bond cleavage. The argument, which was used to rationalize the same effect in the hydrocarbon (Figure 4.12), is still valid here. The discrepancy reflects the opposite polarity of the two transition states, because the conjugated fluorine substituents stabilize positive charge, while destabilize negative charge.[35]

In summary, fluorine substitution effects on the kinetics of the oxiranylcarbinyl radical rearrangements are similar to that in the hydrocarbon system. A complicated thermodynamic fluorine substitution effect was observed.

Conclusion

In this work we have evaluated the dramatic impact of fluorine substituents on the structure and reactivity of simple and fused cyclopropylcarbinyl radicals and oxiranylcarbinyl radicals. DFT calculations (B3LYP/6-311+G(2df,2p)//B3LYP/6-31G(d)) were found to give satisfactory results with respect to predicting activation barriers and heats of reaction for the various fluorinated cyclopropylcarbinyl radical and oxiranylcarbinyl radical ring opening reactions.

A refined stereoelectronic influence, not the polar effect which has been considered the dominate factor, is invoked and believed to be responsible for the kinetics and regiochemistry of all of these radical systems.

Several radical rearrangements, which have no barriers, were found. Experimental studies of such low barrier and even no barrier systems should provide important insight into controversial issues related to the possibility of conformational control of rates and regiochemistry in fast cyclopropylcarbinyl radical systems and the efficacy of their use as radical clocks in very fast competitive situations.

CHAPTER 5
KINETIC STUDIES OF 2,2-DIFLUOROCYCLOPROPYLCARBINYL RADICAL RING OPENING

Introduction

Knowledge of the rate constants of radical reactions is necessary both for mechanistic work and for planning of radical based conversions in synthesis. For alkyl radicals, the linchpin kinetic values are the rate constants for simple unimolecular rearrangements, of referred to as "radical clocks",[174] such as the cyclization of the 5-hexenyl radical and ring opening of the cyclopropylcarbinyl radical. The rate constants of the same radical rearrangements were measured by ESR or LFP, and were then used to obtain rate constants of other radical reactions by extensive competition kinetic studies.[117]

Cyclopropylcarbinyl radicals, in particular, have attracted tremendous research interest. At ambient temperature, with a rate constant for ring opening of 1.2 x $10^8 s^{-1}$, [140] the simple cyclopropylcarbinyl radical is the best calibrated radical. Its alkyl and aromatic substituted derivatives[117,119,121] comprise a fast rearranging radical family with rate constants ranging from $10^7 s^{-1}$ to as high as10^{12} s^{-1}. They have been extensively used in the mechanistic studies of P-450 catalyzed oxidations of unactivated hydrocarbons, but contradictory results were obtained. Some examples of this family are depicted in Figure 5.1.

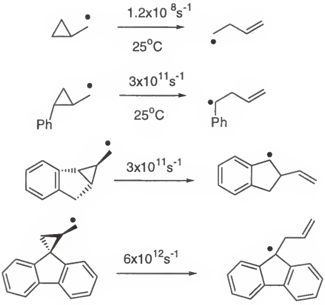

Figure 5.1 Measured rate constants of cyclopropylcarbinyl radicals ring opening.

The 2,2-difluorocyclopropylcarbinyl radical rearrangement was found to occur with exclusive distal C-C bond session, and it was assigned a rate constant of higher than $10^8 s^{-1}$ by Dolbier in a competition kinetic study, using neat Bu_3SnH as radical trapping reagent.[50] More recently, our DFT calculations provided a standard activation enthalpy of 1.6 kcal/mol and standard activation entropy of –2 cal mol^{-1} K^{-1} (Chapter 4),[156] and by utilizing transition state theory this provides a rate constant of $1.5 \times 10^{11} s^{-1}$ at 25 °C.

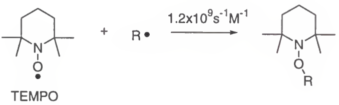

Figure 5.2 Radical quenching reaction with TEMPO

With the fast radical quenching reagent such as 2,2,6,6-tetramethylpiperidin-1-oxyl (TEMPO) and hydrogen atom transfer reagent such as phenylselenol (PhSeH) available, which can trap radicals with rate constants of about $10^9 s^{-1} M^{-1}$, it become more feasible to measure the rate constant of the ultrafast 2,2-difluorocyclopropylcarbinyl radical ring opening. In this study, we are going to present the result of its experimental kinetic study.

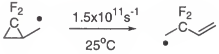

Figure 5.3 Calculated rate constant of 1,1-difluorocyclopropylcarbinyl radical ring opening

First Attempt to Measure the Radical Ring Opening Rate

Synthesis of Radical Precursor

In our first attempt to measure the rate of radical ring opening, we chose to use a Barton type[175] alkyl-PTOC compound as the radical precursor, **55**, where PTOC=[((1H)-pyridine-2-thione)oxy]carbonyl. The synthesis of this radical precursor is depicted in Figure 5.4.

The silylether **51**, the protected 3-buten-1-ol, was difluorocyclopropanated using Seyferth's reagent to give **52**, which was then deprotected to provide alcohol **53**. The oxidation of the alcohol gave acid **54**. Because the final product **55** is a light sensitive compound, during its synthesis the flask was wrapped with aluminum foil. The first unsuccessful attempt to prepare the PTOC ester involoved esterification of the acyl chloride of **54** with **50** which was made from its sodium salt by a literature procedure.

The radical precursor **55** was finally made by a DCC coupling reaction between **50** and **54**, but it decomposed easily on the silica gel even in absolute dark. Because the ^{19}F NMR of the reaction mixture indicated that this reaction was very clean, it was used directly for the next radical generating step after a filtration.

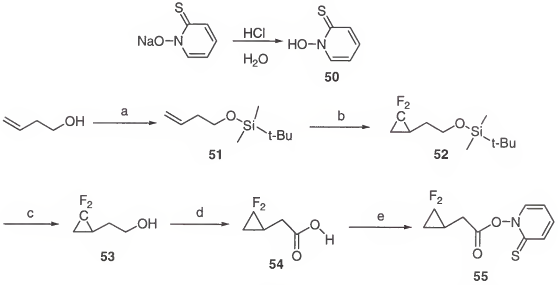

Figure 5.1 (a).t-BuMe$_2$SiCl; (b). PhHgCF$_3$, NaI. (c). FeCl$_3$, CH$_3$CN. (d) Cr$_3$O, H$_2$SO$_4$. (e) **50,** DCC.

Preliminary Kinetic Study

The kinetic studies were carried out in NMR tubes, using THF as solvent and PhSeH as the radical trapping reagent using a concentration up to 2.5 M and 10 equivalents excess relative to the radical precursor. At room temperature, after shining the light for 30 min, the radical precursor **55** was totally decomposed to give one ring opened and two ring closed products, as indicated by ^{19}F NMR. After vacuum transfer, the two ring closed products remained in the non-volatile residue. The ring opened product was identified as alkene **56** by comparing with its known ^{19}F NMR spectrum.[50] One of the ring closed products was identified as acid **54** by comparing its spectra with that of an authentic sample. The other ring-closed product was assigned as **57** with the assistance of GCMS. No sign of 1,1-difluoro-2-methyl cyclopropane was observed. This method was therefore abandoned.

By assuming that the unseen 1,1-difluoro-2-methylcycopropane was a maximum of 5% of **56**, we could estimate that the ring opening process for 2,2-difluorocyclopropylcarbinyl radical should have a rate constant of greater than 3 x $10^{10}s^{-1}$ taking the rate constant of 1.2 x $10^{9}M^{-1}$ s^{-1} for PhSeH reacting with a carbon radical.[176]

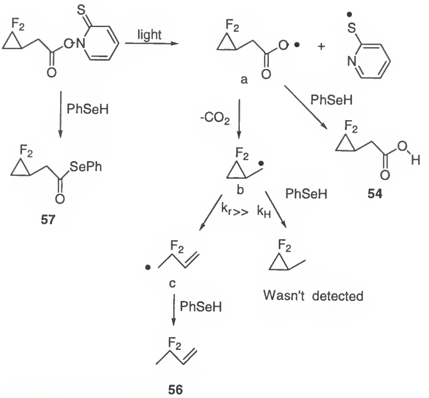

Figure 5.2 The reaction profile of **56**

The reaction profile is depicted in Figure 5.2. Radical precursor **55** decompose with the cleavage of O-N bond to give two radicals, **a** and **b**. Due to high activity of the hydrogen transfer reagent PhSeH towards radicals, a substantial amount of radical **a** was trapped before it underwent decarboxylation to give acid **54**. The rest of the radical a decarboxylated to generate 2,2-difluorocyclopropylcarbinyl radical **b**, which ring opened very rapidly, compared to the trapping reaction, to give radical **c** which was then trapped by PhSeH to give ring opened product **56**. The polar process of **55** in the presence of PhSeH yielded the substitution product **57**.

Second and Successful Attempt at Measuring the Rate of Radical Ring Opening

Syntheses of Radical Precursor

Another fast radical trapping reagent, [177] TEMPO, a free radical, which can react with carbon radical with a rate constant of $1.2 \times 10^9\ M^{-1}s^{-1}$, has also been used as a radical clock in free radical reactions. In this method, a peroxide ester is generally utilized as the radical precursor.[178-180] In our current study, the target radical precursor was perester **58** and its synthesis is depicted in Figure 5.3.

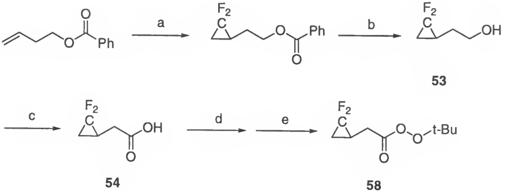

Figure 5.3 (a). $FSO_2CF_2COOTMS$, NaF, 125°C. (b). NaOH, H_2O. (c). CrO_3, H_2SO_4. (d). ClCOCOCl. (e). HOOt-Bu

The first step of the synthesis used the new gem-difluorocyclopropane synthesis methodology that has been described in Chapter 2. The neat cyclopropanation provided nearly pure product with only 1.5 equivalent of $FSO_2CF_2COOTMS$, as indicated by both ^{19}F and ^{1}H NMR. Without purification, the reaction mixture was hydrolyzed in a one-pot reaction to provide the alcohol **53** in a yield of 63% for the two step synthesis. Alcohol **53** was then oxidized to acid **54** by CrO_3 in 1.5 M sulfuric acid. This acid was treated with oxalyl chloride to make the acyl chloride, which was then reacted with anhydrous t-butyl hydroperoxide to give the desired perester **58.**

Kinetics of Thermal Decomposition of *t*-Butyl Perester 58

The kinetics of thermal decomposition of *t*-butyl perester **58** were carried out in cyclohexane with 5 % (v/v) of 1,4-cyclohexadiene, 0.6 M TEMPO/cyclohexane and 1.0 M TEMPO/cyclohexane at 99.3 °C, respectively. The reaction mixtures were degassed by 3 freeze/thaw cycles and sealed *in vacuo* in capillary tubes. The reactions were monitored with ^{19}F NMR using another capillary tube containing certain amount of $PhCF_3$ in cyclohexane solution as a external fluorine standard.

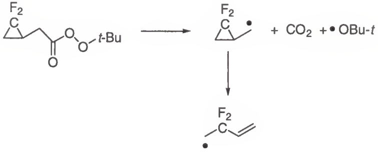

Figure 5.4 The thermal decomposition of **58**

For decomposition in cyclohexane without TEMPO, only ring-opened products were observed through the course of the reaction, indicating that the homolytic cleavage and decarboxylation of the perester **58** followed by radical ring opening was the only reaction sequence occurring in this reaction system (Figure 5.4).

Bartlett and his coworker[181] showed that the rates of the homolytic decomposition processes of t-butyl peresters were correlated to the stability of the free radicals generated after decarboxylation. The first order rate constant of the decomposition of perester **58** is measured to be $(2.09 \pm 0.18) \times 10^{-5} s^{-1}$ at 99.3 °C which is only 5.5 times faster than that of t-butyl peracetate, which was extrapolated from the activation parameters ($\Delta H^{\neq}$ = 38 kcal/mol, $\Delta S^{\neq}$ = 17 e.u.).[181] This indicates that 2,2-difluorocyclopropylcarbinyl radical is not a stabilized radical compared with a primary radial.

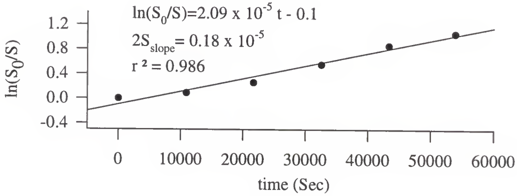

Figure 5.5 Plot of $\ln(S_0/S)$ vs. time of decomposition of perester **58** at 99.3 °C in cyclohexane with 5% (v/v) 1,4,-cyclohexadiene

In the cyclohexane solution of over 10 folders TEMPO respect to the starting perester, the decompositions of perester **58** were found to give two products indicated by ^{19}F NMR spectra. One was a ring opened product, which was identified to be **59**, and the other one was ring closed product, which was identified to be the acid **54**. The products ratios are **59** : **54** = 1 : 3.5 for 1.0 M TEMPO solution and 1 : 2.3 for 0.6 M TEMPO solution. The higher concentration of TEMPO the more acid formed. A polar process[182-184] which was found to be the dominate process in the decomposition acyl peroxide might be responsible for the formation of the acid **54** here.

The decomposition of perester **58** was accelerated in the presence of TEMPO. The observed rate constants were $(3.99 \pm 0.29)\times10^{-5}$ s^{-1} and $(4.90 \pm 0.27)\times10^{-5}$ s^{-1} for 0.6 M and 1.0 M TEMPO solution, respectively.

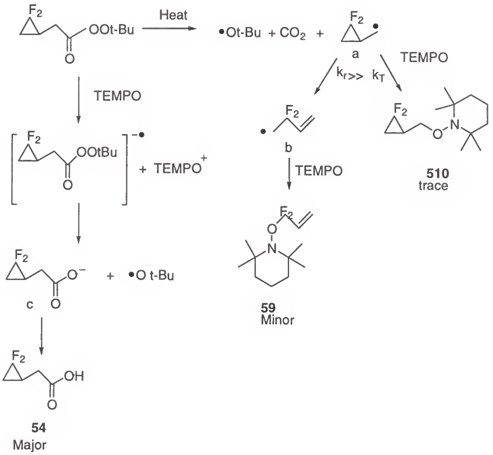

Figure 5.6 Reaction profile of the decomposition of *t*-butyl perester **58** in the presence of TEMPO.

The reaction profile is depicted in Figure 5.6. In the polar process, the radical precursor, **58**, oxidized TEMPO to give a radical anion, which then cleaved to provide the anion **c** and the t-butoxyl radical. The anion **c** obtained a proton from the compound derived from the TEMPO cation to give the acid **54**.[184] The t-butoxyl radical abstracted an H atom from solvent cyclohexane, and the generated cyclohexanyl radical was trapped by TEMPO.

In competition with this polar process, the cleavage of O-O bond in radical precursor **58** and the simultaneous decarboxylation provided 2,2-difluorocyclopropylcarbinyl radical **a** and t-butoxyl radical in a thermally homolytic cleavage process. The radical **a** could either rearrange rapidly to form the ring opened radical **b**, which was then trapped by TEMPO to give the ring opened product **59**, or trapped by TEMPO to give ring closed product **510**, which was too dilute to be detected by NMR.

Even though the yield is low for the homolytic process in this system, fortunately the ratio of product **59** and **510**, which is the value we need to calculated the rate constant of the radical **a** ring opening (*vide infra*), is not effect in this system.

As shown in the reaction profile in Figure 5.6, the reaction rate of ring opening of radical **a**, which is the same as the rate of formation of radical **b** which is trapped by TEMPO to give ring opened product **59** can be expressed as:

$$d[b]/dt = k_r[a] \qquad (1)$$

The reaction rate of TEMPO trapping of radical **a** is:

$$d[\mathbf{510}]/dt = k_T[\mathbf{a}][\text{TEMPO}] \quad (2)$$

(2)/(1) we get:

$$d[\mathbf{510}]/d[\mathbf{b}] = k_T[\mathrm{TEMPO}]/k_r$$

Under pseudo-first-order condition, that is, with over 10-fold excess of TEMPO, the concentration of TEMPO is considered to be constant in the course of the reaction. After integration, with when t =0, **[510]**=**[b]**=0 and **b** is expressed by ring opened product **59**,

$$[\mathbf{510}]/[\mathbf{59}] = [\mathrm{TEMPO}]\ (k_T/k_r) \qquad (3)$$

Syntheses of Authentic Products

The syntheses of products **59** and **510** are depicted in Figure 5.7. In both syntheses, allyl iodide was used as starting material. The photolysis of allyl iodide in the presence of TEMPO and sodium sulfide in acetonitrile produced n-allyloxy-2,2,6,6-tetramethylpiperidine, **511**, which was then difluorocyclopropanated to give **510**.

In the synthesis of **59**, allyl iodide was first cyclopropanated to 2,2-difluorocyclopropylcarbinyl iodide, **512**. The photolysis of **512**, using the same condition of making **511**, provided the desired product **59**. Compound **59**, **510** and **512** were found difficult to be purified. They all decomposed on silica gel during purification and are all thermally unstable at temperature higher than 120 °C.

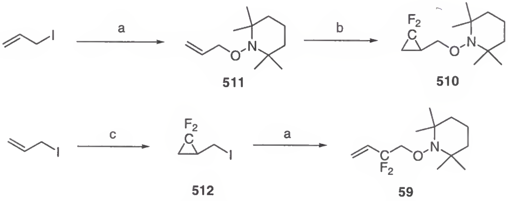

Figure 5.7 (a). TEMPO, *hv*, Na_2SO_3, CH_3CN; (b). $FSO_2CF_2COOTMS$, CsF, 90°C PhCOOMe; (c). $FSO_2CF_2COOTMS$, NaF, 105°C, PhCOOMe.

Product Stabilities

The thermal stability of product mixture of **510** and **59** in degassed cyclohexane solution of 0.8 M TEMPO was tested by prolonged heating at 99.3 °C, the temperature that is going to be used for kinetic study. After 65.5 hours of heating, based on the ^{19}F NMR spectrum, the ratio of the products was not changed and no other new product was formed.

The overall relative respond coefficient of **510** and **59** on HPLC/ESI-MS (*vide infra*) was measured to be **510**: **59** = 0.5784±0.0192 calculated using the integrations of total ion on mass spectra of the respect products, with their 1:1 mixture sample (determined by ^{19}F NMR) under the same condition which was going to be used for the kinetic run. The non-unit coefficient reflected the overall result of the relative stabilities of **510** and **59** on the HPLC column and the relative respond coefficient for the MS integration. This value will be used to calibrate the product ratios in the following kinetic study.

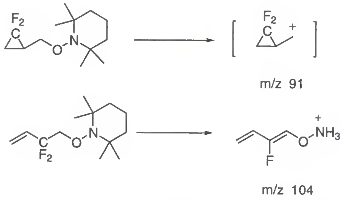

Figure 5.8 The distinct cleavage pattern of **59** and **510** on HPLC/ESI-MS.

Interestingly, under experiment conditions, only **59** yields m/z 104 and only **510** yields m/z 91 as shown in Figure 5.8.

Kinetic Measurement

In the kinetic study, a series of degassed cyclohexane solutions of TEMPO (0.5 M ~1.1 M, over 10 folder excess) and radical precursor **58** were sealed in Pyrex melting point capillary tubes. The reaction mixtures had been maintained at 99.3 °C in thermostated bath for 54 hours and were then analyzed on high pressure liquid chromatograph / mass spectrometry in electrospray ionization ionization mode (HPLC/ESI-MS) using a water symmetry shield RP18, 2.1x 150mm, plus guard column.

Table 5.1 HPLC/ESI-MS ratios of **510** and **59** at different concentration of TEMPO

run	TEMPO concentrations	**510**: **59**
1	0.500	0.00489
2	0.600	0.00650
3	0.700	0.00709
4	0.800	0.00683
5	0.900	0.00958
6	1.000	0.00965
7	1.100	0.00984

In a preliminary kinetic run, the peak of a substantial amount of cyclohexyloxy-2,2,6,6- tetramethylpiperidine (m/z=240) formed by trapping of cyclohexyl radicals generated by hydrogen abstraction from the solvent by *tert*-butoxy radicals partially overlapped with that of product **59**. This problem was overcome by addition of 1,4-cyclohexadiene as a hydrogen atom donor. It readily undergoes hydrogen atom abstraction by *tert*-butoxy radicals, but not by alkyl radicals, to generate cyclohexadienyl radicals, which react with TEMPO not by coupling but by disproportionation to give benzene and the hydroxylamine.[185] Thus, in the kinetic study, a cyclohexane solvent with 5% v/v of 1,4-hexadiene was used. The ratios of **510** and **59** calculated from the integration of total ions of the respect product were listed in Table 5.1.

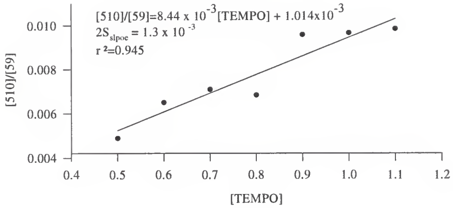

Figure 5.9 Least square plot of **[510]**/**[59]** *vs.* concentration of TEMPO

A least square plot of **[510]**/**[59]** *vs.* the concentration of TEMPO yielded a slop of (8.44 ± 1.3) x 10^{-3} M^{-1} which according to equation (3) is the ratio of k_T/k_r. After corrected by the overall respond coefficient, the ratio is (1.46 ± 0.23) x 10^{-2} M^{-1}. The radical trapping rate constant by TEMPO, k_T, was extrapolated from the activation parameters

$$\log k_T = 9.7 - 0.9/\theta$$

suggested by Beckwith[186] (θ = 2.3RT). At 99.3°C, k_T was calculated to be 1.5 x 10^9 $M^{-1}s^{-1}$. This yielded a rate constant k_r for the 2,2-difluorocyclopropylcarbinyl radical ring opening of 1.0 x $10^{11}s^{-1}$, which is consistent with the rate constant (3.4 x $10^{11}s^{-1}$) extrapolated from the calculated activation parameters ($\Delta S^{\neq}$= -2 e.u., $\Delta H^{\neq}$=1.6 kcal/mol, parameters were obtained at 298.15 °C) using conventional transition state theory at UB3LYP/6-311+G(2df,2p)//UB3LYP/6-31G(d) level of theory (Chapter 4)[156] and earlier experimental result.[49]

Conclusions

A competition methodology had been utilized to determine the rate constant of radical rearrangement of 2,2-difluorocyclopropylcarbinyl radical. The radical was found to rearrange with the distal C-C bond on the ring to CF_2 group cleavage to give 2,2-difluoro-3-butenyl radical. Using TEMPO as the radical quenching reagent the rate constant was measured to be 1.0 x $10^{11}s^{-1}$, which is consistent with the earlier computational results. This provides another successful case to demonstrate the predicating power of modern computational methodology.

The kinetics of thermal decomposition of *tert*-butyl perester indicated that 2,2-difluorocyclopropylcarbinyl radical is not a much stabilized radical compared with primary alkyl radicals.

CHAPTER 6

REACTIVITY AND REGIOCHEMICAL BEHAVIOR OF THE 2, 2-DIFLUOROCYCLOPROPYL CARBINYL CATION

Introduction

Cyclopropylcarbinyl cation has attracted the attention of many chemists over the last 40 years since J. D. Roberts' pioneering solvolytic studies[187,188] and it is therefore a well-studied system both experimentally and theoretically.[189] [190-194]. A pentacoordinated tricyclobutonium structure (Figure 6.1 a) was initially proposed, designated as a "nonclassical" ion by Roberts. However, it was soon replaced by a system of equilibrating bridged bicycobutonium ions (Figure 6.1 b) as further experimental results were not consistent with the tricyclobutionium species (Figure 6.2).[195]

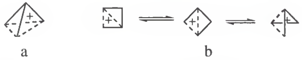

Figure 6.1 nonclassical ion (a) and equilibrating bridged ions

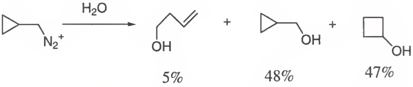

Figure 6.2 Product distributions for the trapping the cyclopropylcarbinyl cation

The NMR studies carried out by Olah, Roberts and coworkers in superacid media[196] suggested an equilibration involving nonclassical bicyclobutonium ions and the bisected cyclopropylcarbinyl cation (Figure 6.3) and this was corroborated by *ab initio* calculations,[197] which revealed that the two structures have very similar energies and can interconvert with a low barrier.

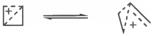

Figure 6.3 The equilibration between nonclassical bicyclobutonium and the bisected cyclopropylcarbinyl cation

Consistent with cation delocalization, the cyclopropylcarbinyl cation is a highly stabilized cation comparing even with the benzyl cation (Table 6.1).[198] From the molecular orbital point of view, the stability is rationalized by the excellent overlap of the π-Walsh orbitals with the adjacent unoccupied p orbital (Figure 6.4). As a result, the positive charge is delocalized over the ring system, the proximal C-C bond being lengthened and the distal C-C bond being shortened.

Table 6.1 Stabilization energies relative to CH_3^+ (kcal/mol)

Ion	Energies
CH_3^+	0
CH_3—CH_2^+	36
Ph—CH_2^+	55
C_3H_6—CH_2^+	58 [a]
HO—CH_2^+	60

a. C_3H_6 = cyclopropyl

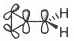

Figure 6.4 Bisected cyclopropylcarbinyl cation

The unusual stability of cyclopropylcarbinyl cations had been inferred from rapid rates of solvolysis reactions of cyclopropylmethyl derivatives. Hart and his co-workers have provided a striking demonstration of the effect of cyclopropyl groups on cation stability(Table 6.2).[199] Each replacement of an isopropyl by a cyclopropyl group results in a rate enhancement of 10^2-10^3 in solvolysis rate.

Table 6.2 Relative first-order rate constants for solvolyses in dioxanin (X= *p*-nitrobenzoate)

Compound	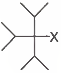	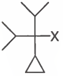	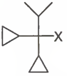
Relative rates	1.00	246	23,500

The effects of substituents at the β carbon of the cyclopropyl ring on solvolysis rates of cyclopropylmethyl derivatives are shown in Table 6.3.[200,201] A cation stabilizing group such as β-methyl can accelerate the rate around 10 times, and a β-alkoxy substituent can accelerate the rate nearly 1000 times. However compared with methyl and alkoxy groups, phenyl substituent has an only small effect on the solvolyses rate.

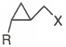

Table 6.3 Relative first-order rte constants for solvolyses of cycloporpylmethyl derivatives substituted at the *trans-β* carbon.

R	Relative rate
H[a]	1
Methyl[a]	11
Ethoxy[a]	940
Phenyl[b]	2.19

a. 3,5-dinitrobenzoates in 60% aqueous acetone at 100 °C.
b. *β*-Naphthalenesulfonates in 90% aqueous dioxane at 25 °C.

The substituents not only influence the kinetics of the solvolyses of the cyclopropylmethyl derivetives, but also determine the regiochemistry of the ring opening to form the more stable isomeric acyclic cation as shown in Figure 6.5.[202]

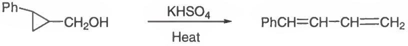

Figure 6.5 With a phenyl on the ring the only product observed was derived from the proximal C-C bond cleavage on the ring

By manipulating the differences in regiochemistry that different substituents exert on the radical and cation ring openings, Newcomb developed a mechanistic probe that could distinguish between a radical and carbocation intermediate (Figure 6.6).[203] In evaluating the efficacy of this probe, it should be remembered that in addition to its ability to differentiate between the intermediacy of a radical and a carbocation, it should ideally play simply the role of an "observer" of the reaction. That is, it should not exert a significant mechanistic influence upon the reaction system it is testing.

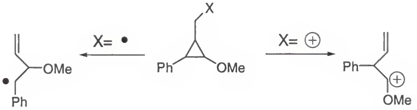

Figure 6.6 Newcomb's probe that could distinguish radical and cation mechanism

If the diagnostic probe itself has a steric or electronic bias so as to favor or disfavor one of the possible mechanistic pathways, then the interpretation of the results from use of such a probe may be ambiguous. This is certainly one of the potential flaws of any cyclopropylcarbinyl system that purports to distinguish carbocation from radical intermediate, because although the cyclopropyl group should exert little if any kinetic influence upon a radical-forming process, it is well recognized to greatly enhance the formation of carbocations (*vide supra*). Carbocation-stabilizing substituents such as alkoxy groups will serve to make such enhancements greater. Therefore, experimental results obtained from use of most of the present cyclopropyl carbinyl probes need to be interpreted with care in those cases where a carbocation intermediate is detected.

Fluorine substitution effects on the cyclopropylcarbinyl cation formation were overlooked during the "golden era" of carbocation research. There are only a few qualitative studies that have recently appeared in the literature.[139,204,205] Because β-fluorine substituents destabilize carbocations, whereas α-fluorines are stabilizing, it appeared likely to us that reactions involving the 2,2-difluorocyclopropyl-carbinyl cation (Figure 6.7 a), would undergo rearrangement via a regiospecific cleavage of the *proximal* bond to form the1,1-difluorobut-3-enyl cation (Figure 6.7 b).

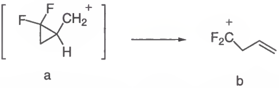

Figure 6.7 2,2-difluorocyclopropylcarbinyl cation (a) may ring opening with proximal C-C bond cleavage on the ring to the CF_2 group

The 2,2-difluorocyclopropylcarbinyl radical (Figure 6.8 a), as discussed in previous chapter, undergoes an extraordinarily-fast, regiospecific unimolecular ring-opening distal to the geminal fluorine substituents to form the 2.2-difluoro-3-butenyl radical (Figure 6.8 b).[156] Its calculated activation enthalpy of 1.6 kcal/mol and activation entropy of –2 e.u.(Chapter 4) , and the experimental rate constant of 1.0 x $10^{11}s^{-1}$ at 99.3 °C (Chapter 5) qualifies this system as a "hypersensitive" probe of reactions involving radicals as intermediates. Thus, 2,2-difluorocyclopropylcarbinyl moiety potentially has the basic trait of a probe that can distinguish radical and carbocation intermediate and its legitimacy (*vide supra*) of being such a probe has been examined both computationally and experimentally as described below.

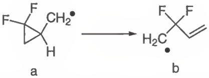

Figure 6.8 2,2-difluorocyclopropylcarbinyl radical ring opening with the distal C-C bond cleavage on the ring.

Computational Studies

Wishing to obtain some computational corroboration of our intuitive presumptions, calculations were carried out trying to locate the 2,2-difluorocyclopropylcarbinyl cation on the potential energy surface at HF/6-31G(d), MP2/6-31G(d) and B3LYP/6-31G(d) levels of theory. However, in all cases, the geometry optimizations starting from the 2,2-difluorocyclopropylcarbinyl cation (Figure 6.7 a) structure all ended up with the optimized 1,1-difluoro homoallylic cation (Figure 6.7 b). The B3LYP/6-31G(d) optimized geometry of the 1,1-difluoro-homoallylic cation is depicted in Figure 6.9. The planar geometry of the CF_2+ site of the 1,1-difluoro-homoallylic cation, and its unusually short C-F bonds (1.272 Å) are consistent with stabilization of the carbocation by its fluorine substituents. The 1.340 Å C-C bond indicated a fully characterized double bond. The Mulliken charge of the CF_2 group is +0.55, and that of the CH_2 at the original carbinyl position is +0.21.

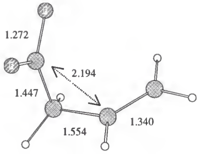

Figure 6.9 B3LYP/6-31G(d) optimized structure of 1,1-difluoro homoallylic cation. Distance is in Å.

The attempt to locate a *2,2*-difluoro homoallylic cation (Figure 6.10 a) also ended up as the 1,1-difluoro homoallylic cation. These results indicate that on the potential energy surface, 2,2-difluorocyclopropylcarbinyl cation, at least in the gas phase, is *not* a minimum, and also that there are no saddle points connecting a 2,2-difluorocyclopropylcarbinyl to a 1,1-difluoro homoallylic cation; thus there is no activation barrier for this transformation. Another possible cation, the 3, 3-difluorocyclobutyl cation (Figure 6.10 b), was able to be located, but it is 17.8 kcal/mol higher in energy than the 1,1-difluoro homoallylic cation. The most stable cation of the formula $C_4H_5F_2^+$ (Figure 6.10 c) that of α,α-difluorocyclopropylcarbinyl was located and is 8.4 kcal/mol more stable than the 1,1-difluoro-homoallylic cation. However, because the bridged bicycobutonium ion, which is the intermediate required for the scramble, was not located, it is not likely that (6.10 c) is going to be formed from (6. 7 a).

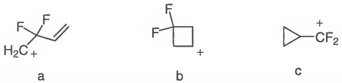

Figure 6.10 Cations that could be derived from 2,2-difluorocyclopropylcarbinyl cation

Compared to the cyclopropylcarbinyl cation, the 1,1-difluoro homoallylic cation is destabilized by 5.2 kcal/mol (B3LYP/6-311+g(2df,2p)//B3LYP/6-31G(d)) as shown in the hypothetical reaction (Figure 6.11), which indicates the conjugative stabilizing effect of fluorine toward α cation, was largely offset by the inductive destabilizing effect toward the non α cation distributed on the whole molecule.

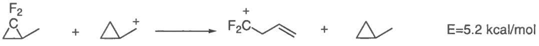

Figure 6.11 Relative hydride affinity of cyclopropylcarbinyl cation and 2,2-difluorocyclopropylcarbinyl cation

With a methyl group at the carbinyl position of 2,2-difluorocyclopropylcarbinyl cation, the cation behaved the same as did (6.7 a) at the HF/6-31G(d) level of theory. The structure of the ring-opened cation has been depicted in Figure 6.12. The Mulliken charge of the CF_2 group is +0.63.

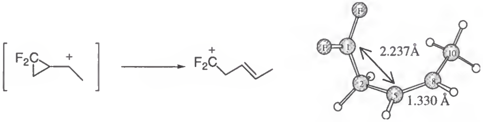

Figure 6.12 Calculated structure of 2,2-difluorocyclopropylcarbinyl cation with a methyl group at the carbinyl position

When the methyl substituent is at the 3 position on the ring, the regiochemistry of the ring opening is apparently altered. At HF/6-31G(d) level of theory, the geometry optimization starting from the ring closed carbinyl cation ended up with the cation observed by the lengthening of C-C bond distal to the CF_2 group (Figure 6.13). The Mulliken charge of the CH group at C3 is +0.26, the CH_2 group at C7 is 0.34 and the CF_2

group is 0.26. The distance of C2-C3 is 2.030Å. This is not a well-defined ring opened cation, more likely being a delocalized cation.

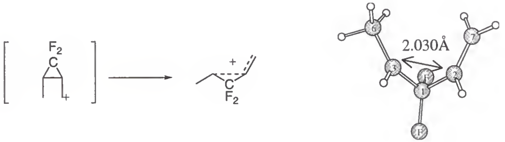

Figure 6.13 Calculated structure of 2,2-difluorocyclopropylcarbinyl cation with a methyl group on the ring

Therefore, according to this computational result, it can be predicted that a solvolysis, such as that depicted in Figure 6.14, should *not* proceed *via* the cyclopropylcarbinyl cation intermediate, but should proceed, *via* synchronous ionization and cleavage of the C-C bond proximal to the CF_2 group, directly to the 1,1-difluoro homoallylic cation (Figure 6.7 b). This result will lead to attachment of the nucleophile to the fluorinated carbon, with the reaction thus exhibiting a regiochemistry different from that of the radical. The rate of the solvolysis will be substantially slower than that of the non-fluorinated system. The same results will be obtained when a methyl group is attached to the carbinyl position.

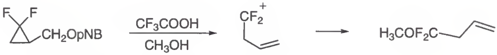

Figure 6.14 Predicated solvolysis reaction

With a methyl group at the 3 position on the ring, the solvolysis reaction should give the ring opened product with the C-C bond cleavage distal to CF_2 group which has the same regiochemistry of radical ring opening, as well as the ring closed product (Figure 6.15).

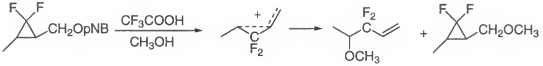

Figure 6.15 Predicated reaction

Experimental Studies

Syntheses of Cation Precursors and Authentic Products

The cation precursor 2,2-difluorocyclopropylcarbinyl tosylate **64** (not the p-nitrobenzoate because of its stability in both acetic acid and trifluoroacetic acid) was synthesized in a straight forward manner(Figure 6.16). The allyl p-nitrobenzoate **61** was synthesized by esterification of allyl alcohol with p-nitrobenzoate chloride in the presence of pyridine in THF. The ester was cyclopropanated using 2.5 equivalents $FSO_2CF_2COOTMS$, a difluorocarbene reagent described in chapter 2 to give ester **62** with 75% conversion at 97°C without solvent. This was the very first reaction that showed the exceptional efficiency of this carbene reagent towards electron deficient alkenes. Without purification, the ester **62** was hydrolyzed in one pot in 10% aqueous NaOH to provide 2,2-difluorocyclopropylcarbinol **63** in an overall 57% of yield for the two steps. The alcohol **63** was tosylated with tosylate chloride in pyridine at 4 °C to give the desired 2,2-difluorocyclopropylcarbinyl tosylate **64**.

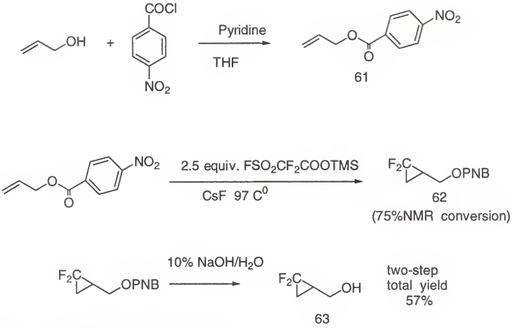

Figure 6.16 Synthesis of cation precursor

Synthesis of the authentic ring closed products, 2,2-difluorocyclopropylcarbinyl acetate and 2,2-difluorocyclopropylcarbinyl trifluoroacetate, were first attempted unsuccessfully via the cyclopropanation of the respective allyl ester in neat reaction before the final difluorocyclopropanation procedure was developed. Allyl acetate gave some product in a very low yield, and the small amount of product was difficulate to isolate. Allyl trifluoroacetate gave no sign of difluorocyclopropane formation.

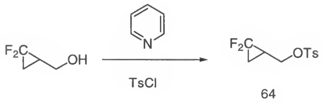

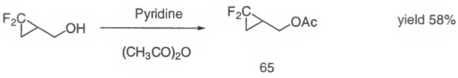

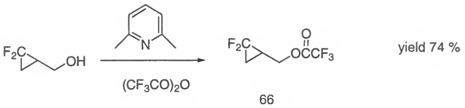

Figure 6.17 Synthesis cation precursor and authentic products

The acetate **65** was successfully synthesized from the esterification reaction of alcohol **63** with acetic anhydride in the presence of pyridine. However, the same reaction failed for trifluoroacetic anhydride. By replacing pyridine with 2,6- lutidine, the trifluoroacetate **66** was finally synthesized (Figure 6.17). The ring-opened products could be isolated carefully from the solvolysis reaction mixtures.

Results and Discussion

The kinetic studies were carried out in sealed capillary tubes using $PhCF_3$ as the ^{19}F NMR internal standard. As shown in the ^{19}FNMR spectrum, the solvolysis of 2,2-difluorocyclopropylcarbinyl tosylate **64**, in glacial acetic acid at 96.6 °C, gave a product mixture exhibiting two triplet product peaks and a set of new difluorocyclopropyl peaks, which were later assigned as ring-opened **67** and **68** and non-ring-opened products **65**, respectively, by comparison with the authentic samples. The total NMR mass balance was 92% (Figure 6.18). The formation of **67** and **68** reflect exclusively the regiochemistry of ring-opening that had been predicted computationally. The ring closed product **65** was proved to be stable under these reaction conditions in a control experiment. Therefore, the ratio of ring opened products to the ring closed products represents the actual product distribution of the tosylate solvolysis without secondary reactions having occurred.

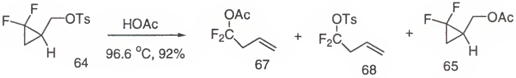

67 : 68 : 65 = 39 : 4.4 : 56.5

Figure 6.18 The acetolysis experiment of **64**

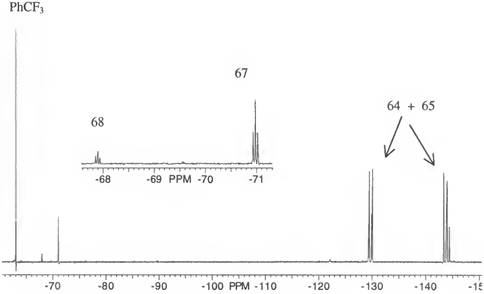

Figure 6.19 ^{19}F NMR spectrum of **64** acetolysis

The rate of solvolysis was measured by monitoring the disappearance of the starting ester **64** using ^{19}FNMR to give an observed first order rate constant $(1.0 \pm 0.1) \times 10^{-5}\ s^{-1}$. Assuming that the ring-opened and ring-closed products derived from competing S_N1 and S_N2 processes, respectively, the partial rate factors for the two processes could be calculated. Giving the ratio of ring opened and ring closed product 44 : 56, the S_N1 process, in which tosylate **64** undergoes heterolytic cleavage to (presumably) form ring-opened cation (Figure 6.7 b), which then is trapped by either HOAc or TsO^- to give products **67** and **68**, was assigned a first-order rate constant (k_Δ) of $(4.4 \pm 0.1) \times 10^{-6} s^{-1}$, and the process involving solvent participation, which led to ring-closed product **65**, was assigned a pseudo first-order rate constant (k_s) of (5.8 ± 0.1) x $10^{-6}s^{-1}$ (Figure 6.19) (Table 6.4).

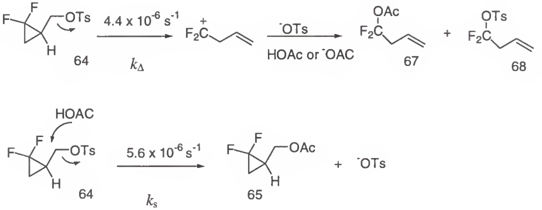

Figure 6.19 The S_N1 process led to ring opened products **67** and **68**. The S_N2 process led to the ring closed product **65**.

In order to confirm that competitive unimolecular and bimolecular reactions were involved, and that all three products do not derive from an equilibrated or delocalized common intermediate carbocation, additional acetolysis experiments were carried out in 0.200M and 0.400M NaOAc/HOAc solutions. This provided the observed solvolysis rate constants (2.87 ± 0.07) x 10^{-5} s^{-1} and (4.7 ± 0.3) x 10^{-5} s^{-1} respectively, which were attributed to $k_\Delta = 4.6 \times 10^{-6}$ s^{-1}, $k_s = 2.4 \times 10^{-5}$ s^{-1} for 0.200 M solution and $k_\Delta = 4.7 \times 10^{-6}$ s^{-1}, $k_s = 4.2 \times 10^{-5}$ s^{-1} for 0.400 M solution based on the product distributions (Table 6.4).

Correcting k_s by subtracting the background k_s(HOAc) (which is the k_s in pure HOAc), one can obtain the pseudo first-order rate constants $k_s(^-OAc)$ that reflect the rates of nucleophilic attack by acetate ion. The values for $k_s(^-OAc)$, 1.8 (±0.1) and 3.6 (±0.4) x $10^{-5}s^{-1}$ for 0.200M and 0.400M [^-OAc], respectively, clearly demonstrate the dependence on [^-OAc], hence the S_N2 nature of the process that leads to non-ring-opened product **65**.

On the other hand, the values of k_Δ for the three reactions increase only slightly, consistent with the influence of a small salt effect on the ionization in a S_N1 process (Figure 6.19).

Table 6.4 Kinetic Results for Solvolyses of 2,2-Difluorocyclopropylcarbinyl Tosylate in NaOAc/HOAc Solutions at 96.6 °C.

Conditions	Pure HOAc	0.200M NaOAc	0.400M NaOAc
k_{obs} ($10^{-5}s^{-1}$)	1.0 ±0.1	2.87 ±0.07	4.7 ±0.3
Mass Balance (%)	92	92	90
Ratio 65/(67+ 68)	57:43	84:16	90:10
k_S ($10^{-6}s^{-1}$)	5.8	24	42
k_Δ ($10^{-6}s^{-1}$)	4.4	4.6	4.7

These results only demonstrate the prevalence of S_N1 and S_N2 processes in the formation of ring opened and ring closed products, respectively, but do not completely rule out the possibility, within experimental kinetic error that some of **65** might be formed via the S_N1 process, a possibility that conceptually influences the description of the carbocation (Figure 6.20).

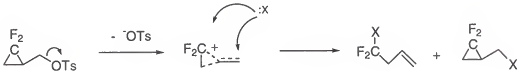

Figure 6.20 Common ion mechanism

However, when the solvolysis was carried out in trifluoroacetic acid, a solvent of high ionizing power but poor nucleophilicity, only ring-opened products were formed, under conditions where the potential ring-closed product, 2,2-difluorocyclopropylcarbinyl trifluoroacetate **66**, was demonstrated to be stable to the solvolytic conditions (Figure 6.21). Thus, a common ion mechanism and as that depicted in Figure 6.20 can be effectively excluded. The rate constant of this solvolysis is $k_\Delta = (8.8 \pm 0.8) \times 10^{-5} s^{-1}$ at 52.1°C with a mass balance of 92% throughout the reaction.

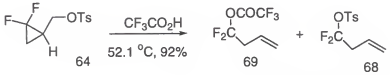

69: 68 = 2.1 : 1

Figure 6.21 Only ring opened products were observed in the solvolysis of **64** in trifluoroacetic acid

The above solvolytic results are completely consistent with the ionization of **64** proceeding directly and regiospecifically to the homoallylic carbocation (Figure 6.7 b), as had been predicted computationally.

Our results would appear to be at odds with an earlier report by Schlosser which indicated that solvolysis of 2,2-difluoro-3,3-dimethylcyclopropylcarbinyl tosylate proceeded with regiospecific *distal* ring-opening (Figure 6.22).[204] However, calculations at HF/6-31G(d) level of theory indicated that even a *single* methyl group on the cyclopropane ring is apparently sufficient to alter the regiochemistry in favor of distal ring-opening (*vide supra*). This simply indicates, of course, that the stabilization provided by a methyl group must be sufficiently greater than that provided by the two fluorine substituents in order to overcome the *de*stabilization of the β-fluorines.

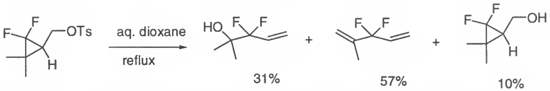

Figure 6.22 With two methyl substituents on the ring the products derived from the distal cleavage to the CF_2 group on the ring were observed

With the 2,2-difluorocyclopropylcarbinyl radical and cation both undergoing requisite, ultra-fast ring-opening, but with opposite regiochemistries, the system certainly qualifies as a hypersensitive probe capable of distinguishing between the two types of mechanisms.

Table 6.5 Relative rate (k_Δ) of acetolysis of tosylates at 96.6°C

Substrates	Relative Rate
Cyclopropylcarbinyl tosylate	8.4×10^4
2,2-difluoro cyclopropylcarbinyl tosylate	1
Isobutyl tosylate	0.56

In evaluating the efficacy of this probe, the acetolysis rate of the tosylate **64** which reflects the ease of cation formation, was compared with those of isobutyl tosylate[206] and cyclopropylcarbinyl tosylate[207] (which we extrapolated from their respective activation parameters) (Table 6.5).

At 96.6 °C, the 8.4×10^4 times decrease of acetolysis rate of 2,2-difluorocyclopropylcarbinyl tosylate relative to that of cyclopropylcarbinyl tosylate, revealed a substantial inductive destabilizing influence on its ionization transition state due to the fluorine substituents on the ring, a result which is consistent with the computational result (Figure 6.11).

More strikingly, the rate constant (k_Δ) in the acetolysis of **64** is only 1.8 times greater than that of isobutyl tosylate at 96.6 °C, which means that the net result of such diminished reactivity is to essentially eliminate the rate enhancing effect of the cyclopropylcarbinyl moiety relative to a typical primary substrate, such as isobutyl tosylate. Therefore, as a result, the 2,2-difluorocyclopropylcarbinyl system exhibits *no* kinetic bias towards either the radical or the carbocation mechanism.

As the smallest atom next to hydrogen, fluorine substituents should impose very little or no steric influence in a system to be tested, especially when they are compared with phenyl substituents. The stereoelectronic influence should also not pose a problem for the 2,2-difluorocyclopropylcarbinyl system. The distinct ^{19}FNMR of ring closed and ring opened products provide a convenient analysis method for mechanistic study.

Conclusion

On the basis of our kinetic and computational studies indicating that the 2,2-difluorocyclopropylcarbinyl radical and cation systems, are sterically and electronically benign, but exhibit high rearrangement reactivity and regiospecificity, we concluded that the 2,2-difluorocyclopropyl carbinyl system should be capable of acting as an ideal, hypersensitive probe of radical and/or carbocation mechanisms.

An extensive study of substitution effects on this probe is necessary in order to define its limitations. Such experiments are crucial to interpreting the results form future mechanistic studies. The preliminary computational findings, that the property of the probe will be preserved with an alkyl substituent at the carbinyl position while, diminished with an alkyl substituent on the ring, need to be demonstrated experimentally.

CHAPTER 7
EXPERIMENTAL

General Methods

All ^{1}H NMR spectra were recorded at 300 MHz, ^{13}C spectra at 75 MHz and ^{19}F spectra at 282 MHz on Varian VXR-300 and Gemini-300 NMR spectrometers. The chemical shifts of ^{1}H signals are reported in parts per million (ppm) down field relative to tetramethylsilane (TMS) (δ=0.00) in $CDCl_3$. ^{13}C signals are expressed in ppm using the central peak of the $CDCl_3$ signal as internal standard (δ=77.00). ^{19}F NMR are reported in ppm using $CFCl_3$ as internal standard (δ=0.00).

Kinetic studies at the temperature lower than 250 °C were carried out in an oil-bath within a Statim temperature controller. A fused-salt bath (±0.1 °C) were used for high temperature (> 250 °C) kinetic studies.

GC analyses were done on a Hewlett-Packard HP5890 instrument, equipped with a HP 3396A integrator.

Preparative gas chromatographic separations were carried out with a 20 foot x 0.25 inch copper column packed with 20% SE-30 on Chromosorb P.

High resolution mass spectra were obtained on a Finnegan MAT-95 spectrometer.

The kinetic plots were obtained using least square method. The errors were report as 2σ (2S) with 95% interval.

All reagents, unless otherwise specificed, were purchased form Aldrich, Fisher, or Acros, and used as received. Dichloromethane was distilled form calcium hydride and used immediately. Diethyl ether and tetrahydrofuran (THF) were distilled form sodium bensophenone ketyl and used immediately.

All calculations were performed with the Gaussion94(W) and Gaussion98W[131] program systems on IBM RS/6000 SP2 cluster, or intel-based PCs. All stationary points were characterized by harmonic frequency analysis, minima and transition structure giving rise to zero or exactly one negative eigenvalue, repectively, in the second derivative matrix. Hatree-Fork and Density functional theory frequencies and resultant zero-point energies have been scaled by a factor of 0.8929 and 0.9804, respectively.

Experimental of Chapter 2

General Remarks

The reagent, fluorosulfonyldifluoroacetic acid, was provided by Professor Qing-Yun Chen from Shanghai Institute of Organic Chemistry, China

Synthesis of Compounds

Trimethylsilyl fluorosulfonyldifluoroacetate (**21**)

A dry 1L three neck-round bottom flask, equipped with a magnetic stirring bar and an addition funnel, was charged with 150g (0.85mol, 1 equiv.) of fluorosulfonyldifluoroacetic acid. Under N_2, at 0 ^{0}C, 329 g (3.05 mol, 3.6 equiv.) of TMS chloride was added dropwise. The generated HCl was absorbed by10% NaOH aqueous solution. Upon the complete of the addition, the reaction mixture was stirred at room temperature over night and distilled (27mmHg, 62 ~ 63 ^{0}C) to afford 166 g (0.66 mol) (Yield, 78%) of product. ^{1}H NMR δ 0.395 (s); ^{13}C NMR δ 155.131(t, $J_{(C\text{-}F)} = 27.0$ Hz), 112.223(dt, $J_{d(C\text{-}F)} = 31.5$ Hz, $J_{t(C\text{-}F)} = 299.0$ Hz), -1.050. ^{19}F NMR δ 40.581 (1F, s), -103.744 (2F, s). HRMS (CI), $C_5H_{10}O_4S_1Si_1F_3$ calculated: $(M+1)^+$, 251.0012, found 251.0015.

General exploration procedure of difluorocyclopropanation

A dry two-neck pear shape flask, equipped with a magnetic stirring bar, was charged with initiator (NaF, KF or CsF), olefin and solvent. Under N_2 and at elevated temperature, trimethylsilyl fluorosulfonyldifluoroacetate(21) was added slowly using a syringe pump through a Teflon® needle. Upon the completion of addition, the reaction mixture was stirred for 20 minutes and cooled to room temperature. Certain amount of α,α,α-trifluorotoluene was added as internal standard to calculate the ^{19}F MNR yields. The reaction conversions were estimated by ^{1}HNMR integration of products and starting materials assuming no significant amount of by-products were formed. Products were purified either by column chromatography (10% diethyl ether/hexanes) or distillation.

2,2-difluorocyclopropylcarbinyl benzoate (**22**)

Neat reaction. Column chromatography purification. (10% diethyl ether/hexanes).Colorless liquid. ^{1}H NMR δ 8.040 (2H,m), 7.562(1H, tt, J_t= 7.5 Hz, J_t= 1.5 Hz), 7.435(2H, m), 4.450(1H, dddd, $J_{d(H\text{-}H)}$=12.0 Hz, $J_{d(H\text{-}H)}$=7.5 Hz, $J_{d(F\text{-}H)}$=2.7 Hz, J_d=1.5 Hz), 4.293(1H, ddd, $J_{d(H\text{-}H)}$=12.0 Hz, $J_{d(H\text{-}H)}$=8.1 Hz, J_d= 1.8 Hz), 2.083(1H, dddt, J_d=13.2 Hz, J_d=11.4 Hz, J_d=7.8 Hz, J_t=7.8 Hz), 1.561(1H, tdd, J_t=11.4 Hz, J_d=7.8 Hz, J_d= 4.5 Hz), 1.285(1H, dtd, J_d= 13.2 Hz, J_t= 7.8 Hz, J_d=3.9 Hz); ^{13}C NMR δ166.367, 133.164, 129.774, 129.652, 128.397, 112.994(t, $J_{t(C\text{-}F)}$ = 282.5Hz), 61.621(d, $J_{d(C\text{-}F)}$ = 5.5Hz), 21.116(t, $J_{t(C\text{-}F)}$ = 11.6 Hz), 15.040(t, $J_{t(C\text{-}F)}$ $J_{t(C\text{-}F)}$ $J_{t(C\text{-}F)}$= 11.1 Hz); ^{19}F NMR δ129.646(1F, ddddd, $J_{d(F\text{-}F)}$= 160.0 Hz, $J_{d(F\text{-}H)}$=13.0 Hz, $J_{d(F\text{-}H)}$=11.6 Hz, $J_{d(F\text{-}H)}$= 4.0 Hz, $J_{d(F\text{-}H)}$=2.5 Hz, $J_{d(F\text{-}H)}$= 0.6 Hz), 143.781(1F, ddddd, $J_{d(F\text{-}F)}$=160.0 Hz, $J_{d(F\text{-}H)}$=13.3 Hz, $J_{d(F\text{-}H)}$=4.8 Hz, $J_{d(F\text{-}H)}$= 2.0 Hz, $J_{d(F\text{-}H)}$=0.6 Hz); HRMS (CI) $C_{11}H_{11}O_2F_2(M+1)^+$, calc. 213.0727, found 213.0752.

2-(2',2'-difluorocyclopropyl)ethyl benzoate (**23**)

Neat reaction. Column chromatography purification. (10% diethyl ether/hexanes).Colorless liquid. ^{1}H NMR δ 8.040(2H, m), 7.553(1H, m), 7.430(2H, m), 4.390(2H, m), 1.960(1H, m), 1.880(1H, m), 1.650(1H, ddq, J_d = 13.8 Hz, J_d =11.1Hz, J_q

= 7.2 Hz), 1.440(1H, tdd, J_t = 11.7 Hz, J_d = 7.8 Hz, J_d = 4.2 Hz), 1.003(1H, dtd, J_d = 12.9 Hz, J_t = 7.5 Hz, J_d = 2.4Hz); ^{13}C NMR δ 166.501, 133.017, 130.053, 129.552, 128.390,113.909(t, $J_{t(F\text{-}C)}$=283.5 Hz), 63.660(d, $J_{d(F\text{-}C)}$= 2.0 Hz), 26.384(d, J_d= 4.1 Hz), 19.707(t, $J_{t(F\text{-}C)}$= 11.1 Hz), 15.902(t, $J_{t(F\text{-}C)}$= 10.6 Hz); ^{19}F NMR δ -129.434(1F, dddtd, $J_{d(F\text{-}F)}$ = 155.8 Hz, $J_{d(F\text{-}H)}$= 13.8 Hz, $J_{d(F\text{-}H)}$= 12.7 Hz, $J_{t(F\text{-}H)}$ = 3.7 Hz, $J_{d(F\text{-}H)}$= 1.1 Hz), -144.322(1F, dddt, $J_{d(F\text{-}F)}$= 155.8 Hz, $J_{d(F\text{-}H)}$= 12.7 Hz, $J_{d(F\text{-}H)}$= 4.2Hz, $J_{t(F\text{-}H)}$= 1.4 Hz); HRMS (CI), $C_{12}H_{13}O_2F_2(M+1)^+$, calc. 227.0884, found 227.0889.

Preparation of 3-(2',2'-difluorocyclopropyl)propyl benzoate **(24)**

A 25 ml dry two-neck round bottom flask, equipped with a magnetic stirring bar, was charged with 2.3 mg of initiator NaF and 0.900g (4.8 mmol, 1 equivalent) of 4-pentenyl benzoate. Under N_2 and at 105 °C, 1.8g (7.2 mmol, 1.5 equivalent) of trimethylsilyl fluorosulfonyldifluoroacetate(21) was added slowly using a syringe pump through a Teflon® needle over a period of 5 hours (When 1.3 equivalent of difluorocarbene was added, the conversion is 97% and after 1.5 equivalent of carbene precursor was added, no starting material remained in the reaction mixture). Upon the completion of the addition, the reaction mixture was stirred for 20 minutes and cooled to room temperature and diluted with 30 ml of diethyl ether. The solution was washed with water, 5% sodium bicarbonate, water and brine and dried over sodium sulfate. The solvent was removed under reduced pressure. Purification of products on flash column chromatography (10% diethyl ether/hexanes) provided 0.98g of colorless liquid (Yield, 86%). ^{1}H NMR δ 8.020(2H, d, J_d = 7.8 Hz), 7.530(1H, t, J_t = 7.3 Hz), 7.412(2H, t, J_t = 7.6 Hz), 4.333(2H, t, J_t = 6.4 Hz), 1.876(2H, p, J_p= 6.8 Hz), 1.60(2H, m), 1.52 (1H, m), 1.362 (1H, tdd, J_t= 11.1 Hz, J_d= 7.5 Hz, J_d= 4.0 Hz), 0.904(1H, dtd, J_d= 13.2 Hz, J_t= 7.1

Hz, J_d= 3.5 Hz); ^{13}CNMR δ 166.408, 132.835, 130.144, 129.409, 128.261, 114.319(t, $J_{t(F-C)}$= 283.5 Hz), 64.013, 27.893(d, $J_{d(F-C)}$= 1.5 Hz), 23.479(d, $J_{d(F-C)}$= 3.5 Hz, 21.880(t, $J_{t(F-C)}$= 10.6 Hz), 15.977(t, $J_{t(F-C)}$= 10.6 Hz); ^{19}F NMR δ -128.636(1F, dt, $J_{d(F-F)}$= 155.8 Hz, $J_{t(F-H)}$= 12.7 Hz), -145.219(1F, dd, $J_{d(F-F)}$= 155.8 Hz, $J_{d(F-H)}$= 12.7 Hz); HRMS (CI) calculated: $C_{13}H_{15}O_2F_2$, (M+1)$^+$, 241.1040, found: 241.1000.

Cis-7,7-difluoro-trans-2-benzoatebicyclo[4.1.0] heptane (***cis*-25**)

Neat reaction. Column chromatography purification (10% diethyl ether/hexanes).Colorless liquid. ^{1}H NMR δ 8.073 (2H, d, J_d= 7.5 Hz), 7.568(1H, t, J_t = 7.5 Hz), 7.450(2H, t, J_t =7.5 Hz), 5.440(1H, dtd, J_d= 10.2 Hz, J_t = 6.6 Hz, J_d = 3.0 Hz), 2.10~1.86(3H, m), 1.76~1.18(5H, m); ^{13}C NMR δ 166.261, 132.982, 130.291, 129.690, 128.334, 114.993(t, J_t= 285.1 Hz), 67.805(t, $J_{t(F-C)}$= 2.0 Hz), 26.650(dd, $J_{d(F-C)}$= 3.5 Hz, $J_{d(F-C)}$ = 1.1 Hz), 22.127(t, $J_{t(F-C)}$= 11.1 Hz), 21.550(d, $J_{d(F-C)}$ = 3.5 Hz), 20.932(dd, $J_{d(F-C)}$= 12.1 Hz, $J_{d(F-C)}$= 9.1 Hz), 15.746(d, $J_{d(F-C)}$= 2.5 Hz); ^{19}F NMR δ -123.525(1F, dt, $J_{d(F-F)}$= 160.0 Hz, $J_{d(F-H)}$= 12.7 Hz), -148.191(1F, d, $J_{d(F-F)}$= 160.0 Hz); HRMS (CI), calculated: $C_{14}H_{15}O_2F_2$, (M+1)$^+$, 253.1040, found: 253.1008.

Trans-7,7-difluoro-trans-2-benzoatebicyclo[4.1.0] heptane (***trans*-25**)

Neat reaction. Column chromatography purification (10% diethyl ether/hexanes).Colorless liquid. The structure was confirmed by comparing the ^{19}F NMR of hydrolyzed reaction mixture with the literature data. ^{1}H NMR δ 8.073 (2H, dm, J_d= 7.5 Hz), 7.575(1H, tt, J_t = 7.5 Hz), 7.451(2H, tm, J_t =7.5 Hz), 5.362(1H, t, J_t= 4.2 Hz), 1.932(1H, m), 1.84~1.50(6H, m), 1.401(1H, m); ^{13}CNMR δ 165.780, 133.042, 130.297, 129.576, 128.368, 113.331(t, $J_{t(F-C)}$= 284.5 Hz), 64.921, 26.981(t, $J_{t(F-C)}$= 2.5 Hz), 22.474(t, $J_{t(F\text{-}C)}$= 10.9 Hz), 18.094(t, $J_{t(F\text{-}C)}$= 10.6 Hz), 16.478, 15.917; ^{19}F NMR δ 125.994(1F, dt, $J_{d(F\text{-}F)}$= 162.3 Hz, $J_{t(F\text{-}H)}$= 15.0 Hz), 149.677(1F, d, $J_{d(F\text{-}F)}$ = 162.3 Hz); HRMS (CI), calculated: $C_{14}H_{15}O_2F_2$, $(M+1)^+$, 253.1040, found: 253.1039.

N-butyl (2',2'-difluorocyclopropyl)formate **(26)**

A 25ml dry two-neck round bottom flask, equipped with a magnetic stirring bar and a condenser, was charged with 23 mg of initiator NaF, 5.0g (39 mmol, 1 equivalent) of butyl acrylate and 3.6g (39 mmol, 1 equivalent) of toluene. The flask was immersed in a 130 °C oil bath. Under N_2, trimethylsilyl fluorosulfonyldifluoroacetate (21) was added slowly using a syringe pump through a Teflon® needle. After 28 hours and 16g (1.6 equivalent) of (21) was added, ^{1}H NMR indicated that 100% of conversion was achieved. The reaction mixture was distilled (55mmHg, 98~100 °C) to give 6.08g of colorless liquid (Yield, 87%). The liquid became a little cloudy when contacted with air.

Experimental of Chapter 3

General remarks

The kinetic sample were analyzed by GC using a capillary chiral column (length 25m, ∅ 0.25nm, film thickness 0.25μm, stationary phase: polysiloxane-bonded cyclodextrin derivative) which was provided by Prof. V. Schurig and H. Grosenick from Institut für Organische Chemie, Universität Tübingen.

Synthesis of Starting Material

Cis-3-penten-1-ol **(35)**

A 250ml dried round bottom flask equipped with magnetic stirrer, was charged with $Pd/CaCO_3$ Pb poisoned (Lindlar) (0.3 g), 3-pentyne-1-ol (10.6 g, 126mmol), and absolute methanol (200ml). After the system was purged with H_2 three times, with vigorous stirring, 1 atmosphere of hydrogen was introduced. The consumption H_2 indicated the progress of the reaction. About 24hr later, the reaction completed, the reaction mixture was filtered through a celite bed to remove the catalyst and the solvent was removed by distillation. This provided 10.6 g of light yellow liquid product (Yield 98%). ^{1}H NMR, δ 5.62 (1H, dqt, J_d=10.8 Hz, Jq=6.9 Hz, J_t=1.6 Hz), 5.39 (1H, dtq, J_d=10.8 Hz, J_t=7.3 Hz, J_q=1.8 Hz), 3.63 (2H, t, J_t=6.6 Hz), 2.32 (2H, qdq, J_q=6.6 Hz, J_d=1.6 Hz, $J_{q=}$0.9 Hz), 1.63 (3H, ddt, J_d=6.7 Hz, J_d=1.8 Hz, J_t=0.9 Hz), 1.5 (1H, s). ^{13}C NMR, δ 127.2, 126.0, 62.3, 30.5, 12.9; HRMS (EI), calculated: $C_5H_{10}O$ M^+ 86.0732, found: 86.0711.

Cis-3-pentenyl butyrate (36)

Under N_2, an oven dried 250ml 1-neck round bottom flask equipped with magnetic stirrer was charged with dry THF (100ml) and cis-3-penten-1-ol (35) (8.61g, 100mmol). With stirring, at 0 °C, butyryl chloride (10.6g, 100mmol) and dry pyridine (7.9g, 100mmol) were added dropwise consecutively. Upon the completion of the addition, the cooling bath was removed and the reaction mixture was maintained at room temperature over night. After filtration over silica gel, THF was removed under reduced pressure and replaced by diethyl ether (200ml). The organic layer was washed with water, 0.1N NaOH, dried ($MgSO_4$). The solvent was removed under reduced pressure and this gave 13.6g product as yellow liquid (Yield 87%). ^{1}H NMR, δ 5.55 (1H, m), 5.34 (1H, m), 4.05 (2H, t, J_t=7.0 Hz), 2.35 (2H,q, J_q=7.0 Hz), 2.25 (2H, t, J_t=7.3 Hz), 1.62 (5H, m), 0.91 (3H, t, J_t=7.3Hz). ^{13}C NMR, δ173.7, 126.7, 125.3, 63.5, 36.2, 26.5, 18.4, 13.6, 12.8. HRMS (CI positive) calculated: $C_9H_{17}O_2$ $(M+1)^+$ 157.1229, found: 313.2339($2M+1^+$, 100%), 227.1714(10), 225.1864(33), 157.1242($M+1^+$, 28).

Cis-2-(2', 2'-difluoro-3'-methylcyclopropyl) ethyl butyrate **(37)**

A dry three-neck-round-bottom (TNRB) flask equipped with a magnetic stirrer was charged with NaI (40g, 267 mmol) and fitted with a solid-addition tube in which phenyltrifluoromethylmercury $PhHgCF_3$ (25g, 72mmol) was added. Under vacuum (0.5 mmHg) and at 150 °C, the NaI was dried overnight. With the protection of N_2, benzene (150ml) was distilled into the flask directly from Na/Benzophenone and cis-3-pentenyl butyrate (36) (13.0g, 83mmol) was introduced via a syringe. While refluxing, Phenyltrifluoromethylmercury was added over a period of 4 hours and 36 hours later, $PhHgCF_3$ was completely consumed. The reaction mixture was cooled to room temperature and diluted with 50ml benzene. Following the filtration, the filtrate was washed with water and dried over $MgSO_4$. The solvent was evaporated under reduce pressure to give the crude product (mainly product and starting material) which was separated by flash column chromatography (3% diethyl ether/hexanes), this provided 4.8g of product (liquid) (Yield 35%). ^1H NMR, an AB quartet centered at δ 4.10, further split into triplet (2H, J_{ab}=11.0 Hz, J_t=6.4 Hz), δ 2.27 (2H, t, J_t=7.5 Hz), 1.71 (2H, broad q, J_q=6.4 Hz), 1.63 (2H, h, J_h=7.3 Hz), 1.51(2H, m), 1.05 (3H, dddd, J_d=6.4 Hz, J_d=3.2 Hz, J_d=1.2 Hz, J_d=0.6 Hz), 0.93 (3H, t, J_t=7.3 Hz); ^{13}C NMR, δ 173.8, δ 114.7(dd, J_d=291.1Hz, J_d=284.0 Hz), 63.0, 36.1, 21.4, 21.1, 19.0, 18.4, 13.6, 5.6; ^{19}F NMR, δ -127 (1F, dt, $J_{d\ (F\text{-}F)}$=155 Hz, $J_{t\ (H\text{-}F)}$=14Hz), δ -155 (1F, d, $J_{d\ (F\text{-}F)}$=155 Hz); HRMS (CI) calculated: $C_{10}H_{17}F_2O_2$ $(M+1)^+$ 207.1197, found: 413.2252($2M+1^+$, 24), 207.1193(M+1)$^+$, 99.0614(100) ; Elemental analysis, calculated: C 58.22%, H 7.82%, found: C 58.23%, H 7.927%.

Optically active cis-1, 1-difluoro-2-(2'-hydroxyl)ethyl-3-methylcyclopropane (**38**)

A 250ml three-neck-round-bottom flask equipped with magnetic stirrer was charged with 100 ml H_2O, 20ml ethylene glycol. With stirring, at 3 °C PPL (Lipase type II, crude, from porcine pancreas, Sigma, 0.6g) was added. After the pH was adjusted to 6.5 by bubbling CO_2 into the basic solution, 2-(2', 2'-difluoro-3'-methylcyclopropyl) ethyl butyrate (**37**) (4.24g, 20.6mmol) was added. The pH was maintained around 6.5 by the titration of 1.0M NaOH using a syringe pump. After 5ml NaOH solution was added (40% completion), the reaction was quenched by saturating with NaCl. The reaction mixture was extracted with diethyl ether 4 times, dried over Na_2SO_4 and the solvent was removed under reduce pressure. Flush column chromatography purification (15%-50% diethyl ether / hexanes, the best visualization was achieved by using 5% H_2SO_4 in MeOH on TLC), provided 2.6g starting material and 0.63g product (d.e.%=13.6%) (d.e.% was checked by ^{19}F NMR of its (R)-(-)-O- Acetylmandelic acid ester). ^{1}H NMR, δ 3.70 (3H, t, J_t=6.6 Hz), 1.65 (2H, qdd, J_q=6.6 Hz, J_d=2.7 Hz, J_d=0.9 Hz), 1.61~1.48 (2H, m), 1.45 (1H, s), 1.05 (3H, ddd, J_d =6.3 Hz, J_d=3.0 Hz, J_d=1.5 Hz); ^{13}C NMR, δ 115.12 (dd, $J_{d\ (C\text{-}F)}$ =284 Hz, $J_{d\ (C\text{-}F)}$ =290 Hz), 61.98, 24.69, 21.35(t, $J_{t\ (C\text{-}F)}$ =10.3 Hz), 18.97 (t, $J_{t\ (C\text{-}F)}$ =10.3 Hz), 5.72 (d, $J_{d\ (C\text{-}F)}$ =4.6 Hz); ^{19}F NMR, -126.8 (1F, dt sextet, $J_{d\ (F\text{-}F)}$ =154.4 Hz, $J_{t\ (H\text{-}F)}$ =14.2 Hz, $J_{sextet\ (H\text{-}F)}$ =3.0Hz), -154.9 (1F, d, $J_{d\ (F\text{-}F)}$ =154.4 Hz); HRMS (CI positive), calculated: $C_6H_{11}F_2O$ (M+1)$^+$ 137.0778, found: 137.0773(M+1$^+$, 2%), 119.0723(15), 117.0759(14), 99.0616(100), 87.0577(32), 77.0221(14), 73.0482(12), 55.0464(16).

Optically active 2-(2', 2'-difluoro-3'-methylcyclopropyl) ethyl butyrate (optically active **37**)

A dry 50ml three -neck-round-bottom flask equipped with a magnetic stirrer was charged with optically active cis-1, 1-difluoro-2-(2'-hydroxyl)ethyl-3-methylcyclopropane (38) (0.59g, 4.3mmol) and 10ml dry THF, and with stirring cooled to 0 °C. Butyryl chloride (0.62g, 5.8mmol) and pyridine (0.41g, 5.2mmol) were dropped in consecutively. Upon the completion of the addition, the reaction mixture was maintained at 0 °C for 5 minutes and raised to room temperature with removing of the cooling bath.. After 5hrs, the reaction mixture was filtered and the solvent was evaporated under reduced pressure. The residue was purified by flash chromatography (10%diethylether / hexanes). This yielded 0.68g of product. (Yield 77%)

Higher optically active cis-1, 1-difluoro-2-(2'-hydroxyl)ethyl-3-methylcyclopropane (Higher optically active **38**)

Following the prior enzyme resolution procedure, 0.68g of the optically active 37 was hydrolyzed to give 90mg of alcohol with d.e.% of 28.5% (d.e. was checked by ^{19}F NMR of its (R)-(-)-O- Acetylmandelic acid ester).

Optically active cis-1, 1-difluoro-2-ethyl-3-methylcyclopropane (**39**)

Under N_2, a dried 25ml three-neck-round-bottom flask, equipped with a condenser and a magnetic stirrer, was charged with optically active alcohol (Higher optically active 38) (89mg, 0.65mmol), pentafluorophenyl chlorothionoformate (249mg, 0.95mmol), 10mg N-hydroxysuccinimide and 3ml toluene with stirring. After the solid was dissolved, pyridine (150mg, 1.9mmol) was dropped in and 30minutes later, the reaction mixture was filtered into a 50ml TNRB flask. More toluene (7ml) and tributyltin hydride (0.623g) were added. After purged with N_2 and with refluxing, 2ml-toluene solution of AIBN radical initiator (7.2mg) was added dropwise over a period of 25 minutes. The product was collected in a dry-ice trap and purified on preparative GC with a d.e.% of 30.2% (d.e .was checked by GC with the chiral column). ^{1}H NMR δ 1.43 (m, 4H), 1.05 (dd, 3H, J = 6.5, $^4J_{HF}$ = 3.4 Hz), 1.00 (t, 3H, J = 7.2 Hz); ^{13}C NMR δ 115.7 (t, J_{CF} = 287.6 Hz), 26.2 (dd, $^2J_{CF}$ = 10.0, 10.5 Hz), 19.1 (dd. $^2J_{CF}$ = 10.0, 10.5 Hz), 14.7 (d, $^3J_{CF}$ = 5.9 Hz), 13.6 (s), 5.3 (d, $^3J_{CF}$ = 6.6 Hz); ^{19}F NMR, δ -125.6 (1F, dt, $J_{d\ (F\text{-}F)}$ = 154.8 Hz, $J_{t\ (H\text{-}F)}$ = 14.7 Hz), -155.7 (1F, d, $J_{d\ (F\text{-}F)}$ =154.8 Hz); HRMS (EI), calculated: $C_6H_{10}F_2$ (M^+) 120.0751; found: 120.0745(M^+, 2%), 91.0332(100%).

Trans-3-penten-1-ol **(310)**

Under the protection of N_2, a 1000ml TNRB flask equipped with a magnetic stirrer, a dry ice condenser and an addition funnel, was charged with liquid ammonium (400ml), dry diethyl ether (50ml) and sodium (8g). Upon the dissolvation of the Na, a dry diethyl ether solution (100ml) of 3-pentyne-1-ol (8.30g) was dropped in slowly. After 4 hours of gentle reflux of the NH_3 solution, the reaction was quenched with NH_4Cl (9.5g) and the temperature was raised to room temperature to evaporate the NH_3. To the residue, 300 ml of ice water was added and extracted with diethyl ether (5x80ml). The organic layer was washed with water, brine, dried over $MgSO_4$ and evaporated to give 7.66g pure trans product (yield, 87%). ^{1}H NMR, δ 5.55(1H, dqt, J_d=15.3 Hz, J_q=6.3 Hz, J_t=1.22 Hz), 5.4(1H, dtq, J_d=15.3 Hz, J_t=6.9 Hz, J_q=1.5 Hz), 3.60(2H, t, J_t=6.3 Hz), 2.23(2H, qm, J_q=6.3 Hz), 1.68(3H, dm, J_d=6.3), 1.5(1H, broad); ^{13}C NMR, δ 128.62, 127.01, 61.99, 35.95, 18.04; HRMS (CI), calculated: $C_5H_{11}O$ $(M+1)^+$ 87.0810, found: 87.0724.

Trans-3-pentenyl butyrate **(311)**

By following the procedure of making cis-3-pentenylbutyrate (36), 9.2g of trans-3-pentenylbutyrate was obtained (yield, 62%). ^{1}H NMR, δ 5.50(1H, dqt, J_d=15.3 Hz, J_q=6.3, J_t=1.2Hz), 5.36(1H,dtq, J_d=15.3 Hz, J_t=6.6 Hz, J_q=1.5 Hz), 4.04(2H, t, J_t=6.9 Hz), 3.80(2H, qm, J_q=6.7 Hz), 3.77(2H, t, J_t=7.5 Hz), 3.14~3.17(3H, ddd, J_d=6.3 Hz, J_d=1.4 Hz, J_d=0.5 Hz), 3.08~3.21(2H, sextet, J_{sextet}=7.5 Hz), 2.44(3H, t, J_t=7.5 Hz); ^{13}C NMR, δ 173.71, 127.82, 126.34, 63.82, 36.21, 31.99, 18.45, 17.97, 13.64; HRMS (CI), calculated $C_9H_{17}O_2$ $(M+1)^+$ 157.1229, found: 157.1246.

Trans-2-(2', 2'-difluoro-3'-methylcyclopropyl)ethyl butyrate **(312)**

By following the procedure of making cis-2-(2', 2'-difluoro-3'-methylcyclopropyl) ethyl butyrate (**37**), 6.39g of trans-2-(2', 2'-difluoro-3'-methylcyclopropyl) ethyl butyrate was obtained (yield, 56%). ^{1}H NMR, δ 4.10(2H, t, J_d=6.4 Hz), 2.26(2H, t, J_t=7.5 Hz), 1.57~1.86(2H, m), 1.62(2H, sextet, J_{sextet}=7.5 Hz), 1.13(3H, d, J_d=5.2 Hz), 1.00~1.21(2H, m), 0.92(3H, t, J_t=7.5 Hz); ^{19}F NMR, δ -140.27(1F, dm, $J_{d(F-F)}$ =155.8 Hz), -141.49(1F, dd, $J_{d(F-F)}$=155.5 Hz, $J_{d(F-H)}$=13.8 Hz); ^{13}C NMR, δ 173.61, 115.88(t, $J_{t(F-C)}$=286 Hz), 62.98, 36.14, 26.15, 25.97, 22.49, 18.40, 13.66, 11.14; HRMS (CI), calculated $C_{10}H_{17}O_2F_2$ $(M+1)^+$ 207.1197, found: 207.1195.

Trans-1, 1-difluoro-2-(2'-hydroxyl)ethyl-3-methylcyclopropane **(313)**

By following the enzymatic hydrolysis procedure of making cis-1, 1-difluoro-2-(2'-hydroxyl)ethyl-3-methylcyclopropane (**38**), and quenching the reaction at 30% completion, 0.55g of racemic product was obtained. ^{1}H NMR, δ 3.68(2H, t, J_t=6.4 Hz), 1.73(1H, s), 1.68(2H, qm, J_q=6.5 Hz), 1.13~1.16(3H, dd, J_d=5.0 Hz), 1.06~1.21(2H, m);

^{13}C NMR, δ116.25(t, $J_{t(C-F)}$=287 Hz), 61.86, 29.85, 25.90, 22.53, 11.16; ^{19}F NMR, δ -140.12(1F, dm, $J_{d(F-F)}$=155.4 Hz), -141.22(1F, ddm, $J_{d(F-F)}$=155.4, $J_{d(H-F)}$=14.7 Hz); HRMS (CI), calculated: $C_6H_{11}OF_2$ $(M+1)^+$ 137.0778, found: 137.0756.

(R)-(-)-O-Acetylmandelate Ester of trans-1, 1-difluoro-2-(2'-hydroxyl)ethyl-3-methylcyclopropane and resolution for trans compound (resolved **314**)

A 50ml dried TNRB flask was charged with alcohol (**313**) (0.45g) and dry CH_2Cl_2 (25ml). To this solution, (R)-(-)-O-Acetylmandelic acid (0.85g), 1.20g DCC and 20mg DMAP were added. After stirred for 4hrs at room temperature, the solution was filtered to remove DCU and the solvent was removed under reduced pressure. The racemic residue was resolved on flash column chromatograph at –70 °C (silica gel, 10% diethyl ether/hexanes). The combination of later fractions gave a sample to consist of d.e.%=66.1% indicated by ^{19}F NMR. After the evaporation of the solvent under reduced pressure, 0.3g of yellowish oil was obtained. ^1H NMR, δ 7.47 (m), 7.38 (m), 5.92 (s), 5.90 (s), 4.18 (m), 2.20 (s), 1.67 (m), 1.05 (d, J = 4.9 Hz), 1.02 (d, J = 4.9 Hz); ^{19}F NMR, δ -140.25 (1F, ddd, $J_{d(F-F)}$ = 160.6, $J_{(H-F)}$ = 14.5 Hz, 10.7 Hz) (apparent triplets, the peaks of two diasteromers overlap), -141.5 (dd, $J_{d(F-F)}$ = 160.6 Hz, $J_{d(H-F)}$ = 11.9 Hz) (the peaks of two diasteromers are separated by 0.12 ppm); GCMS 270 (14.3), 116 (6.0), 149 (28.2), 107 (87.9), 77 (2.1), 43 (100).

Optically active trans-1, 1-difluoro-2-(2'-hydroxyl)ethyl-3-methylcyclopropane (optically active **313**)

A 100ml TNRB flask was charged with resolved (R)-(-)-O-Acetylmandelic ester (0.29g) (resolved 314) and aqueous NaOH (60ml 0.5N). This solution was refluxed for 3 hours, cooled to room temperature and extracted with diethyl ether (5x20ml). The organic layer was washed with water, brine and dried over Na_2SO_4. After removal of the solvent under reduced pressure, the residue was purified on flash column chromatograph (silica gel, 20%ehter/hexanes). This provided 0.084g of product (yield 63%).

Optically active trans-1, 1-difluoro-2-ethyl-3-methylcyclopropane (**315**)

By following the procedure of making cis-1, 1-difluoro-2-ethyl-3-methylcyclopropane (39), optically active (315) was obtained (d.e.%=66.1%). ^1H NMR (500 MHz), δ 1.25 (2H, m), 1.18 (2H, m), 0.88 (3H, dd, $J_{d\,(H\text{-}H)}$=7.1 Hz, $J_{d\,(F\text{-}H)}$=3.4 Hz), 0.79 (3H, t, J_t=7.2 Hz); ^{19}F NMR, δ –140.38(1F, dd, $J_{d(F\text{-}F)}$=156.9 Hz, $J_{d(H\text{-}F)}$=14.8 Hz), -141.9 (1F, dd, $J_{d(F\text{-}F)}$=156.9 Hz, $J_{d(H\text{-}F)}$=14.8 Hz); HRMS (EI) calculated: $C_6H_{10}F_2$ $(M)^+$ 120.0751, found: 120.0749.

Kinetic Studies

Preparation of sample for kinetic studies

Toluene solutions of optically active *cis*- and *trans*-1,1-difluoro-2-ethyl 3-methylcyclopropane (39 and 315) were diluted until the best resolution on the chiral column was achieved (conc. ~0.4%). 15μl of these solutions were sealed in capillary glass tubes. Racemic *cis*-samples were used for the epimerization study. An equilibrium sample was obtained by heating the sample at 298.1 °C for 48 hrs, and then at 274.5 °C for 48 hrs (Keq=2.43) and for 60hrs (Keq=2.44)

GC conditions

Injection amount: 0.01 μl; Injector temperature: 200 °C; Detector temperature 180 °C; oven temperature 24 °C; Head pressure 10 psi; Carrier: N_2. Under this condition, the two pairs of enantiomers (cis and trans compound 39 and 315) were well resolved with retention times of 10.36 mins (trans), 13.76 (cis), 15.45 (trans), 16.34 (cis).

Mass balance

Mass balance was checked at 274.5 °C with *n*-hexane as internal standard (retention time 6.4min). The recovered mass after 62 hours was 92%.

Summary of kinetic results

Racemization rate constants for *cis*-compound:

$$T=210.1\ ^{o}C,\ k_{r\text{-}cis}=(1.92\pm0.08)\ x10^{-6}\ s^{-1}$$
$$T=210.9\ ^{o}C,\ k_{r\text{-}cis}=(4.14\pm0.37)\ x10^{-6}\ s^{-1}$$
$$T=220.8\ ^{o}C,\ k_{r\text{-}cis}=(1.31\pm0.05)\ x10^{-5}\ s^{-1}$$
$$T=230.4\ ^{o}C,\ k_{r\text{-}cis}=(2.14\pm0.03)\ x10^{-5}\ s^{-1}$$
$$T=240.7\ ^{o}C,\ k_{r\text{-}cis}=(5.58\pm0.22)\ x10^{-5}\ s^{-1}$$

Arrhenius function of cis-compound racemization:

$$\ln k=(30.6\pm2.0)-(2.08\pm0.10)\ x10^{4}/T$$
$$\log k=(13.3\pm0.9)-\ (2.08\pm0.10)\ x10^{4}/2.303T$$
$$\log A=13.3\pm0.9$$
$$Ea=41.3\pm2.0\ kcal/mol$$

When $T=274.5\ ^{o}C$,

$k=6.43x10^{-4}\ s^{-1}$

$\ln(k/T) \sim 1/T$ plot of cis-compound racemization

$$\ln(k/T)=(-2.03\pm0.07)x10^{4}/T + (23.4\pm1.4)$$

when $T=274.5\ ^{o}C$,

$k=6.35x\ 10^{-4}\ s^{-1}$

$\Delta H^{\neq} = 40.4 \pm 1.4$ kcal/mol

$$\Delta S^{\neq} = -0.7 \pm 2.7 \text{ kcal/mol}$$

$$Ea = 41.5 \pm 1.4 \text{ kcal/mol}$$

Epimerization rate constant at 274.5 °C:

$$k_{tc}+k_{ct}=(8.73\pm0.17)\times10^{-6}\ s^{-1}$$

$$K_{eq}=k_{ct}/k_{tc}=2.44$$

$$k_{tc}=(2.53\pm0.05)\times10^{-6}\ s^{-1}$$

$$k_{ct}=(6.20\pm0.12)\times10^{-6}\ s^{-1}$$

Epimerization rate constant at 298.1 °C:

$$k_{tc}+k_{ct}=(5.32\pm0.08)\times10^{-5}\ s^{-1},$$

$$K_{eq}=k_{ct}/k_{tc}=2.50,$$

$$k_{tc}=(1.52\pm0.02)\times10^{-5}\ s^{-1,} \qquad k_{ct}=(3.80\pm0.06)\times10^{-5}\ s^{-1}$$

Racemization rate constant for *trans*-compound at 274.5 °C:

$$k_{tr}=(1.54\pm0.02)\times10^{-5}\ s^{-1}$$

Kinetic data

Racemization of optically active cis-1-ethyl-2, 2-difluoro-3-methylcyclopropane

Table 7.1 Racemization data of optically active cis-1-ethyl-2, 2-difluoro-3-methylcyclopropane at 201.1°C

	t (sec.)	d.e. (%)	$d.e_o/d.e$	$\ln(d.e_o/d.e)$
1	0.00	30.2	1.00	0.00
2	1.66×10^4	27.9	1.08	0.770
3	3.21×10^4	26.5	1.14	0.131
4	5.81×10^4	23.9	1.26	0.231
5	7.68×10^4	22.2	1.36	0.307
6	9.24×10^4	21.7	1.39	0.329
7	1.10×10^5	19.3	1.56	0.445

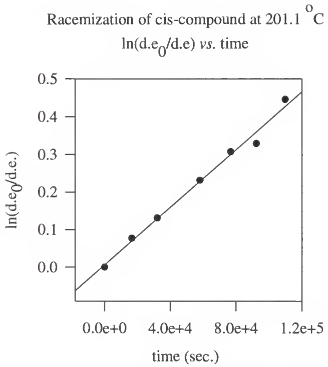

$\ln(d.e_0/d.e.) = 3.83\times10^{-6}\, t + 6.09\times10^{-3}$

$r^2 = 0.990$

$2S_{slope} = 0.16\times10^{-6}\ s^{-1}$

Figure 7.1 Plot of $\ln(d.e._0/d.e)$ vs. time at 201.1°C

Table 7.2 Racemization data of optically active cis-1-ethyl-2, 2-difluoro-3-methylcyclopropane at 210.9 °C

	t (sec.)	d.e. (%)	d.e$_o$/d.e	ln(d.e$_o$/d.e)
1	0.00	30.2	1.00	0.00
2	1.66×10^4	26.4	1.14	0.131
3	3.13×10^4	21.8	1.39	0.329
4	4.82×10^4	20.6	1.47	0.385
5	6.55×10^4	17.5	1.73	0.548

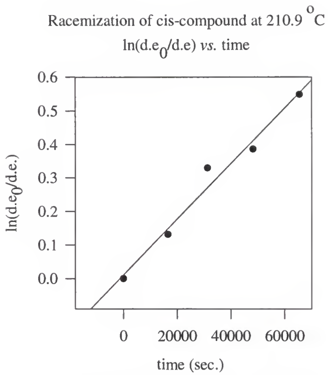

$\ln(d.e_0/d.e.) = 8.28 \times 10^{-6}\, t + 1.10 \times 10^{-2}$

$r^2 = 0.976$

$2S_{slope} = 7.4 \times 10^{-7}\ s^{-1}$

Figure 7.2 Plot of ln(d.e.$_0$/d.e) vs. time at 210.9°C

Table 7.3 Racemization data of optically active cis-1-ethyl-2, 2-difluoro-3-methylcyclopropane at 220.8 °C

	t (sec.)	d.e. (%)	$d.e._o/d.e.$	$\ln(d.e._o/d.e.)$
1	0.00	30.2	1.00	0.00
2	$3.60x10^3$	28.4	1.06	0.0583
3	$8.40x10^3$	24.8	1.22	0.199
4	$1.50x10^4$	21.0	1.44	0.365
5	$2.10x10^4$	17.6	1.72	0.542

Racemization of cis-compound at 220.8 ^oC

$\ln(d.e_0/d.e)$ *vs.* time

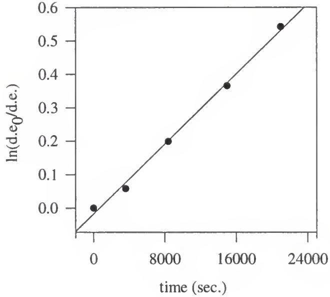

$\ln(d.e_0/d.e.) = 2.62 \times 10^{-5}\, t - 1.85 \times 10^{-2}$

$r^2 = 0.996$

$2S_{slope} = 9 \times 10^{-7}\ s^{-1}$

Figure 7.3 Plot of $\ln(d.e._0/d.e)$ vs. time at 220.8°C

Table 7.4 Racemization data of optically active cis-1-ethyl-2, 2-difluoro-3-methylcyclopropane at 230.4 °C

	t (sec.)	d.e (%)	$d.e_0/d.e$	$\ln(d.e_0/d.e)$
1	0.00	30.2	1.00	0.00
2	1.80×10^3	28.6	1.06	0.0583
3	3.84×10^3	25.8	1.17	0.157
4	5.40×10^3	24.2	1.25	0.223
5	7.20×10^3	22.4	1.35	0.300
6	9.00×10^3	20.7	1.46	0.378

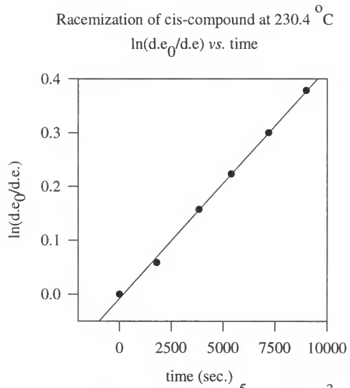

$\ln(d.e_0/d.e.) = 4.27 \times 10^{-5}\ t - 7.91 \times 10^{-3}$

$r^2 = 0.998$

$2S_{slope} = 5 \times 10^{-7}\ s^{-1}$

Figure 7.4 Plot of $\ln(d.e._0/d.e)$ vs. time at 230.4 °C

Table 7.5 Racemization data of optically active cis-1-ethyl-2, 2-difluoro-3-methylcyclopropane at 240.7 °C

	t (sec.)	d.e. (%)	$d.e_0/d.e.$	$\ln(d.e_0/d.e.)$
1	0.00	30.2	1.00	0.00
2	1.25×10^3	27.3	1.11	0.104
3	2.40×10^3	23.5	1.29	0.255
4	3.60×10^3	20.6	1.47	0.385
5	4.82×10^3	18.4	1.64	0.495
6	6.02×10^3	15.3	1.97	0.678

Racemization of cis-compound at 240.7 °C

$\ln(d.e_0/d.e)$ *vs.* time

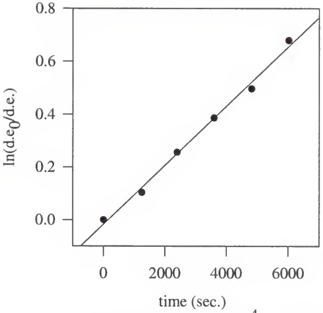

$\ln(d.e_0/d.e.) = 1.116 \times 10^{-4}\, t - 1.71 \times 10^{-2}$

$r^2 = 0.994$

$2S_{slope} = 4 \times 10^{-6}\ s^{-1}$

Figure 7.5 Plot of $\ln(d.e._0/d.e)$ vs. time at 240.7 °C

Table 7.6 Temperature dependence of Racemization of optically active cis-1,1-difluoro-2-ethyl -3-methylcyclopropane

	T (°C)	1/T (k^{-1})	k (s^{-1})	lnk	k/T	ln(k/T)
1	201.1	$2.109\text{x}10^{-3}$	$1.92\text{x}10^{-6}$	−13.2	$4.05\text{x}10^{-9}$	−19.3
2	210.9	$2.066\text{x}10^{-3}$	$4.14\text{x}10^{-6}$	−12.4	$8.55\text{x}10^{-9}$	−18.6
3	220.8	$2.024\text{x}10^{-3}$	$1.31\text{x}10^{-5}$	−11.2	$2.65\text{x}10^{-8}$	−17.5
4	230.4	$1.986\text{x}10^{-3}$	$2.14\text{x}10^{-5}$	−10.8	$4.25\text{x}1{-}^{-8}$	−17.0
5	240.7	$1.946\text{x}10^{-3}$	$5.58\text{x}10^{-5}$	−9.79	$1.09\text{x}10^{-7}$	−16.0

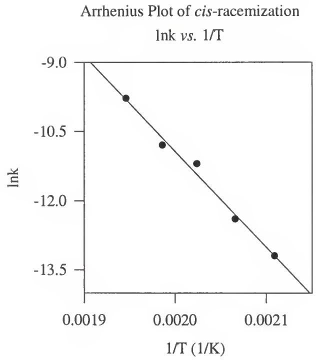

$\text{lnk} = 30.6 - 2.08 \text{ x}10^4 / \text{T}$

$r^2 = 0.988$

$2S_{slope} = 1\text{x}10^3 \text{ K}$

$2S_{interception} = 2.0$

Figure 7.6 Arrhenius plot of cis-compound racemization

Table 7.7 Racemization of optically active trans-1,1-difluoro-2-ethyl -3-methylcyclopropane at 274.5°C

	t (sec.)	d.e.(%)	d.e$_0$/d.e	ln(d.e$_0$/d.e.)
1	0.0000	6.610e+1	1.000e+0	0.0000
2	1.200e+3	6.354e+1	1.040e+0	3.922e-2
3	2.400e+3	6.124e+1	1.079e+0	7.603e-2
4	3.600e+3	5.876e+1	1.125e+0	1.178e-1
5	4.820e+3	5.626e+1	1.175e+0	1.613e-1
6	6.000e+3	5.421e+1	1.219e+0	1.980e-1

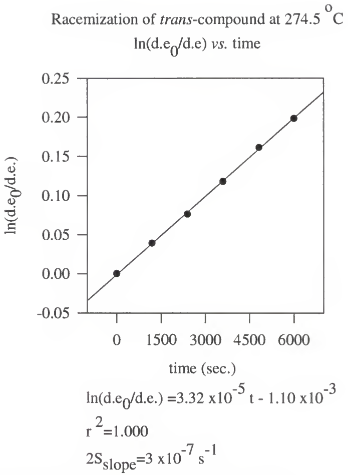

Figure 7.7 Plot of racemization of trans-compound at 274.5°C

Table 7.8 Epimerization at 298.1 °C ($Keq=k_{ct}/k_{tc}=2.50$, Xe=0.714)

	Time (sec.)	X	Xe/(Xe-X)	ln[Xe/(Xe-X)]
1	1.810×10^3	0.083	1.13	0.122
2	3.655×10^3	0.137	1.24	0.215
3	5.460×10^3	0.188	1.36	0.307
4	8.360×10^3	0.267	1.60	0.470
5	1.440×10^4	0.390	2.20	0.788

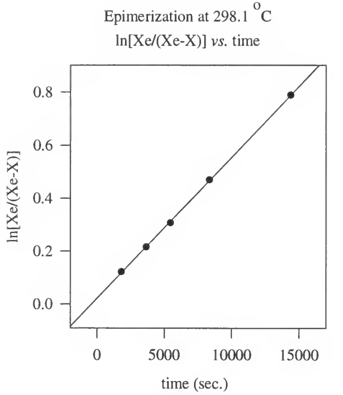

$\ln[Xe/(Xe-X)] = 5.32 \times 10^{-5}\, t + 2.21 \times 10^{-2}$

$r^2 = 0.999$

$2S_{slope} = 8 \times 10^{-7}\ s^{-1}$

Figure 7.8 Plot of epimerization at 298.1 °C

Table 7.9 Epimerization at 274.5 °C ($Keq=k_{ct}/k_{tc}=2.44$, Xe=0.709)

	Time (sec.)	X	$(Xe-X_0)/(Xe-X)$	$\ln[(Xe-X_0)/(Xe-X)]$
1	0.000	4.84e+0	1.00e+0	0.000
2	2.17e+4	1.54e+1	1.19e+0	1.74e-1
3	4.70e+4	2.73e+1	1.51e+0	4.15e-1
4	6.44e+4	3.21e+1	1.70e+0	5.32e-1
5	8.54e+4	3.97e+1	2.12e+0	7.49e-1
6	1.08e+5	4.52e+1	2.57e+0	9.43e-1

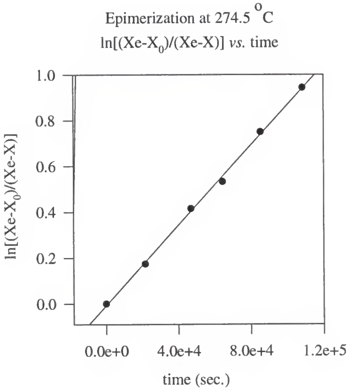

$\ln[(Xe-X_0)/(Xe-X)] = 8.73 \times 10^{-6}\, t - 7.26 \times 10^{-3}$

$r^2=0.999$

$2S_{slope}=1.7\times10^{-7}\ s^{-1}$

Figure 7.9 Plot of epimerization at 274.5 °C

Supplementary Data of Chapter 4

Part 1. Simple Cyclopropylcarbinyl Radical Ring Opening

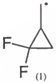
(1)

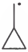
(2)

Table 7.10 Total energy[a], ZPE[b] S^2 of cyclopropylcarbinyl radical and 2,2-difluorocyclopropylcarbinyl radical.

	Radical (1)	Radical (2)
HF	-353.172252959	-155.466319303
ZPE	53.29142	63.44636
MP2	-353.99853177341	-155.96039502924
PMP2	-354.00113075	-155.96287521
S^2	0.7673	0.7662
B3LYP	-355.007489191	-156.543073505
S^2	0.7547	0.7545

a. In hartree, using HF/6-31g* optimized geometry and 6-31G(d) basis set for single point energy calculation.
b. In kcal/mol, zero point energy calculated at HF/6-31(G(d) level.

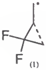
(1)

(2)

Table 7.11 Total energy[a], ZPE[b] and S^2 of ring opening transition states of cyclopropylcarbinyl radical and 2,2-difluorocyclopropylcarbinyl radical.

	Transition state (1)	Transition state (2)
HF	-353.162310266	-155.447903059
ZPE	52.09743	62.22286
MP2	353.98233460787	-155.93425019224
PMP2	353.99480231	-155.94816735
S^2	0.9149	0.9431
B3LYP	-355.002298124	-156.530685705
S^2	0.7722	0.7768

a. In hartree, using HF/6-31G(d) optimized geometry and 6-31G(d) basis set for single point energy calculation. b. In kcal/mol, zero point energy calculated at HF/6-31G(d) level.

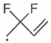

(1)

(2)

Table 7.12 Total energy[a], ZPE[b] and S^2 of ring opened products of cyclopropylcarbinyl radical and 2,2-difluorocyclopropylcarbinyl radical.

	Product (1)	Product (2)
HF	-353.191792231	-155.474018781
ZPE	52.34024	62.70402
MP2	-354.00576650016	-155.95949882367
PMP2	-354.01208936	-155.96227803
S^2	0.8455	0.7722
B3LYP	-355.020956758	-156.546978252
S^2	0.7547	0.7538

a. In hartree, using HF/6-31G(d) optimized geometry and 6-31G(d) basis set for single point energy calculation. b. In kcal/mol, zero point energy calculated at HF/6-31G(d) level.

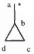

Table 7.13 Total energy[a], ZPE[b] , Thermal energy (E_T)[b] and Enthropy (S)[c] of fluroinated cyclopropylcarbinyl radicals.

reaction	Position of CF_2	B3LYP/6-311G+(2df,2p)	ZPE	E_T	S
2	none	-156.601446522	59.56999	62.715	70.376
1	c	-355.146260087	49.67329	53.690	78.491
3	c, d	-553.676384621	39.65511	44.645	88.245
5	a, c	-553.693540509	41.51141	46.048	86.678
6	a	-355.154924974	51.75695	55.358	77.729
4[d]	a, b, c, d	-851.470243125	26.13145	32.345	100.480

a. In hartree, using geometry optimized at B3LYP/6-31G(d) level.

b. In kcal/mol. zero-point energy calculated at B3LYP/6-31G(d) level at 298.15 K, 1 atm.

c. in e.u.

d. 4 is perfluoro radical.

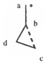

Table 7.14 Total energy[a], ZPE[b], Thermal energy (E_T)[b] and Enthropy (S)[c] of ring opening transition state of fluorinated cyclopropylcarbinyl radical.

reaction	Position of CF_2	B3LYP/6-311+G(2df,2p)	ZPE	E_T	S
2	none	-156.589923038	58.86245	61.697	68.246
1	d	-355.142093291	48.93218	52.544	76.469
1’	c	-355.131976221	49.47857	53.125	77.560
3	c, d	-553.669816912	39.35020	43.976	85.945
5	a, d	-553.682853881	39.64645	44.232	86.463
5’	a, c	-553.674641961	40.17171	44.812	87.847
6	a	-355.135392757	49.66930	53.410	78.389
4[d]	a, b, c, d	-851.457852247	24.79039	31.065	101.054

a. In hartree, using geometry optimized at B3LYP/6-31G(d) level;
b. In kcal/mol. zero-point energy calculated at B3LYP/6-31G(d) level at 298 K, 1 atm;
c. In e.u.
d. 4 is perfluoro radical.

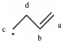

Table 7.15 Total energy[a], ZPE[b] Thermal energy (E_T)[b] and Enthropy (S)[c] of ring opening product of fluorinated cyclopropylcarbinyl radical.

reaction	Position of CF_2	B3LYP/6-311G+(2df,2p)	ZPE	E_T	S
2	none	-156.607382123	58.78995	62.319	73.766
1	d	-355.161995174	49.12789	53.342	80.990
1’	c	-355.163942619	50.95282	54.982	81.808
3	c, d	-553.706860860	40.81967	45.740	89.621
5	a, d	-553.705311356	39.61072	44.721	91.150
5’	a, c	-553.711330040	41.61875	46.495	91.597
6	a	-355.155578551	49.51727	53.825	83.165
4[d]	a, b, c, d	-851.501136725	26.19480	32.600	103.828

a. In hartree, using geometry optimized at B3LYP/6-31G(d) level;
b. In kcal/mol. zero-point energy calculated at B3LYP/6-31G(d) level at 298 K, 1 atm;
c. In e.u.
d. 4 is perfluoro radical.

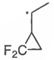

(7)

Table 7.16 Total energy[a], ZPE[b] and S^2 of 2, 2-difluorocyclopropylcarbinyl radical with methyl on the radical center

radical	B3LYP/6-31G(d)	ZPE	S^2	B3LYP/6-311+G(2df,2p)
8	-394.329771254	67.65543	0.7551	-394.478254225

a. In hartree, using geometry optimized at B3LYP/6-31G(d) level;

b. In kcal/mol. zero-point energy calculated at B3LYP/6-31G(d) level;

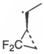

7a

7b

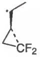

7c

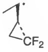

7d

Table7.17 Total energy[a], ZPE[b] and S^2 of ring opening transition state of 2, 2-difluorocyclopropylcarbinyl radical with methyl on the radical center

reaction	B3LYP/6-31G(d)	ZPE	S^2	B3LYP/6-311+G(2df,2p)
7a	-394.323935466	66.71495	0.7747	-394.474207962
7b	-394.321339476	66.60624	0.7764	-394.471180723
7c	-394.313093909	67.22433	0.7800	-394.463321097
7d	-394.311824618	67.35847	0.7804	-394.461745486

a. In hartree, using geometry optimized at B3LYP/6-31G(d) level;

b. In kcal/mol. zero-point energy calculated at B3LYP/6-31G(d) level;

7a

7b

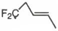

7c

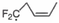

7d

Table 7.18 Total energy[a], ZPE[b] and S^2 of ring opened product of 2, 2-difluorocyclopropylcarbinyl radical with methyl on the radical center

reaction	B3LYP/6-31G(d)	ZPE	S^2	B3LYP/6-311+G(2df,2p)
7a	-394.343673668	66.87626	.7554	-394.495125761
7b	-394.340128870	66.99589	.7560	-394.490889283
7c	-394.344891493	68.76635	.7520	-394.496198457
7d	-394.342636011	68.87700	.7520	-394.494024759

a. In hartree, using geometry optimized at B3LYP/6-31G(d) level;
b. In kcal/mol. zero-point energy calculated at B3LYP/6-31G(d) level;

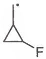

(9)

Table 7.19 Total energy[a], ZPE[b] and S^2 of cis and trans-2- fluorocyclopropylcarbinyl radical

radical	B3LYP/6-31G(d)	ZPE	S^2	B3LYP/6-311+G(2df,2p)
9-cis	-255.770997947	54.80271	0.7549	-255.868995701
9-trans	-255.771337840	54.65450	0.7549	-255.870184817

a. In hartree, using geometry optimized at B3LYP/6-31G(d) level;
b. In kcal/mol. zero-point energy calculated at B3LYP/6-31G(d) level;

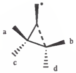

Table 7.20 Total energy[a], ZPE[b] and S^2 of ring opening transition state of cis and trans-2- fluorocyclopropylcarbinyl radical

reaction	Position of F	B3LYP/6-31G(d)	ZPE	S^2	B3LYP/6-311+G(2df,2p)
9a	a	-255.760697398	54.00892	0.7793	-255.860674298
9b	b	-255.756974528	54.12727	0.7786	-255.857288144
9c	c	-255.761405598	53.93059	0.7783	-255.862344588
9d	d	-255.758433448	54.13526	0.7780	-255.858546143

a. In hartree, using geometry optimized at B3LYP/6-31G(d) level;
b. In kcal/mol. zero-point energy calculated at B3LYP/6-31G(d) level;

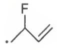

9ac

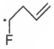

9bd

Table 7.21 Total energy[a], ZPE[b] and S^2 of ring opened product of cis and trans-2-fluorocyclopropylcarbinyl radical

product	B3LYP/6-31G(d)	ZPE	S^2	B3LYP/6-311+G(2df,2p)
9ac	-255.777891182	54.18395	0.7549	-255.880112795
9bd	-255.779888725	54.88721	0.7532	-255.881179194

a. In hartree, using geometry optimized at B3LYP/6-31G(d) level;

b. In kcal/mol. zero-point energy calculated at B3LYP/6-31G(d) level;

Charge distribution (CHelpG)

Table 7.22 Transition structure of ring opening of cyclopropylcarbinyl radical (2)

1	C	-.328701
2	C	.005136
3	C	-.200044
4	C	-.173726
5	H	.098351
6	H	.124781
7	H	.092904
8	H	.106689
9	H	.093373
10	H	.084947
11	H	.096292

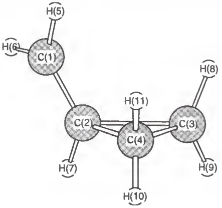

C2-C3 bond is going to break

Table 7.23 cyclopropylcarbinyl radical (2)

1	C	-.307229
2	C	.025819
3	C	-.205348
4	C	-.205107
5	H	.126561
6	H	.095956
7	H	.081314
9	H	.093824
8	H	.100244
10	H	.093769
11	H	.100196

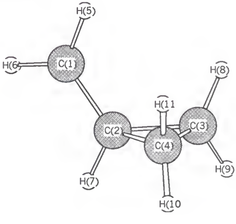

Table 7.24 transition structure of 2,2-difluorocyclopropylcarbinyl radical (1)

1	C	-.239011
2	C	-.108158
3	H	.101623
4	H	.109605
5	C	-.322451
6	C	.682475
7	H	.111808
8	H	.141454
9	H	.130697
10	F	-.314206
11	F	-.293835

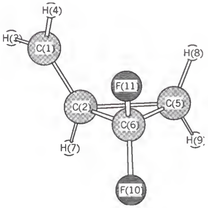

C2-C5 bond will break

Table 7.25 2,2-difluorocyclopropylcarbinyl radical (1)

1	C	-.263737
2	C	-.043564
3	H	.103077
4	H	.114027
5	C	-.295889
6	C	.584812
7	H	.093974
8	H	.121474
9	H	.133915
10	F	-.279862
11	F	-.268226

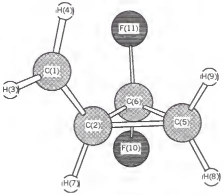

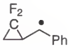

11

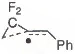

11ts1

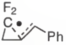

11ts2

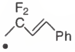

11p1

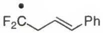

11p2

Table 7.27 Potential Energy(E), ZPE, Thermal Energy (TE),S^2 of radical 11 and its ring opening transition states and products. (B3LYP/6-31G(d))

substrates	E (Hartree)	ZPE (kcal/mol)	TE (kcal/mol)	S^2
11	-586.084042979	101.75307	108.197	0.7790
11ts1	-586.072613488	100.36513	106.775	0.7923
11ts2	-586.060264875	100.96744	107.413	0.7910
11p1	-586.084738591	100.40327	107.431	0.7575
11p2	-586.085530100	102.20324	109.040	0.7521

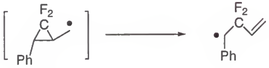

12

Table 7.28 Potential Energy scan of radical 12 (UB3LYP/6-31G(d))

Point	Bond length (Å)	B3LYP/6-31G(d) (hartree)
1	2.50216	-586.09823
2	2.45216	-586.09793
3	2.40216	-586.09711
4	2.35216	-586.09576
5	2.30216	-586.09389
6	2.25216	-586.09158
7	2.20216	-586.08882
8	2.15216	-586.08570
9	2.10216	-586.08230
10	2.05216	-586.07876
11	2.00216	-586.07527
12	1.95216	-586.07206
13	1.90216	-586.06939
14	1.85216	-586.06746
15	1.80216	-586.06631
16	1.75216	-586.06583
17	1.70216	-586.06573
18	1.65216	-586.06565
19	1.60216	-586.06517
20	1.55216	-586.06382
21	1.50216	-586.06107

Radical cation

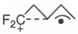

16

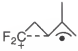

17

Table 7.29 Potential Energy (E) of radical cation 16 and 17 (B3LYP/6-31G(d))

	E (Hartree)	S^2
16	-393.451180846	0.7697
17	-432.769943653	0.7702

Part 2. Fused Ring System

19

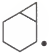

20

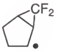

21

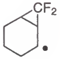

22

Table 7.30 Total energies (E)[a], ZPEs,[b] Thermal energies (E_t)[b] and standard entropies (S)[c] of the cyclopropyl carbinyl radical ring opening in [n.1.0] system.[d]

radicals	E	ZPE	E_t	S
19	-234.044949850	82.98975	86.420	
19tse	-234.032482031	81.79496	85.141	74.175
19tsi	-234.030539376	82.21990	85.489	73.589
19pe	-234.049722895	81.81451	85.856	79.983
19pi	-234.061409623	82.77281	86.437	
20	-273.374531686	101.46002	105.578	80.701
20tse	-273.362675100	100.36339	104.349	79.697
20tsi	-273.360375229	100.79796	104.681	78.609
20pe	-273.381428225	100.35876	105.022	85.609
20pi	-273.380985179	101.28877	105.621	82.218
21	-432.590778372	73.08821	77.442	83.100
21tse	-432.575048246	72.50023	76.736	83.088
21tsi	-432.584314950	72.30587	76.443	81.545
21pe	-432.606898949	73.90578	78.472	86.845
21pi	-432.620046802	73.07579	77.610	85.216
22	-471.921312817	91.69360	96.691	88.159
22tse	-471.905674246	91.05957	95.961	89.109
22tsi	-471.913931698	90.90227	95.676	86.364
22pe	-471.939186700	92.46773	97.621	91.134
22pi	-471.938194855	91.29966	96.500	89.625

A. Energy in Hartree, calculated at uB3LYP/6-311+G(2df,2p)//UB3LYP/6-31G(d)
b. Zero point energy, in kcal/mol, thermal energy is calculated at standard state.
c. In cal $mol^{-1}K^{-1}$
d. ts = transition state, p = product, e = external, i = internal

Part 3. Oxiranylcarbinyl Radical Rearrangement

23

24

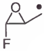
25

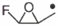
26

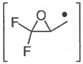
27

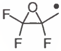
28

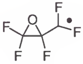
29

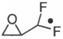
30

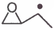
31

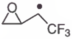
32

Table 7.31 Total energies (E)[a], ZPEs,[b] Thermal energies (E_t)[b] and standard entropies (S)[c] of the oxiranylcarbinyl radical ring opening system.[d]

radicals	E	ZPE	E_t	S
23	-192.512376354	44.56023	47.442	68.478
23tso	-192.507120926	44.42851	47.023	66.969
23tsc	-192.493038400	43.32110	46.063	67.619
23po	-192.520046451	44.13484	47.136	70.012
23pc	-192.523378255	44.86099	47.848	69.292
24	-291.790845697	39.44940	42.723	72.933
24tso	-291.779879392	39.42891	42.390	71.187
24tsc	-291.768682509	38.43927	41.536	71.799
24po	-291.793809798	39.92367	43.202	74.354
24pc	-291.799232952	39.93637	43.300	74.012
25	-291.793030885	39.80708	43.079	73.048
25tso	-291.791512193	39.52632	42.520	71.550
25tsc	-291.773503258	39.16314	42.233	72.213
25po	-291.804873844	40.13208	43.418	74.575
25pc	-291.799659159	40.45557	43.959	76.266
26	-291.792898134	39.89114	43.118	72.718
26tso	-291.792272499	39.62291	42.579	71.281
26tsc	-291.771922042	39.14824	42.217	72.391
27po	-391.086799817	35.40115	39.028	77.497
27pc	-391.080178145	35.81935	39.651	80.621
28	-490.346248929	29.56611	33.712	81.220
28tso	-490.345016038	29.32392	33.161	79.432
28tsc	-490.324216452	29.43226	33.283	80.404
28po	-490.353596663	30.37894	34.457	82.065
28pc	-490.351558431	30.97399	35.159	85.321
29	-688.881004631	21.22388	26.108	89.970

29tso	-688.876590550	20.31158	25.153	89.280
29tsc	-688.851501967	19.94037	24.902	90.938
29po	-688.885825892	21.01076	26.058	90.933
29pc	-688.875753432	21.27978	26.510	95.915
30	-391.059910544	36.45130	39.947	77.276
30tso	-391.052422618	35.34820	38.821	76.908
30tsc	-391.030943827	34.00373	37.671	77.828
30po	-391.067316401	35.13424	38.892	79.979
30pc	-391.057888815	35.01502	39.054	81.914
31	-231.844959806	62.52854	55.385	79.302
31tso	-231.841058288	62.29483	65.849	75.646
31tsc	-231.824391102	60.71570	64.329	75.260
32	-529.680306115	48.59732	53.421	91.554
32tso	-529.673359595	48.12972	52.762	88.346
32tsc	-529.661424716	46.98232	51.759	88.587

Experimental of Chapter 5

General Remarks

High pressure liquid chromatography (HPLC) was performed with a Beckman Instruments (Fullerton, CA) system gold, model 126 pump with a water (Milford, MA) symmetry shield RP18, 2.1 x 150, plus guard column and a Finnigan MAT (San Jose, CA) LCQ in electrospray ionization (ESI) mode mass spectrometry detector. The mobile phases are, A: 0.5% HOAc and 20 mM NH_4Oac in H_2O, B: 0.5% HOAc in 1:1 MeOH: iPrOH. The gradient is at 0.2 ml/min. All the kinetic samples were degassed by 3 freeze/thaw cycles (liquid N_2) and sealed *in vacuo* in melting point capillary tubes. All the kinetic studies were performed at 99.3 ± 0.1°C.

Kinetic Studies

Decomposition of *tert*-butyl perester without TEMPO

A cyclohexane solution of perester (**58**) (25 mg in 300μl cyclohexane with 5 % v/v 1,4-cyclohexenadiene) was used for the kinetic study. The disappearance of **58** was monitored with ^{19}F NMR using another capillary tube sealed with cyclohexane solution of $PhCF_3$ as external standard. The kinetic data are listed in Table 7.5.1.

Table 7.32 Kinetic data of thermal decomposition of perester **58** in cyclohexane

point	Time (s)	Integration[a] S	S_0/S	$\ln(S_0/S)$
1	0.0000	25.3100	1.0000	0.0000
2	10920.0000	23.2500	1.0886	0.0849
3	21660.0000	19.5700	1.2933	0.2572
4	32520.0000	14.6200	1.7312	0.5488
5	43320.0000	10.7500	2.3544	0.8562
6	53880.0000	8.8200	2.8696	1.0542

a. The peak at –131.1 ppm in ^{19}F NMR spectrum was used for integration.

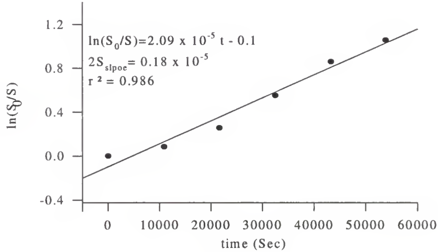

Figure 7.10 Plot of $\ln(S_0/S)$ vs. time of decomposition of **58** in cyclohexane with 5% v/v 1,4-cyclohexadiene.

Rate constant $k_0 = (2.09 \pm 0.18) \times 10^{-5}\ s^{-1}$

Decomposition of *tert*-butyl perester **58** with 0.6 M TEMPO

A cyclohexane solution of perester (**58**) (10 mg in 1ml cyclohexane with 0.600 M TEMPO) was used for the kinetic study. The disappearance of **58** was monitored with ^{19}F NMR using another capillary tube sealed with cyclohexane solution of $PhCF_3$ as external standard. The kinetic data are listed in Table 7.5.2.

Table 7.33 Kinetic data of thermal decomposition of perester **58** in cyclohexane solution of 0.6 M TEMPO

point	Time (s)	Integration[a] S	S_0/S	$\ln(S_0/S)$
1	0	34.68	1	0
2	9600	22.65	1.53	0.426
3	14400	18.66	1.86	0.620
4	20100	13.19	2.63	0.967
5	25440	12.05	2.88	1.057
6	32280	9.85	3.52	1.259

a. Peaks at –138.0 ppm were used for integration.

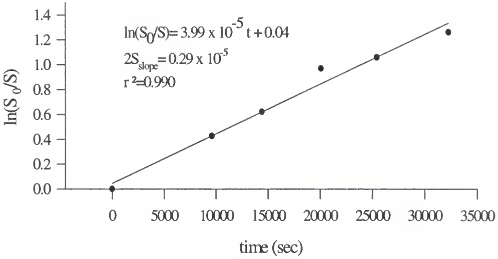

Figure 7.11 Plot of $\ln(S_0/S)$ vs. time of decomposition of **58** in cyclohexane with 0.6 M TEMPO.

Rate constant $k_{0.6} = (3.99 \pm 0.29) \times 10^{-5}\ s^{-1}$

Decomposition of *tert*-butyl perester **58** cyclohexane with 1.0 M TEMPO

Table 7.34 Kinetic data of thermal decomposition of perester **58** in cyclohexane solution of 1.0 M TEMPO

point	Time (s)	Integration[a] S	S_0/S	$\ln(S_0/S)$
1	0.0000	41.59	1	0
2	3600	32.93	1.263	0.233
3	6960	25.62	1.623	0.485
4	11460	21.75	1.912	0.648
5	15120	19.54	2.129	0.755
6	18780	16.23	2.563	0.941
7	22560	12.81	3.247	1.178

a. Peaks at –133.8 ppm were used for integration.

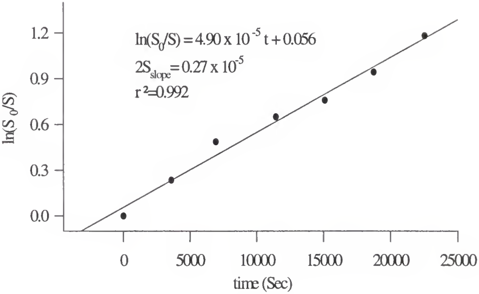

Figure 7.12 Plot of $\ln(S_0/S)$ vs. time of decomposition of **58** in cyclohexane with 1.0 M TEMPO.

Rate constant $k_{1.0} = (4.90 \pm 0.27) \times 10^{-5}\ s^{-1}$

Identification of product **510** and **59** and calibration of relative overall respond coefficient on HPLC/ESI-MS

The authentic samples of **510** and **59** were analyzed on HPLC/ESI-MS to obtain the values of retention times and ionization patterns. The ring closed product **510** was easier to elute compared to the ring opened product **59**. Interestingly, under experiment conditions, only **59** yields m/z 104 and only **510** yields m/z 91. As shown below in Figure 5.8.

Three experimental run were carried out to determine the relative overall respond coefficient of **510** and **59** using a 1:1 mixture calculated from its ^{19}FNMR spectrum. The integration of the total ions on mass spectrum and the ratios were listed in table 7.5.4.

Table 7.35 Integrations and ratios of **510** and **59** on HPLC/ESI-MS using 1:1 mixture determined with ^{19}F NMR.

run	Integration **510** (10^9)	Integration of **59** (10^9)	Ratio (**510**: **59**)
1	5.496	9.868	0.5570
2	5.576	9.385	0.5942
3	6.178	10.576	0.5841
average	5.750	9.943	0.5784
± std. dev.	0.3725	0.599	0.0192

Relative overall respond coefficient (**510** : **59**) = 0.5784 ± 0.0192

HPLC/ESI-MS ratios of **510** and **59** in various concentrations of TEMPO

A series of degassed cyclohexane solution of perester (**58**) (25 mg in 10ml cyclohexane with 5 % v/v 1,4-cyclohexenadiene) with the concentrations TEMPO (sublimed) of 0.5, 0.6, 0.7, 0.8, 0.9, 1.0, 1.1 M, respectively, were maintained at 99.3 ± 0.1 °C for 54 hours and were analyzed on HPLC/ESI-MS. The kinetic data are listed in Table 7.5.5 and the plot is depicted in Figure 7.5.4.

Table 7.36 HPLC/ESI-MS integrations of total ions of **510** and **59** at different concentration of TEMPO in cyclohexane with 5% v/v of 1,4-cyclohexadiene

run	[TEMPO]	Integration **510** (10^7)	integration **59** (10^7)	**510**: **59**
1	0.500	3.132	640.0	0.00489
2	0.600	5.922	911.0	0.00650
3	0.700	7.990	1126.0	0.00709
4	0.800	5.722	837.8	0.00683
5	0.900	7.251	756.7	0.00958
6	1.000	9.419	975.8	0.00965
7	1.100	8.860	900.1	0.00984

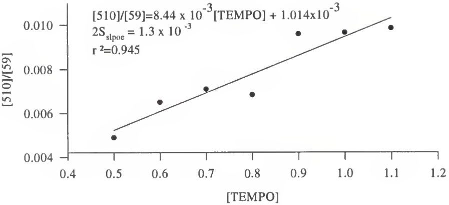

Figure 7.13 Plot of **[510]**/**[59]** *vs.* concentrations of TEMPO

After corrected by the relative overall respond coefficient: slope = $(1.46 \pm 0.22) \times 10^{-2}$ M^{-1}, which is equal to the ratio of TEMPO trapping (k_T) and radical ring opening (k_r):

$$k_T : k_r = (1.46 \pm 0.22) \times 10^{-2}$$

because $k_T = 1.5 \times 10^9 M^{-1}s^{-1}$, so

$$k_r = (1.0 \pm 0.15) \times 10^{11} s^{-1}$$

Synthesis of Kinetic Precursor and Authentic Products

1,1-difluoro-2-(2'-hydroxyl)ethyl-cyclopropane (**53**)

Under N_2, a 25 ml two-neck-round bottom flask equipped with a condenser and a magnetic stirring bar was charged with 3.74 g (21 mmol, 1 equivalent) of 3-butenyl benzoate and 10 mg dry NaF. At 125 °C, 8 g (30 mmol, 1.5 equivalent) of trimethylsilyl fluorosulfonyldifluoroacetate (**21**) was added using a syringe pump with a Teflon® needle. After the addition was completed in 12 hours, the ^{1}H NMR spectrum of the reaction mixture indicated a complete conversion of the starting alkene and that the reaction mixture was nearly the pure cyclopropanated ester except a very little TMS signal. The reaction mixture was transferred into a 100 ml one-neck-round bottom flask equipped with a condenser. Into this flask, charged with 40 ml 10% NaOH/H_2O solution. After refluxing for 3 hours, the reaction mixture was cooled to room temperature and extracted with diethyl ether (5 x 20 ml). The combined organic layer was washed with water, 0.1 M HCl, water and brine, and was dried over Na_2SO_4. The solvent was vaporized under reduced pressure. The vacuum distillation of the residue (5 mmHg, 55-58 °C) provided 1.6 g (131 mmol) of colorless liquid product with an overall yield of 62 % for the one-pot-two-step synthesis. ^{1}H NMR δ 3.74 (1H, q, J=5.1 Hz), 1.7 (3H, m), 1.43 (1H, tdd, J_t = 11.0 Hz, J_d = 7.6 Hz, J_d = 4.2 Hz), 0.97 (1H, dtd, $J_{d\,(H\text{-}F)}$ = 12.9 Hz, J_t = 7.6 Hz, J_d = 3.4Hz); ^{13}C NMR δ 114.522 (t, $J_{F\text{-}C}$ =282 Hz), 61.973 (d, $J_{F\text{-}C}$ = 2.0 Hz), 30.156 (t, $J_{F\text{-}C}$= 3.5 Hz), 19.719 (t, $J_{F\text{-}C}$ = 10.5 Hz), 16.067 (t, $J_{F\text{-}C}$ = 11.0 Hz); ^{19}F NMR δ -129.1 (1F, dt, $J_{d\,(F\text{-}F)}$ = 155.7 Hz, $J_{t\,(F\text{-}H)}$ = 12.7 Hz), -144.3 (1F, ddd, $J_{F\text{-}F}$ =155.7 Hz, $J_{F\text{-}H}$ = 13.0 Hz, $J_{F\text{-}H}$ = 4.2 Hz); HRMS $C_5H_9OF_2$ $(M+1)^+$, calculated 123.0621, found 123.0612.

2',2'-difluorocyclopropyl acetic acid (**54**)

A 250 mol round bottom flask equipped with a magnetic stirring bar was charged with 6 g CrO_3 and 100 ml 1.5 M H_2SO_4. At 0°C, 100 ml acetone solution of 1.45 g (12 mmol) of alcohol (**53**) was added dropwise. Upon the completion of the addition, the temperature was raised to room temperature. After 4 hour of stirring, the reaction mixture was extracted with diethyl ether (4x50ml). The combined organic layer was washed with brine and then extracted with 2.0 M of $NaOH/H_2O$ (4 x 50 ml). The aqueous layer was acidified with H_2SO_4 to pH < 1 and extracted with diethyl ether (4 x 50 ml). The combined organic layer was washed with water, brine and dried over Na_2SO_4. The solvent was vaporized under reduced pressure. This afforded 1.8 g (12mmol) colorless liquid with some ether, which later solidified to white solid pure product with a 100% yield. ^{1}H NMR δ 11.6 (1H, broad), 2.56 [2H, ab pattern, a 2.62 (ddt, J_d = 17.6 Hz, J_d = 7.33, J_d = 1.5 Hz), b 2.51 (dddd, J_d = 17.6 Hz, J_d = 7.6 Hz, J_d = 2.7 Hz, J_d = 1.2 Hz)], 1.87 (1H, ddq, J_d = 13.2 Hz, J_d =11.2Hz, J_q = 7.3 Hz), 1.56 (1H, tdd, J_t = 11.7 Hz, J_d = 7.8 Hz, J_d = 4.6 Hz), 1.09 (1H, dtd, J_d = 12.9 Hz, J_t = 7.8 Hz, J_d = 3.7Hz); ^{13}C NMR δ 177.822, 113.160 (dd, $J_{d\ (C\text{-}F)}$ = 283 Hz, $J_{d\ (C\text{-}F)}$ = 280 Hz), 31.959 (d, $J_{d\ (C\text{-}F)}$ = 5.0 Hz), 17.843 (t, $J_{t\ (C\text{-}F)}$ = 11.6 Hz), 16.260 (t, $J_{t\ (C\text{-}F)}$ = 11.0 Hz); ^{19}F NMR δ -130.7 (1F, dt, $J_{d\ (F\text{-}F)}$ = 160.1 Hz, $J_{t\ (H\text{-}F)}$ = 12.8 Hz), -143.9 (1H, ddd, $J_{d\ (F\text{-}F)}$ = 160.1 Hz, $J_{t\ (H\text{-}F)}$ = 12.8 Hz, $J_{t\ (H\text{-}F)}$ = 4.3 Hz); HRMS $C_5H_7O_2F_2$ $(M+1)^+$, calculated 137.0414, found 137.0443; elemental analysis, calculated C: 44.13%, H: 4.44%, found C: 44.03%, H: 4.37%.

tert-butyl per(2',2'-difluorocyclopropyl)acetate (**58**)

Under N_2, a 10ml two-neck-round-bottom flask equipped with a magnetic stirring bar was charged with 0.70 g (5 mmol, 1 equivalent) of acid (**54**), 5 ml pentane. After the acid was dissolved in pentane, 0.73 g (5.7 mmol, 1.1 equivalent) of oxalyl chloride was added dropwise. The reaction mixture was stirred overnight.

Under N_2, a 25 ml two-neck-round-bottom flask equipped with a magnetic stirring bar was charged with 0.405 g (4.5 mmol, 0.9 equivalent)*tert*-butyl hydroperoxide anhydrous (obtained by keeping 90% *tert*-butyl hydroperoxide with 4 Å molecular sieve (molecular sieve was changed 4 times)), 0.71g pyridine and 5 ml pentane. At 0°C, the above prepared acyl chloride pentane solution was added dropwise. Upon the completion of the addition, the reaction mixture was stirred at room temperature for an hour, diluted with 20 ml of pentane and washed with water, cold 15% (w/w) H_2SO_4, water, saturated sodium bicarbonate, brine and dried over Na_2SO_4. The solvent was removed under reduced pressure. The crude product was purified using flash column chromatograph (hexane to 10% diethyl ether). The product has a very weak UV absorption on TLC. This provided 0.84 g (4 mmol) of colorless liquid with an overall yield of 81%. ^{1}H NMR δ 2.51 [2H, ab pattern, a 2.57 (ddt, $J_d = 16.8$ Hz, $J_d = 7.5$, $J_d = 1.5$ Hz), b 2.45 (dddd, $J_d = 16.8$ Hz, $J_d = 7.5$ Hz, $J_d = 2.4$ Hz, $J_d = 1.2$ Hz)], 1.88 (1H, ddq, $J_d = 12.9$ Hz, $J_d = 11.4$Hz, $J_q = 7.5$ Hz), 1.57 (1H, tdd, $J_t = 11.9$ Hz, $J_d = 8.1$ Hz, $J_d = 4.5$ Hz), 1.33 (9H, s), 1.09 (1H, dtd, $J_d = 12.9$ Hz, $J_t = 7.8$ Hz, $J_d = 3.6$Hz); ^{13}C NMR δ 168.578, 112.750 (t, $J_{t(C\text{-}F)} = 284$ Hz), 83.784, 29.435(d, $J_{d(C\text{-}F)} = 4.5$ Hz), 26.006, 17.787 (t, $J_{t(C\text{-}F)} = 11.0$ Hz), 16.157 (t, $J_{t(C\text{-}F)} = 11.0$ Hz); ^{19}F NMR δ -130.644 (1F, dt, $J_{d(F\text{-}F)} = 157.9$ Hz, $J_{t\,(F\text{-}H)} = 12.7$ Hz), -

143.9 (1F, ddd, $J_{d(F\text{-}F)} = 157.9$ Hz, $J_{d(F\text{-}H)} = 12.7$ Hz, $J_{d(F\text{-}H)} = 4.2$ Hz); Elemental analysis calculated C: 51.92%, H: 6.78, found C: 51.86%, H: 6.93%.

N-allyloxy-2,2,6,6-tetramethylpiperidine (**511**) (CAS 131531-08-3)

A quartz tube was charged with 1.67 g (10mmol, 1 equivalent) of allyl iodide, 1.9 g (12 mmol, 1.2 equivalent) of TEMPO, 2.52 g of Na_2SO_3 and 100 ml CH_3CN. The reaction mixture was thoroughly purged with N_2 and then irritated in UV reactor with occasionally shaking. After one day's irritation, the color of the reaction mixture faded from red-brown to light orange and the ^{1}H NMR indicated a complete conversion. Into the reaction, 200 ml of water was added and the mixture was extracted with diethyl ether (50ml x 6). The combined organic layer was washed with water, brine and dried over Na_2SO_4. The solvent was removed under reduced pressure. The crude produce was distilled (~ 1 mmHg, 65 °C-75°C) to afford 0.8 g of colorless product which was further purified on silica gel flash chromatograph column (10% diethyl ether/ hexanes, $R_f = 0.64$). ^{1}H NMR δ 5.91 (1H, ddt, $J_d = 17.3$ Hz, $J_d = 10.5$ Hz, $J_d = 5.6$ Hz), 5.28 (1H, dq, $J_d = 17.3$ Hz, $J_q = 2.0$ Hz), 5.13 (1H, dtd, $J_d = 10.5$ Hz, $J_t = 1.5$ Hz, $J_d = 2.0$), 4.29 (2H, dt, $J_d = 5.4$ Hz, $J_t = 1.7$), 1.46 (4H, m), 1.34 (2H, m), 1.17 (6H, s), 1.12 (6H, s); ^{13}C NMR δ 134.347, 116.252, 59.943, 39.844, 33.134, 20.360, 17.342; HRMS $C_{12}H_{24}NO$ $(M+1)^+$ calculated 198.1858, found 198.1867.

N-(2',2'-difluorocyclopropyl)methoxy-2,2,6,6-tetramethylpiperidine (**510**)

Under N_2, a 5 ml two-neck-pear-shape flask equipped with a magnetic stirring bar was charged with 200 mg (1mmol) of **511**, 136 mg (1mmol) of methyl benzoate and 2 mg of CsF. At 90°C, after 1 g (4 equivalent) of trimethylsilyl fluorosulfonyldifluoroacetate (**21**) was added the complete conversion of reaction was achieved. The reaction mixture was purified on silica gel flash chromatograph column (1:1 hexanes/benzene, R_f= 0.5) to remove methyl benzoate. The crude product was further purified on silica gel flash chromatograph column (3% ethyl acetate /hexanes) to provide relative pure light yellow liquid product, which is unstable on silica gel. ^{1}H NMR 3.80 [2H, ab pattern, a 3.85 (dddd, J_d = 10 Hz, J_d = 6.8 Hz, J_d = 3.2 Hz, J_d = 1.5 Hz), b 3.75 (ddd, J_d = 10 Hz, J_d = 8.3 Hz, J_d = 2.0 Hz)], 1.81 (1H, m), 1.46 (1H, M), 1.45 (4H, m), 1.33 (2H, m), 1.15 (6H, s), 1.12(6H, s), 1.11(1H, m); ^{13}C NMR δ 113.854 (t, $J_{t\,(C\text{-}F)}$ = 281 Hz), 59.993 (d, $J_{d\,(C\text{-}F)}$ = 12.5 Hz), 39.798, 33.174, 21.395 (t, $J_{t\,(C\text{-}F)}$ = 11.0 Hz), 20.260, 17.289, 14.785 (t, $J_{d\,(C\text{-}F)}$ = 11.0 Hz); ^{19}F NMR δ -129.6 (1F, dtt, $J_{d\,(F\text{-}F)}$ = 157.9 Hz, $J_{t\,(F\text{-}H)}$ = 12.8 Hz, $J_{t\,(F\text{-}H)}$ = 8.5 Hz), -143.3 (1F, ddd, $J_{d\,(F\text{-}F)}$ = 157.9 Hz, $J_{d\,(F\text{-}H)}$ = 12.8 Hz, $J_{d\,(F\text{-}H)}$ = 4.3 Hz); HRMS $C_{13}H_{23}NOF_2$ M^+, calculated 247.1748, found 247.1689.

2,2-dilfuorocyclopropylcarbinyl iodide (**512**)

Under N_2, a 25 ml two-neck-round-bottom flask equipped with a magnetic stirring bar was charged with 2.5 g (15 mmol, 1 equivalent) of allyl iodide, 2.04 g (15mmol, 1 equivalent) of methyl benzoate and 2 mg of NaF. At 105°C, 7.5 g (30 mmol, 2 equivalent) of trimethylsilyl fluorosulfonyldifluoroacetate (**21**) was added using a syringe pump with a Teflon® needle in a period of 10 hours. The reaction mixture was distilled twice (130mmHg, 76°C- 92°C) to afford 1.9 g purple curd product. The color of the reaction mixture changed from light brown to deep purple. The crud product was further purified by a fast silica gel flash chromatograph purification (pentane, R_f = 0.34, TLC UV light visualization). Pentane was removed at 160 mmHg at room temperature. This to afford relative pure colorless liquid product which is sensitive to light and unstable on

silica gel. ^{1}H NMR δ 3.21 [2H, ab pattern, a 3.27 (m), b 3.13 (dddd, J_d = 10.5 Hz, J_d = 8.6 Hz, J_d = 2.4 Hz, J_d = 1.2 Hz)], 2.09 (1H, dddt, J_d = 12.1 Hz, J_d = 11.2 Hz, J_d =8.6Hz, J_d = 7.3 Hz), 1.59 (1H, tdd, J_t = 11.5 Hz, J_d = 8.1 Hz, J_d = 5.1 Hz), 1.03 (1H, dtd, J_d = 13.4 Hz, J_t = 7.8 Hz, J_d = 3.9Hz); ^{13}C NMR δ 115.838 (t, $J_{(C\text{-}F)}$ = 282 Hz), 26.410 (t, $J_{(C\text{-}F)}$ = 11.0 Hz), 20.314 (t, $J_{(C\text{-}F)}$ = 10.5 Hz), -0.536 (d, $J_{(C\text{-}F)}$ = 5.6 Hz); ^{19}F NMR δ -126.5 (1F, dt, $J_{d\ (F\text{-}F)}$ = 157.9 Hz, $J_{d(H\text{-}F)}$ = 10.7Hz), -145.8 (1F, ddd, $J_{(F\text{-}F)}$ = 157.9 Hz, $J_{(H\text{-}F)}$ = 12.8 Hz, $J_{(H\text{-}F)}$ = 4.3 Hz); HRMS (CI pos methane),C_4H_5IF $(M+1\text{-}HF)^+$, calculated 198.9420, found 198.9410, $C_4H_5F_2$ $(M+1\text{-}HI)^+$ calculated 91.0359, found 91.0379 (100).

N-(2',2'-difluoro)-3-butenoxy-2,2,6,6-tetramethylpiperidine (**59**)

A quartz tube was charged with 217 mg (1mmol, 1 equivalent) of 2,2-difluorocyclopropylcarbinyl iodide, 188 mg (1.2 mmol, 1.2 equivalent) of TEMPO, 252 mg of Na_2SO_3 and 10 ml CH_3CN. The reaction mixture was thoroughly purged with N_2 and then irritated in UV reactor with occasionally shaking. After one day's irritation, the color of the reaction mixture faded from red-brown to light orange and the ^{19}F NMR spectrum of reaction showed two quartet peaks indicated a complete conversion. Into the reaction mixture, 20 ml of water was added and the mixture was extracted with diethyl ether (5ml x 6). The combined organic layer was washed with water, brine and dried over Na_2SO_4. The solvent was removed under reduced pressure. The crude product was further purified on silica gel flash chromatograph column (3% ethyl acetate /hexanes, R_f =5.2 for 10% ethyl acetate/hexanes) to provide relative pure colorless liquid product, which is unstable on silica gel. ^{1}H NMR δ 6.03 (1H, dq, J_d = 17.8 Hz, J_q = 11.2 Hz), 5.72 (1H, dtd, J_d = 17.6 Hz, J_t = 2.4 Hz, J_d = 1.0 Hz), 5.50 (1H, d, J_d = 11.0 Hz), 4.02 (2H, t, $J_{t(H\text{-}F)}$= 12.5 Hz), 1.46 (4H, m), 1.34 (2H, m), 1.17 (6H, s), 1.11 (6H, s); ^{13}C NMR δ 131.542 (t,

$J_{d\,(C\text{-}F)}$ = 25.7 Hz), 120.164 (t, $J_{d\,(C\text{-}F)}$ = 9.6 Hz), 118.388 (t, $J_{d\,(C\text{-}F)}$ = 239.7 Hz), 60.537, 39.864, 32.940, 20.240, 17.162; ^{19}F NMR δ -105.6 (q, J_q = 12.8 Hz); HRMS $C_{13}H_{24}ONF_2$ $(M+1)^+$, calculated 248.1826, found 248.1783.

Experimental of Chapter 6

Synthesis of Cation Precursor and Authentic Samples

Allyl p-nitrobenzoate (**61**)

A 250 ml dry three-neck round bottom flask, equipped with a magnetic stirring bar, a condenser and an additional flask, was charged with dry THF (80 ml) and allyl alcohol (8.68g, 150 mmol, 1 equiv.; Aldrich) and pyridine (11.9 g, 150 mmol, 1 equiv.). At 0 ^{0}C, the dry THF (100 ml) solution of p-nitrobenzoate chloride (32.4g, 180 mmol, 1.2 equvi.; Acros) was added dropwise. After addition complete, the reaction mixture was stirred at room temperature for 8 hours and then filtered. Solvent was removed under reduced pressure and 400ml of ethylacetate was added. The solution was washed with water, 5% $NaHCO_3$, water, brine, dried(Na_2SO_4) and the solvent was removed under reduced pressure. This yielded 15.3g of yellow liquid(yield 49%); ^{1}H NMR δ 8.23(4H, aromatic AA'XX'), 6.02 (1H, ddt, $J_{d\,(H\text{-}H)}$ = 17.1 Hz, $J_{d\,(H\text{-}H)}$ = 10.5 Hz, $J_{t\,(H\text{-}H)}$ = 5.9 Hz), 5.41(1H, d and pseudo-q, $J_{d\,(H\text{-}H)}$ = 17.1 Hz, $J_{q\,(H\text{-}H)}$ = 1.4 Hz), 5.31 (1H, d and pseudo-q, $J_{d\,(H\text{-}H)}$ = 10.5 Hz, $J_{q\,(H\text{-}H)}$ = 1.4 Hz), 4.84 (2H, dt, $J_{d\,(H\text{-}H)}$ = 5.9 Hz, $J_{t\,(H\text{-}H)}$ = 1.4 Hz); ^{13}C NMR δ 164.278, 150.490, 135.454, 130.701, 123.490, 119.090, 66.391; HRMS (CI), $C_{10}H_{10}O_4N$ $(M+1)^+$, calculated: 208.0610, found: 208.0604.

2,2-difluorocyclopropylcarbinyl p-nitrobenzoate (**62**)

A 100 ml dry three-neck round bottom flask, equipped with a magnetic stirring bar, was charged with allyl p-nitrobenzoate (12.25g, 59.2 mmol, 1 equiv.) and a small portion of CsF. At 97 ^{0}C and with stirring, trimethylsilyl fluorosulfonyldifluoroacetate (32.4g, 130 mmol, 2.2 equiv.) was added dropwise using a syringe pump at the rate of 1.67 ml/hour. After the addition was completed, the reaction mixture (total 16.69g) was cooled to room temperature and a small portion of the reaction mixture (0.125g) was taken for flash column chromatography purification (silica gel, 10% diethylether/hexanes) (R_f = 0.28, 20% diethylether/hexanes). This provided 0.28g of (62), represented an isolated yield of 48.9%; ^{1}H NMR δ 8.24 (4H, aromatic AA'XX'), 4.52 (1H, dddd, $J_{d\,(H\text{-}H)}$ = 12.0 Hz, J_d = 7.5 Hz, J_d = 2.7 Hz, J_d = 1.2 Hz), 4.32 (1H, ddd, J_d = 12.0 Hz, J_d = 8.1 Hz, J_d = 1.8 Hz), 2.10 (1H, m), 1.60(1H, m), 1.31 (1H, m); ^{13}C NMR δ 164.451, 150.630, 135.094, 130.801, 123.563, 112.760(t, $J_{t\,(F\text{-}C)}$ =283.1 Hz), 62.608 (d, J_d = 5.5 Hz), 20.862(t, $J_{t\,(F\text{-}C)}$ =11.1 Hz), 15.107(t, $J_{t\,(F\text{-}C)}$ =11.6 Hz); ^{19}F NMR δ -129.75(1F, dtt, $J_{d\,(F\text{-}F)}$ = 161.1 Hz, $J_{t\,(F\text{-}H)}$ = 12.1 Hz, $J_{t\,(F\text{-}H)}$ = 3.7 Hz), -143.68(1F, ddd, $J_{d\,(F\text{-}F)}$ = 161.1 Hz, $J_{d\,(F\text{-}H)}$ = 13.3 Hz , $J_{d\,(F\text{-}H)}$ = 4.5 Hz); HRMS (CI), $C_{11}H_{10}O_4F_2N_1$ $(M+1)^+$, calculated 258.0578, found 258.0585.

2,2-difluorocyclopropylcarbinol (**63**)

Into the reaction mixture of (62), 80 ml of aqueous solution (10% NaOH) was added and the mixture was heated to 80 ^{0}C with stirring. After 2 hours at this temperature, this reaction mixture was cooled down to room temperature, 200 ml of water was added, the mixture was extracted with diethylether (100ml x 5). The combined ether layer was washed with 5% $NaHCO_3$, H_2O, brine, dried (Na_2SO_4), and the ether removed under reduced pressure. Distillation (60mmHg, 76 ~ 80 ^{0}C) of the residue provided 3.7 g of colorless liquid (two-step yield 58%); ^{1}H NMR δ 3.75 (1H, dddd, $J_{d\,(H-H)}$ = 12.0 Hz, J_{d} = 6.6 Hz, J_{d} = 3.0 Hz, J_{d} = 1.2 Hz), 3.64 (1H, ddm, $J_{d\,(H-H)}$ = 12.0 Hz, J_{d} = 8.1 Hz), 1.87(1H, m), 1.75(1H, broad), 1.44 (1H, m), 1.14 (1H,m); ^{13}C NMR δ 113.668 (t, $J_{t\,(F-C)}$=282.0 Hz), 59.991(d, J_{d}=5.6 Hz), 24.234 (t, $J_{t\,(F-C)}$=11.1 Hz), 14.480 (t, $J_{t\,(F-C)}$=11.0 Hz); ^{19}F NMR δ -129.1(1F, dt, $J_{d(F-F)}$=160.3 Hz, $J_{d(F-H)}$=12.7 Hz), -144.7 (1F, dd, $J_{d(F-F)}$=160.3 Hz, $J_{d(F-H)}$=12.7 Hz); HRMS (CI), $C_4H_7OF_2$ $(M+1)^+$, calculated 109.0465, found 109.0531(0.23), 91.0363(100).

2,2-difluorocyclopropylcarbinyl tosylate (**64**)

A dry 5-ml round bottom flask was charged with 2,2-difluorocyclopropylcarbinol (115mg, 1.06 mmol, 1 equiv.) and pyridine (1.8ml). At 0 ^{0}C, tosyl chloride (408mg, 2.14 mmol, 2eqv.) was added and the reaction mixture maintained at –5 ^{0}C for 12 hrs. Then, 3 ml of ice water was added and the solution extracted with diethyl ether (2ml x 6). The combined ether layer was washed with 6 M HCl, water, brine, dried (Na_2SO_4 and Na_2CO_3). Removal of the solvent under reduced pressure afforded 146 mg of pure sulfonate (64) (yellow oil, yield 53%). The tosylate was stored in diethyl ether solution over Na_2CO_3 (anhydrous); ^{1}H NMR δ 7.56 (4H, aromatic AA'XX'), 4.06 (2H, d, $J_{d\,(H-H)}$ = 7.8 Hz), 2.42 (3H, s), 1.91 (1H,m), 1.52 (1H, m), 1.18 (1H,m); ^{13}C NMR δ 145.096, 132.790, 129.939, 127.896, 112.300(t, $J_{t\,(F-C)}$ =283.0 Hz), 66.902 (d, J_{d} =5.5 Hz), 21.664, 20.933(dd, $J_{d\,(C-F)}$ =12.1 Hz, $J_{d\,(C-F)}$ =10.6 Hz), 15.294 (t, $J_{t(C-F)}$ =11.6 Hz); ^{19}F NMR δ -129.7(1F, dtdm, $J_{d\,(F-F)}$ =162.3 Hz, $J_{t\,(F-H)}$ = 13.0 Hz, $J_{d\,(F-H)}$ = 4.0 Hz), -143.2 (1H, dddt, $J_{d\,(F-F)}$ =162.3 Hz, $J_{d\,(H-F)}$ = 13.3 Hz, $J_{d\,(H-F)}$ = 4.8 Hz, $J_{t\,(H-F)}$ = 1.7 Hz;

HRMS (CI), $C_{11}H_{13}O_3F_2S$ $(M+1)^+$, calculated 262.0554 , found 263.0541(3.7), 91.0362(100).

2,2-difluorocyclopropylcarbinyl acetate (**65**)

A dry 5-ml round bottom flask was charged with 2,2-difluorocyclopropylcarbinol (100mg, 0.93 mmol, 1 equiv.) and pyridine (1.2ml). At 0 ^{0}C, acetic anhydrous (300mg, 2.94 mmol, 3.2equiv.) was added and the reaction mixture maintained at –5 ^{0}C for 12 hours. Then, 3 ml of ice water was added and the solution extracted with diethyl ether (2ml x 6). The combined ether layer was washed with 6 M HCl, water, brine, dried (Na_2SO_4 and Na_2CO_3). The removal of solvent by distillation afforded 82 mg of colorless liquid (yield 58%); ^{1}H NMR δ 4.19 (1H, dddd, $J_{d\,(H\text{-}H)}$ = 12.0 Hz, J_d = 7.5 Hz, J_d = 2.7 Hz, J_d = 1.2 Hz), 4.03 (1H, ddd, $J_{d\,(H\text{-}H)}$ = 12.0 Hz, J_d = 8.1 Hz, J_d = 1.8 Hz), 2.07(3H, s), 1.93 (1H, m), 1.50 (1H,m), 1.18 (1H, m); ^{13}C NMR δ 170.868, 112.941(t, $J_{t(C\text{-}F)}$ =283.0 Hz), 61.167 (d, J_d= 5.5 Hz), 20.989 (t, $J_{t(C\text{-}F)}$ =11.6 Hz), 20.836, 14.954 (t, $J_{t(C\text{-}F)}$ =11.0 Hz); ^{19}F NMR δ -129.77 (1F, dtdd, $J_{d\,(F\text{-}F)}$ =160.9 Hz, $J_{t(H\text{-}F)}$ =12.1 Hz, $J_{d(H\text{-}F)}$ =3.7 Hz, $J_{d(H\text{-}F)}$ =2.8 Hz), -143.996 (1F, dddt, $J_{d(F\text{-}F)}$ =160.9 Hz, $J_{d(H\text{-}F)}$ =13.3 Hz, $J_{d(H\text{-}F)}$ =4.8 Hz, $J_{t(H\text{-}F)}$ =1.5 Hz); HRMS (CI), $C_6H_9O_2F_2$ $(M+1)^+$, calculated 151.0571, found 151.0643(100).

1,1-difluoro-3-butenyl tosylate (**68**)

A dry NMR tube with valve was charged with 2,2-difluorocyclopropylcarbinyl tosylate (0.2 g), trifluoroacetic acid (0.2 ml) and maintained at 53 ^{0}C for 12 hours. Then, the reaction mixture was cooled down to room temperature. After vacuum transfer, 1ml diethyl ether was added to the residue and the solution was treated with $MgSO_4$ and

Na_2CO_3 at 0 ^{0}C. After filtration of the mixture and removal of the solvent, the residue was purified by flash column chromatography (hexanes: benzene=3:1) which provided (68) (R_f=0.12); ^{1}H NMR δ 7.593 (4H, aromatic AA'XX'), 5.65(1H, m), 5.24(2H, m), 2.83(2H, tdt, $J_{t\,(F\text{-}H)}$ = 12.3 Hz, $J_{d\,(H\text{-}H)}$ = 6.9 Hz, $J_{t\,(H\text{-}H)}$ = 1.2 Hz), 2.45 (3H, s); ^{19}F NMR δ -68.300 (2F, t, $J_{t(H\text{-}F)}$ =12.7 Hz); ^{13}C NMR δ 145.663, 134.035, 129.763, 128.054, 126.262, 123.789(t, $J_{t\,(C\text{-}F)}$ = 276.0 Hz), 121.993, 40.601(t, $J_{t\,(C\text{-}F)}$ = 27.4 Hz), 21.841; HRMS (FAB) $C_{11}H_{13}O_3F_2S$ $(M+1)^+$, calculated 263.0553, found 263.0553 (25), 173.0157(100), 91.0554(36).

1,1-difluoro-3-butenyl trifluoroacetate (**69**)

A dry NMR tube with valve was charged with 2,2-difluorocyclopropylcarbinyl tosylate (0.2 g), trifluoroacetic acid (0.2 ml) and maintained at 53 ^{0}C for 12 hrs. Then, the reaction mixture was cooled down to room temperature. After vacuum transfer, 1 ml $CDCl_3$ was added to the volatile reaction mixture and the solution was treated with $MgSO_4$ and Na_2CO_3 at 0 ^{0}C which gave the $CDCl_3$ solution of 69; ^{1}H NMR δ 5.73 (1H, ddt, $J_{d\,(H\text{-}H)}$ = 17.1 Hz, $J_{d\,(H\text{-}H)}$ = 10.2 Hz, $J_{t\,(H\text{-}H)}$ = 6.9 Hz), 5.33 (1H, dm, $J_{d\,(H\text{-}H)}$ = 10.2 Hz), 5.30 (1H, dm, $J_{d\,(H\text{-}H)}$ = 17.1 Hz), 3.04 (2H, dt, $J_{d\,(H\text{-}H)}$ = 6.9 Hz, $J_{t\,(F\text{-}H)}$ = 12.6 Hz); ^{19}F NMR δ -71.647 (2F, t, $J_{t\,(F\text{-}H)}$ = 12.7 Hz), -75.958 (3F, s); HRMS (CI), $C_6H_6O_2F_5$ $(M+1)^+$, calc. 205.0288, found 205.0296(1.12), $C_4H_5F_2$ $(M+1\text{-}CF_3COOH)^+$, calc. 91.0359, found 91.0372(100)

2,2-difluorocyclopropylcarbinyl trifluoroacetate (**66**)

A dry 5 ml round bottom flask equipped with a magnetic stirring bar was charged (63) (200mg, 1.85 mmol) and 2,6-Luctidine (218mg, 2 mmol, Acros). At 0 ^{0}C, under N_2, trifluoroacetic anhydrous (390 mg) was added dropwise and then the temperature raised up to room temperature. Distillation (65~66 ^{0}C) of the reaction mixture afforded 280 mg colorless liquid (Yield 74%); ^{1}H NMR δ 4.40 (2H, ab pattern), 2.04 (1H, m), 1.62 (1H,m), 1.30 (1H, m); ^{13}C NMR δ 157.356(q, $J_{q(C\text{-}F)}$ =42.8 Hz) , 114.370 (q, $J_{q(C\text{-}F)}$ =285.0 Hz), 112.200 (dd, $J_{d(C\text{-}F)}$ =282.0, $J_{d(C\text{-}F)}$ =284.0 Hz), 64.668 (d, J_{d} = 6.0 Hz), 20.225 (dd, $J_{d(C\text{-}F)}$ =12.6 Hz, $J_{d(C\text{-}F)}$ =11.1 Hz), 15.234 (t, $J_{t(C\text{-}F)}$ =11.6 Hz); ^{19}F NMR δ -75.436 (3F, s), -129.483 (1F, dt, $J_{d\,(F\text{-}F)}$ = 162.3 Hz, $J_{t\,(F\text{-}H)}$ = 10.5 Hz), -143.291(1F, ddd, $J_{d(F\text{-}F)}$ = 162.0 Hz, $J_{d\,(F\text{-}H)}$ = 12.7 Hz, $J_{d\,(F\text{-}H)}$ =6.5 Hz) HRMS (CI), $C_6H_6O_2F_5$ (M+1)$^{+}$, calculated 205.0288, found 205.0283(0.62), 91.0369(100).

Solvolysis Studies

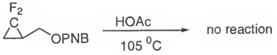

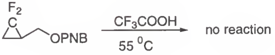

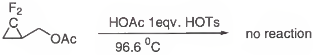

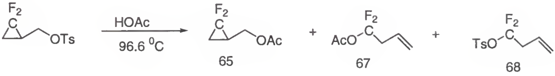

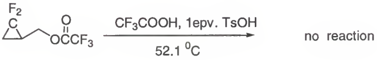

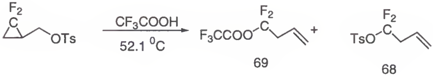

General procedure of kinetic studies

All of the kinetic studies followed this procedure except as described specifically. A capillary tube sealed with C_6D_6, 10mg of starting ester, 0.5mg of α,α,α-trifluorotoluene and 0.5ml solvent were sealed in a dry NMR tube. The tube was maintained at the given temperature in an oil bath and the progress of reaction was monitored by ^{19}F NMR.

Acetolysis of 2,2-difluorocyclopropylcarbinyl acetate

A 2ml vial was charged with TsOH .H_2O (6.3 mg, 0.03mmol), AcOH (50 µl), Ac_2O (6 mg), 2,2-difluorocyclopropylcarbinyl acetate (5-mg, 0.03 mmol) and internal standard α,α,α-trifluorotoluene (1.2mg). The solution was then sealed in capillary tube and maintained at 96.6 ^{0}C for 10 hrs. The ^{19}F NMR indicated no reaction.

Trifluoroacetolysis of 2,2-difluorocyclopropylcarbinyl trifluoroacetate

A 2ml vial was charged with TsOH.H_2O (9.3mg, 0.05mmol), CF_3COOH (50µl), $(CF_3CO)_2O$ (6mg), 2,2-difluorocyclopropylcarbinyl trifluoroacetate (10mg, 0.05 mmol) and internal standard α,α,α-trifluorotoluene (1.8mg). The solution was sealed in capillary tube and maintained at 52.1 ^{0}C for 4 hrs. The ^{19}F NMR indicated no reaction.

Trifluoroacetolysis of 2,2-difluorocyclopropylcarbinyl tosylate

A capillary tube (sealed) with 2,2-difluorocyclopropylcarbinyl tosylate (6mg), α,α,α-trifluorotoluene (0.3mg, internal standard) and trifluoroacetic acid (50µl) was maintained at 52.1 ± 0.2 ^{0}C. In the course of the reaction, two major products were observed. The triplet peak at –69.326 ppm in ^{19}F NMR was assigned as 1,1-difluoro-3-butenyl tosylate (68); the other triplet peak at –73.651ppm was assigned as 1, 1-difluoro-

3-butenyl trifluoroacetate (69). The ratio of 1,1-difluoro-3-butenyl trifluoroacetate: 1,1-difluoro-3-butenyl tosylate had been relatively stable (see Table 7.6.1). The disappearance of starting material followed first-order fashion (Table 7.6.1, Figure 7.6.1). The total mass balance of the reaction is 92.3%.

Acetolysis of 2,2-difluorocyclopropylcarbinyl tosylate

1. In pure HOAc

A capillary tube charged with 2,2-difluorocyclopropylcarbinyl tosylate (10mg), α,α,α-trifluorotoluene (0.5mg) and AcOH (50μl) was maintained at 96.3 ± 0.2 ^{0}C. In the course of the reaction, 3 major products were observed in ^{19}F NMR. The triplet peak at –67.851 ppm was assigned as 1,1-difluoro-3-butenyl tosylate (68); the triplet peak at –70.929 ppm was assigned as 1,1-difluoro-3-butenyl acetate (67); the AB pattern peaks at -129.5 ppm and –144.1 ppm was assigned as 2,2-difluorocyclopropylcarbinyl acetate (65). The disappearance of starting material followed first-order kinetics (Table 7.6.2, Figure 7.6.2). The ratio of ring closed product (65) to total ring opened products [(67) + (68)] was relatively stable at the early stage of the reaction (Table 7.6.2). Total mass balance was 92%.

2. In 0.200 M NaOAc/HOAc

A capillary tube charged with 2,2-difluorocyclopropylcarbinyl tosylate (10mg), α,α,α-trifluorotoluene (0.5mg) and 0.200M NaAc/AcOH (50μl) was maintained at 96.6 ± 0.2 ^{0}C. The same pattern of ^{19}F NMR spectrum as above was obtained and the data are summarized in Table 7.6.3. The disappearance of starting material followed the first-order pattern (Figure 7.6.3). The total mass balance in the course of reaction was 90.3%.

3. In 0.400 M NaOAc/HOAc

A capillary tube charged with 2,2-difluorocyclopropylcarbinyl tosylate (10mg), α,α,α-trifluorotoluene (0.5mg) and 0.400M NaAc/AcOH (50μl) was maintained at 96.6 ± 0.2 ^{0}C. The same pattern of ^{19}F NMR spectrum as above was obtained and the data are summarized in Table 7.6.4. The disappearance of starting material followed the first-order pattern (Figure 7.6.4). The total mass balance in the course of reaction was 90.3%.

Kinetic data

Table 7.37 Trifluoroacetolysis of 2,2-difluorocyclopropylcarbinyl tosylate at (52.1± 0.1 ^{0}C)

	Time (sec.)	(64) ^{a}	$(64)_0/(64)$	$\ln[(64)_0/(64)]$	(69) : (68)
1	0	24.54	1.0000	0.0000	
2	2650	20.02	1.2258	0.2036	2.1
3	3721	16.68	1.4658	0.3824	2.1
4	7339	11.92	2.0587	0.7221	2.1
5	10562	9.87	2.4860	0.9108	2.0
6	12901	7.88	3.1142	1.1360	2.0

a. The relative amount of 2,2-difluorocyclopropylcarbinyl tosylate was represented by the integration of the peak at -145.6 in ^{19}F NMR.

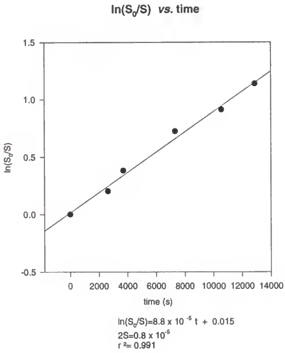

$$k_t = k_\Delta = (8.8 \pm 0.8) \times 10^{-5}\ s^{-1}$$

Figure 7.14 Plot of $\ln(S_0/S)$ vs. time of Trifluoroacetolysis of 2,2-difluorocyclopropylcarbinyl tosylate at (52.1± 0.1 ^{0}C)

Table 7.38 Acetolysis of 2,2-difluorocyclopropylcarbinyl tosylate in pure HOAc at (96.3 ± 0.2) ^{0}C

	Time (sec.)	$(64)^a$	$(64)_0/(64)$	$\ln[(64)_0/(64)]$	$(65)^b:(67)+(68)^c$	(67):(68)
1	0	48.10	1.0000	0.0000		
2	7203	44.21	1.0882	0.0845	1.3	8.8
3	14505	40.52	1.1871	0.1715	1.2	7.8
4	21600	38.61	1.2358	0.2117	1.3	6.9
5	28274	35.71	1.3470	0.2979	2.6	3.2

a. The relative amount of 2,2-difluorocyclopropylcarbinyl tosylate was represented by the integration of the peak at -145.6 in ^{19}F NMR.

b. Because of overlap of the peaks of (65) with starting material, few assumptions were employed to obtain (65)'s total integration. (i). The integration values of the two sets of peaks of AB peak are equal. (ii). The ratio of the integration values of the set of peaks around –144 ppm is 1.15. For example, (-143.3) : (-143.7) = 1.15.

c. Because there were no other significant amount of products were observed, we assumed that only the formations of (65), (67) and (68) contribute to the total rate.

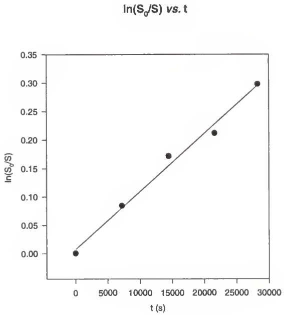

$\ln(S_0/S)=1.0 \times 10^{-5} t + 7.23 \times 10^{-3}$
$2S=0.1 \times 10^{-5}$
$r^2=0.994$

$$k_t = (1.0 \pm 0.1) \times 10^{-5}\ s^{-1}$$

$$k_\Delta = k_t/2.3 = 4.3 \times 10^{-6}\ s^{-1}$$

$$k_s = 1.3\ k_t/2.3 = 5.7 \times 10^{-6}\ s^{-1}$$

Figure 7.15 Plot of $\ln(S_0/S)$ vs. time of acetolysis of 2,2-difluorocyclopropylcarbinyl tosylate in pure HOAc at (96.3 ± 0.2) ^{0}C

Table 7.39 Acetolysis of 2,2-difluorocyclopropylcarbinyl tosylate in 0.200 M NaOAc/HOAc at (96.6 ± 0.2) °C

	Time (sec.)	(64)[a]	$(64)_0/(64)$	$\ln[(64)_0/(64)]$	(65)[b] :[(65)+(67)+(68)]
1	0	93.62	1.0000	0.0000	
2	7093	77.40	1.2096	0.1903	84.0%
3	9793	71.20	1.3149	0.2738	85.7%
4	12793	65.26	1.4346	0.3609	86.5%
5	15493	60.30	1.5525	0.4399	86.9%
6	18253	55.53	1.6859	0.5223	87.5%

a. The relative amount of 2,2-difluorocyclopropylcarbinyl tosylate was represented by the integration of the peak at -145.6 in ^{19}F NMR.

b. Because there were no other significant amount of products were observed, we assumed that only the formations of (65), (67) and (68) contribute to the total rate.

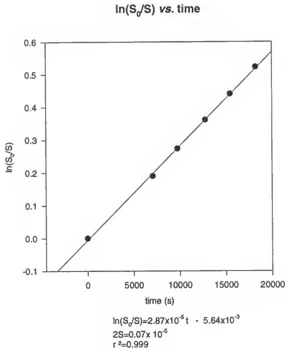

$k_t = (2.87 \pm 0.07) \times 10^{-5}\ s^{-1}$

$k_s = k_t \times 84.0\% = 2.41 \times 10^{-5}\ s^{-1}$

$k_\Delta = k_t - k_s = 4.6 \times 10^{-6}\ s^{-1}$

Figure 7.16 Plot of $\ln(S_0/S)$ vs. time of acetolysis of 2,2-difluorocyclopropylcarbinyl tosylate in 0.200 M NaOAc/HOAc at (96.6 ± 0.2) °C

Table 7.40 Acetolysis of 2,2-difluorocyclopropylcarbinyl tosylate in 0.400 M NaOAc/HOAc at (96.3 ± 0.2) ^{0}C

	Time (sec.)	$(64)^{a}$	$(64)_0/(64)$	$\ln[(64)_0/(64)]$	$(65)^{b}:[(65)+(67)+(68)]$
1	0	95.30	1.0000	0.0000	
2	4753	74.33	1.2821	0.2485	90.0%
3	7503	66.08	1.4422	0.3662	91.9%
4	9783	59.19	1.6100	0.4762	92.6%
5	11643	54.15	1.7600	0.5653	93.4%
6	13653	50.60	1.8834	0.6331	93.7%

a. The relative amount of 2,2-difluorocyclopropylcarbinyl tosylate was represented by the integration of the peak at -145.6 in ^{19}F NMR.

b. Because there were no other significant amount of products were observed, we assumed that only the formations of (65), (67) and (68) contribute to the total rate.

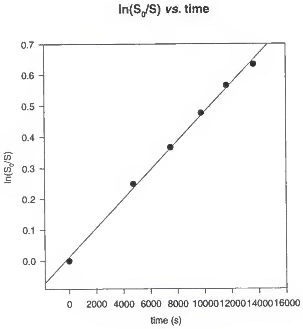

$\ln(S_0/S)=4.7\times10^{-5}\,t + 0.013$

$2S=0.3 \times 10^{-5}$

$r^2=0.997$

$$k_t = (4.7 \pm 0.3) \times 10^{-5}\ s^{-1}$$

$$k_s = k_t \times 90.0\% = 4.2 \times 10^{-5}\ s^{-1}$$

$$k_\Delta = k_t - k_s = 4.7 \times 10^{-6}\ s^{-1}$$

Figure 7.16 Plot of $\ln(S_0/S)$ vs. time of acetolysis of 2,2-difluorocyclopropylcarbinyl tosylate in 0.400 M NaOAc/HOAc at (96.6 ± 0.2) ^{0}C

Computational Data of Chapter 6

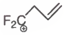

1

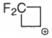

2

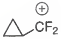

3

Table 7.41 Total energy[a], ZPE[b] of 1, 1-difluoro-homoallylic,3,3-difluorocyclobutyl cation and cyclopropyldifluorocarbinyl cation

cation	B3LYP/6-31G(d)	ZPE	B3LYP/6-311+G(2df,2p)
1	-354.760604562	51.79741	-354.887295042
2	-354.727564618	49.08491	-354.854645032
3	-354.775529869	52.78248	

a. In hartree, using geometry optimized at B3LYP/6-31G(d) level;

b. In kcal/mol. zero-point energy calculated at B3LYP/6-31G(d) level, 298.15K, 1 atm.

APPENDIX
SELECTED ^{19}F NMR, ^{1}H NMR AND GC SPECTRA

The representative ^{19}F NMR spectra of typical difluorocyclopropanes, kinetic studies and optically active samples, ^{1}H NMR spectra of key products in kinetic studies and the GC spectra of the chiral analysis carried out in Chapter 3 are graphically illustrated in this appendix. Full spectral characterization data are presented numerically in their respective areas of Chapter 7.

Fluorine spectrum of compound **22**

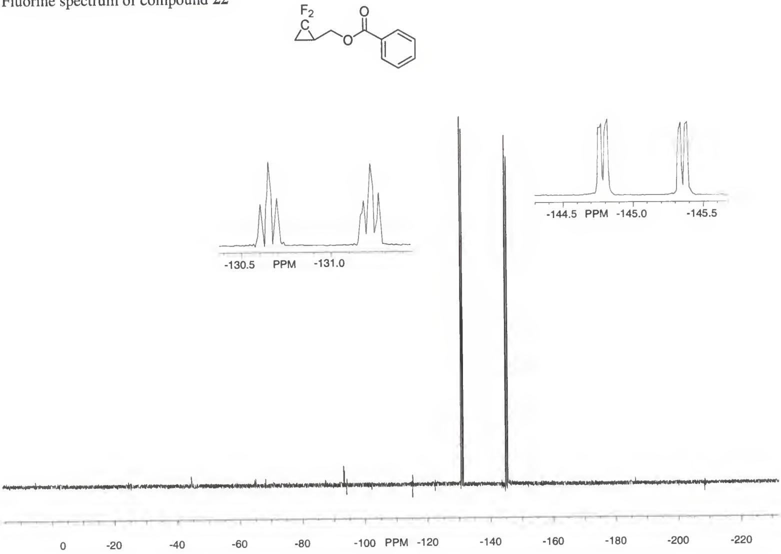

^{1}H NMR spectrum of compound **22**

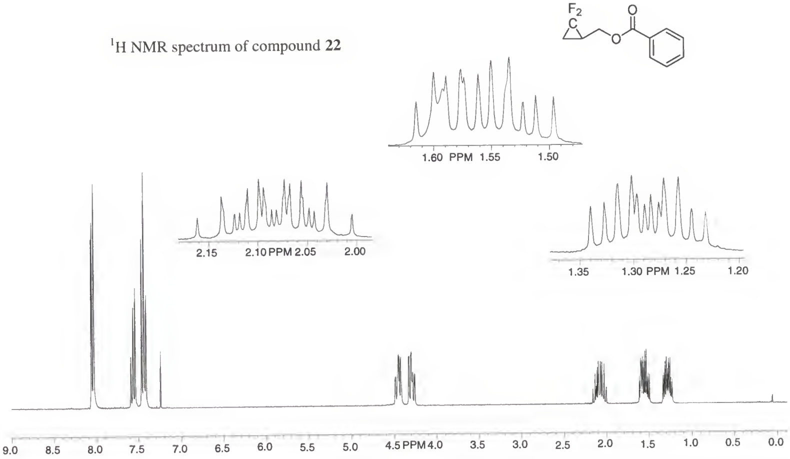

^{19}F NMR of compound **26**

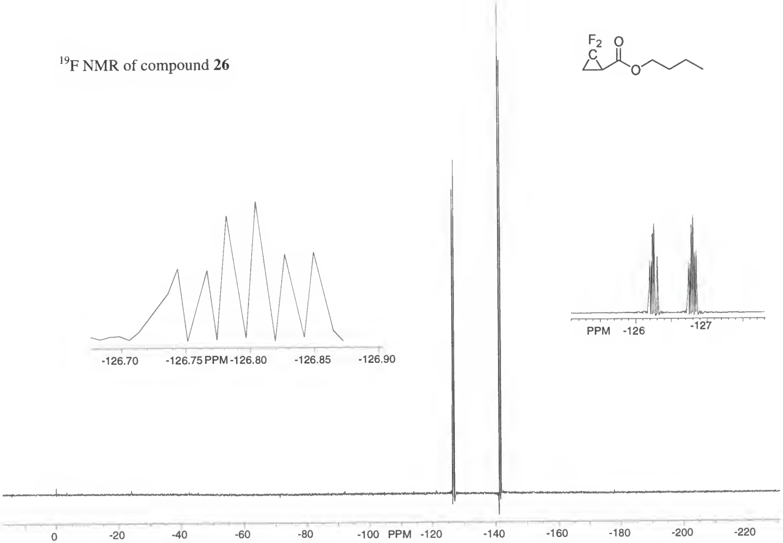

GC spectrum of optically active **39**

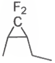

```
        END OF SIGNAL

  Closing signal file M:T01      .BNA

  RUN#      4           JAN  1, 1901  06:48:13

  SIGNAL FILE: M:T01.BNA
  AREA%
        RT        AREA TYPE   WIDTH        AREA%
     1.932        1935   PV    .044       .70232
     2.048        3806   VV    .061      1.38142
     7.585       80654   BV    .215     29.27402
    11.443       65900   PB    .170     23.91893
    13.862      123219   PB    .228     44.72333

  TOTAL AREA= 275514
  MUL FACTOR=1.0000E+00
```

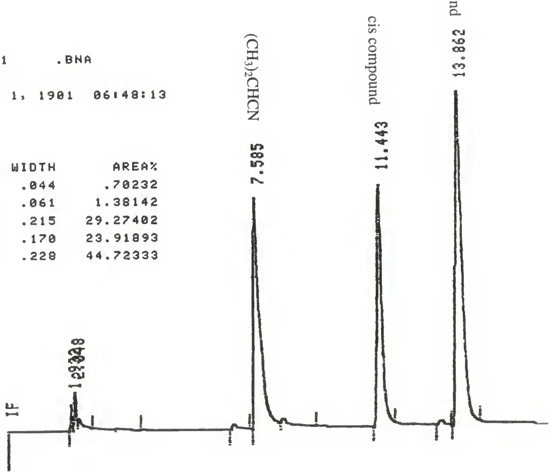

GC spectrum of optically active **315** in chapter 3

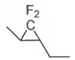

```
Closing signal file M:SIGNAL  .BNC

RUN#   279          FEB 18, 1981  08:40:12

SIGNAL FILE: M:SIGNAL.BNC
AREA%
      RT       AREA TYPE  WIDTH       AREA%
   7.701      24681   PB   .065   10.46826
  16.590      35929   PB   .152   15.23901
  25.254     175160   BB   .362   74.29277

TOTAL AREA= 235770
MUL FACTOR=1.0000E+00
```

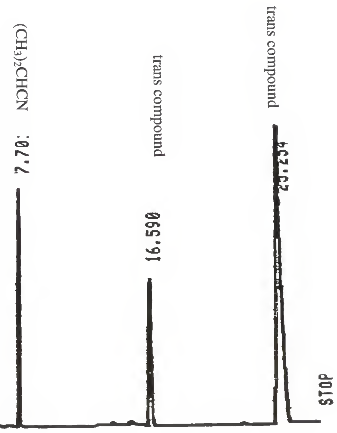

GC spectrum of epimerization reaction mixture in chapter 3

```
RUN#      9    .        JAN  3, 1981   00:25:46

SIGNAL FILE: M:SIGNAL.BNA
AREA%
     RT         AREA TYPE  WIDTH        AREA%
  11.475        8127   PB    .122      2.84404
  13.210       44947   PB    .139     15.72921
  17.583       92785   PB    .206     32.47013
  20.032       44300   PB    .221     15.50279
  21.117       95596   BB    .286     33.45382

TOTAL AREA= 285755
MUL FACTOR=1.0000E+00
```

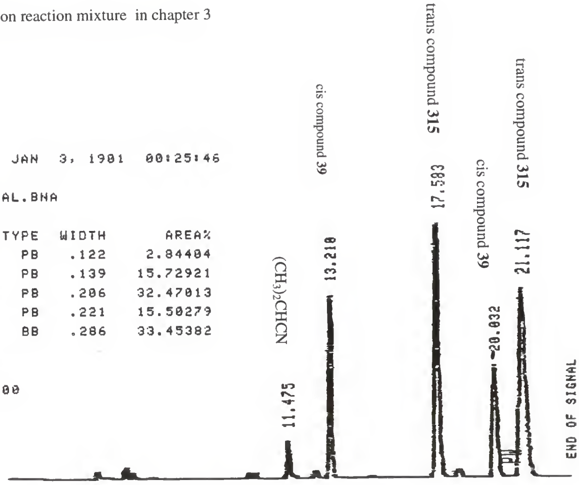

^{19}F NMR spectrum of combination of fractions 16-30 of **314** after flash chromatography at -70°C in chapter 3

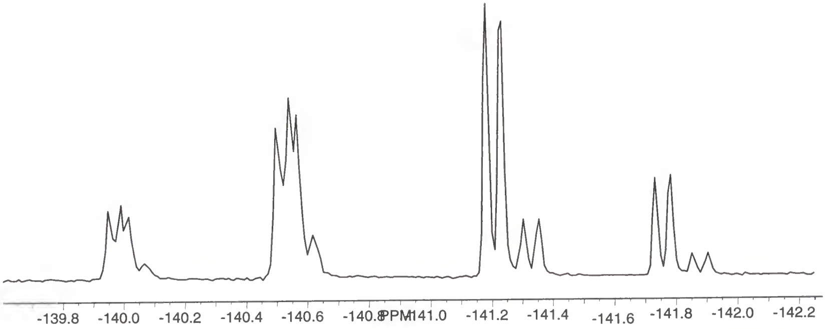

19F NMR spectrum of

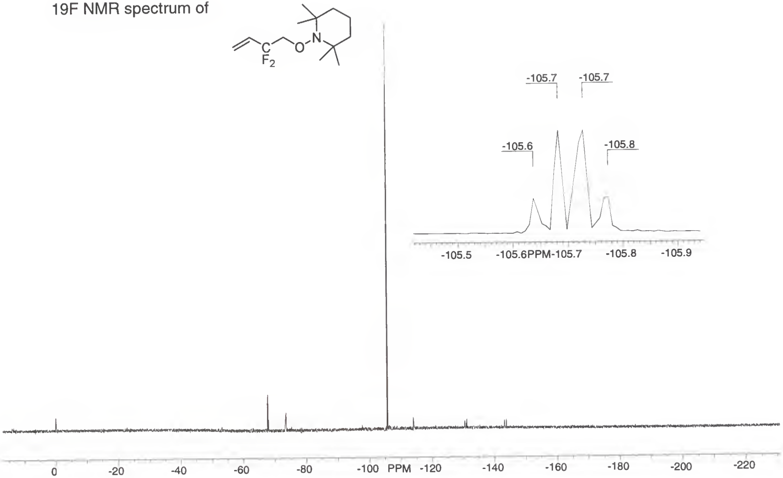

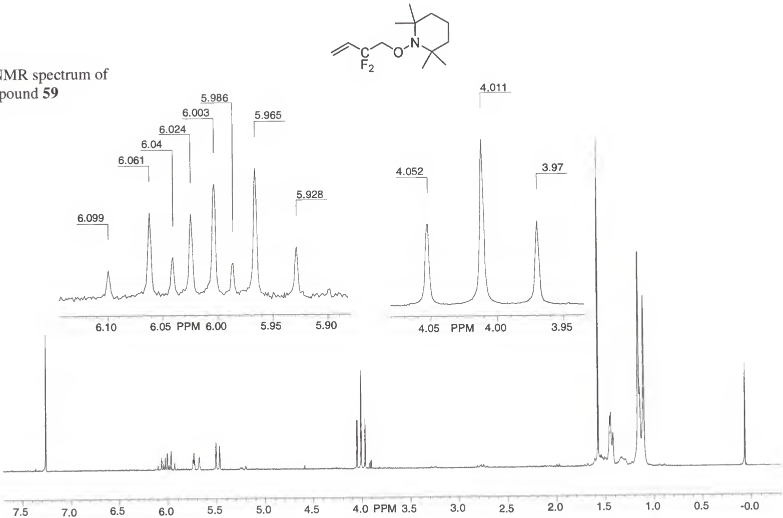

^{1}H NMR spectrum of compound **59**

^{19}F NMR spectrum of **510**

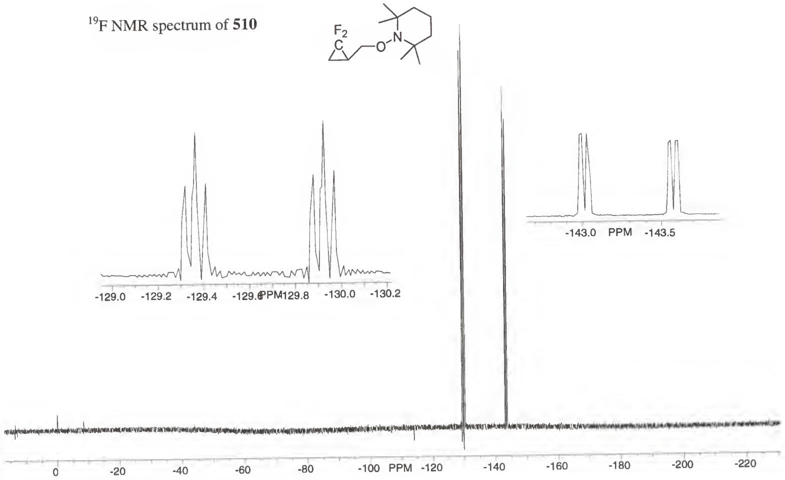

^{19}F NMR of **68**

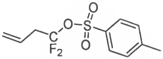
O
S
O
C
F2
O

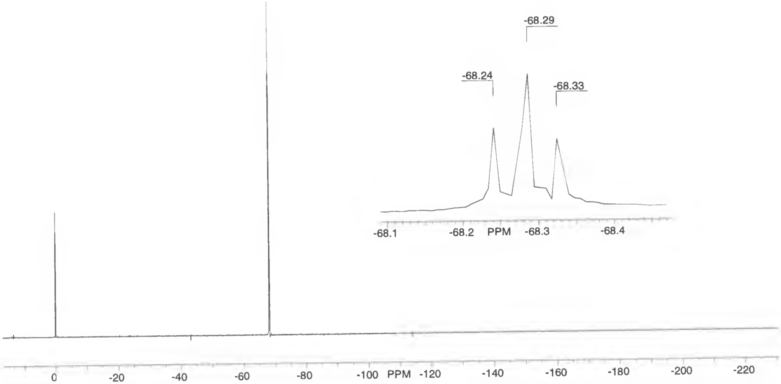
-68.29
-68.24
-68.33
-68.1
-68.2
PPM
-68.3
-68.4
0
-20
-40
-60
-80
-100
PPM
-120
-140
-160
-180
-200
-220

^{1}H NMR spectrum of **68**

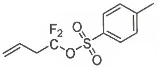

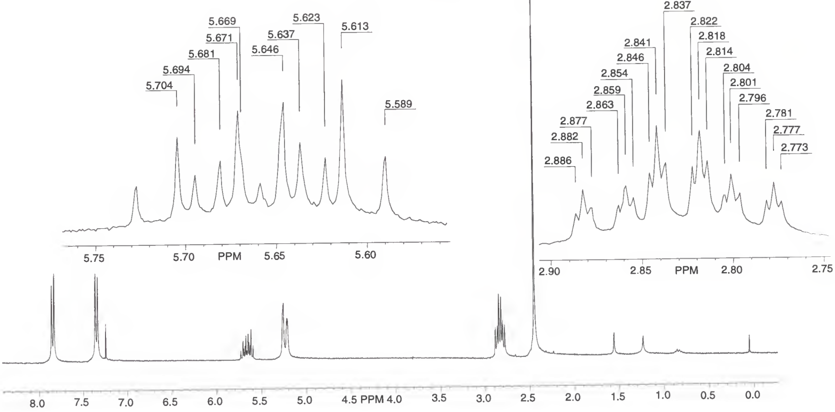

^{19}F NMR spectrum of **66**

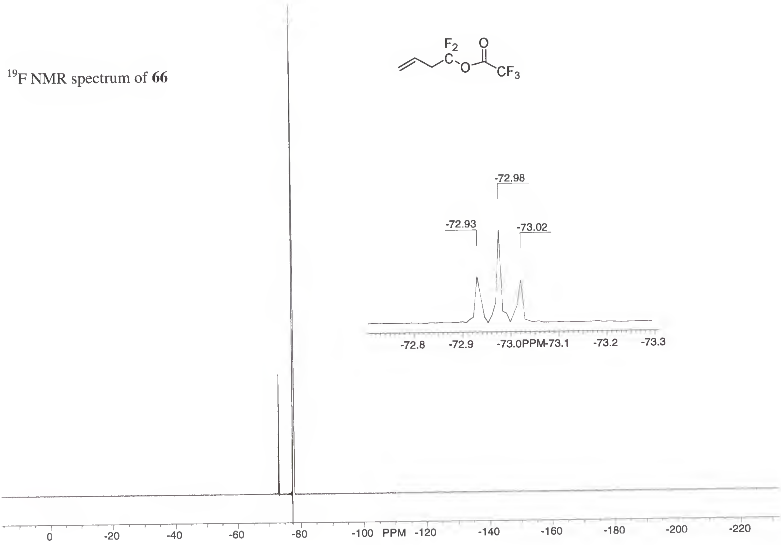

^{19}F NMR spectrum of kinetic study of solvolysis of **64** in 0.2M NaAc/HOAc in chapter 6

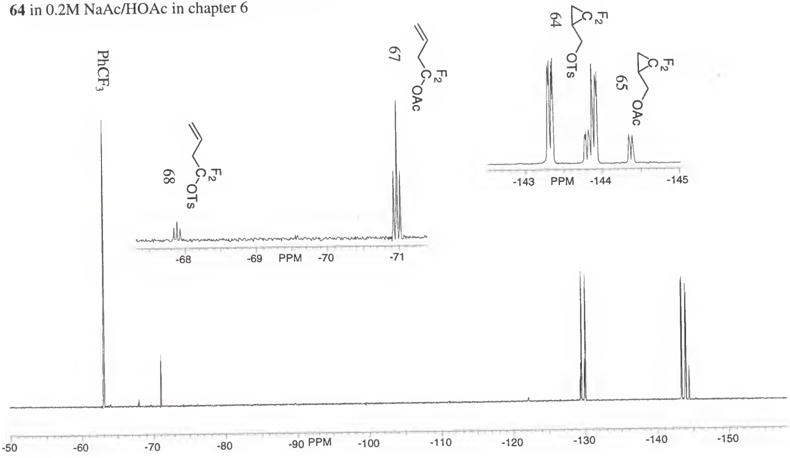

REFERENCES

(1) Freund, A. *Monatsh* **1882**, *3*, 625.

(2) Reboul, M. E. *C. R.* **1873**, *76*, 1270.

(3) Perkin, W. H. *Ber. Dtsch. Chem. Ges.* **1884**, *17*, 54.

(4) *The Chemistry of Cycopropyl Group*; Rappoport, Z., Ed.; John Wiley & Sons: New York, 1995; Vol. 2.

(5) *Advanes in Strain in Organic Chemistry*; Halton, B., Ed.; Jai Press Ltd.: London, 1991; Vol. 1.

(6) *The Chemistry of the Cyclopropyl Group*; Rappoport, Z., Ed.; John Wiley & Sons: New York, 1987.

(7) Greenberg, A.; Liebman, J. F. *Strained Orgainc Molecules*; Academic press: New York, 1978; Vol. 38.

(8) Bastiansen, O.; Hassel, O. *Tidsskr, Kjemi, Bergves. Metallurgi* **1946**, *6*, 71.

(9) Bastiansen, O.; Hassel, O. *Chem. Abstr* **1964**, *40*, 6059.

(10) Rozsondai, B. In *The Chemistry of Cycloporpyl Group*; Z. Roppoport, Ed.; John Wiley & Sons Ltd: Chichester, 1995; Vol. 2, p 139.

(11) Yamamoto, S.; Nakata, M.; Fukuyama, T.; Kuchitsu, K. *J. Phy. Chem.* **1985**, *89*, 3298.

(12) Wiberg, K. B.; Wendeloski, J. J. *J. Am. Chem. Soc.* **1982**, *104*, 5679.

(13) Norden, T. D.; Staley, S. W.; Taylor, W. H.; Harmony, M. D. *J. Am. Chem. Soc.* **1986**, *108*, 7912.

(14) Bak, B.; Skaarup, S. *J. Mol. Struct.* **1971**, *10*, 385.

(15) Hirose, C. *Bull. Chem. Soc. Jpn.* **1974**, *47*, 1311.

(16) Egawa, T.; Fukuyama, T.; Yamamoto, S.; Takabayashi, F.; Kambara, H.; Ueda, T.; Kuchitsu, K. *J. Chem. Phys.* **1987**, *86*, 6018.

(17) Adams, W. J.; Geise, H. J.; Bartell, L. S. *J. Am. Chem. Soc.* **1970**, *92*, 5013.

(18) Ewbank, J. D.; Kirsch, G.; Schäfer, L. *J. Mol. Struct* **1976**, *31*, 39.

(19) IiJima, T. *Bull. Chem. Soc. Jpn.* **1972**, *45*, 1291.

(20) Tamagawa, K.; Iijima, T.; Kimura, M. *J. Mol. Struct.* **1976**, *30*, 243.

(21) Hirota, E.; Endo, Y.; Saito, S.; Yoshida, K.; Yamaguchi, I.; Machida, K. *J. Mol. Spectrosc* **1981**, *89*, 223.

(22) Baeyer, A. V. *Ber. Dtsch. Chem. Ges.* **1885**, *18*, 2277.

(23) Sachse, H. *Ber. Dtsch. Chem. Ges.* **1890**, *23*, 1363.

(24) Mohr, E. *J. Prakt. Chem.* **1918**, *98*, 315.

(25) Cox, J. D.; Pilcher, G. *Thermochemistry of Organic and Organometalic Compounds*; Academic: London, 1970.

(26) Franklin, J. L. *Ind. Eng. Chem* **1949**, *41*, 1070.

(27) Wiberg, K. B. In *The Chemistry of theCyclopropyl Group*; Z. Rappoport, Ed.; John Wiley & Sons: Chichester, 1987, p 1.

(28) Walsh, A. D. *Trans. Faraday Soc.* **1949**, *45*, 179.

(29) Cremer, D.; Kraka, E.; Szabo, K. J. In *The Chemistry of the Cyclopropyl Group*; Z. Rappoport, Ed.; John Wiley & Sons: Chichester, 1995; Vol. 2, p 43.

(30) Jackson, J. E.; Allen, L. C. *J. Am. Chem. Soc.* **1984**, *106*, 591.

(31) Kitchen, D. B.; Jackson, J. E.; Allen, L. C. *J. Am. Chem. Soc.* **1990**, *112*, 3408.

(32) Förster, T. *Z. Phys. Chem. B* **1939**, *43*, 58.

(33) Coulson, C. A.; Moffitt, W. E. *Philos. Mag.* **1949**, *40*, 1.

(34) Forster, H.; Vogtle, F. *Angew. Chem. Int. Ed. Engl.* **1977**, *16*, 429.

(35) Chambers, R. D. *Fluroine in Organic Chemistry*; Wiley: New York, 1973.

(36) *Chemistry of Organic fluroine Compounds II: A Critical Review*; Hudilcky, M.; Pavlath, A. E., Eds.; ACS: Washington, 1995.

(37) Smart, B. E. In *Molecular Structure and Energetics*; J. F. Liebman; A. Greenberg, Eds. VCH: Derrfield Beach, FL, 1986; Vol. 3, p 141.

(38) Mitsch, R. A.; Neuvar, E. W. *J. Phys. Chem* **1966**, *70*, 546.

(39) O'Neal, H. E.; Benson, S. W. *J. Phys. Chem.* **1968**, *72*, 1866.

(40) Roth, W. R.; Kirmes, W.; Hoffmann, W.; Lennartz, H. W. *Chem. Ber.* **1982**, *115*, 2508.

(41) Schaffer, F.; Verevkin, S. P.; Rieger, H. J.; Beckhaus, H. D.; Rüchardt, C. *Leibigs Ann. /Recueil* **1997**, 1333.

(42) Greenberg, A.; Liebman, J. F.; W. R. Dolbier, J.; Medinger, K. S.; Skancke, A. *Tetrahedron* **1983**, *39*, 1533.

(43) Wiberg, K. B.; Marquez, M. *J. Am. Chem. Soc.* **1998**, *120*, 2932.

(44) Sargeant, P. B. *J. Am. Chem. Soc.* **1969**, *91*, 3061.

(45) Jefford, C. W.; Mareda, J.; Gehret, J. C. E.; Karbengele, T.; Graham, W. D.; Gruger, U. *J. Am. Chem. Soc.* **1976**, *98*, 2585.

(46) Dolbier, W. R., Jr. *Acc. Chem. Res.* **1981**, *14*, 195.

(47) Dolbier, W. R., Jr.; Enoch, H. O. *J. Am. Chem. Soc.* **1977**, *99*, 4532.

(48) Flowers, M. D.; Frey, H. M. *Proc. R. Soc. (London, Ser. A)* **1960**, *257*, 121.

(49) Dolbier, W. R., Jr.; Al-Sader, B. H.; Sellers, S. F.; Koroniak, H. *J. Am. Chem. Soc.* **1981**, *103*, 2138.

(50) Dolbier, W. R., Jr.; Sellers, S. F. *J. Am. Chem. Soc.* **1982**, *104*, 2494.

(51) Getty, S. J.; Hrovat, D. A.; Borden, W. T. *J. Am. Chem. Soc.* **1994**, *116*, 1521.

(52) Rüchardt, C. *Angew. Chem. Int. Ed. Engl.* **1970**, *1970*, 830.

(53) Dorigo, A. E.; Houk, K. N.; Cohen, T. *J. Am. Chem. Soc.* **1989**, *111*, 4334.

(54) Wu, Y. D.; Kirmse, W.; Houk, K. N. *J. Am. Chem. Soc.* **1990**, *112*, 4557.

(55) Kirmse, W.; Zeppenfeld, M. *J. Chem. Soc., Chem. Commun* **1977**, 124.

(56) Dolbier, W. R., Jr.; Sellers, S. F.; Al-Sader, B. H.; Fielder, T. H., Jr. *J. Am. Chem. Soc.* **1981**, *103*, 717.

(57) Hoffmann, R. *Tetrahedron Lett.* **1970**, *33*, 2907.

(58) Günther, H. *Tetrahedron Lett.* **1970**, *59*, 5173.

(59) Durmaz, S.; Kollmar, H. *J. Am. Chem. Soc.* **1980**, *102*, 6942.

(60) Bent, H. *Chem. Rev.* **1961**, *61*, 275.

(61) Bernett, W. A. *J. Org. Chem.* **1969**, *34*, 1772.

(62) Coulson, C. A.; Moffitt, W. *J. Chem. Phys.* **1947**, *15*, 151.

(63) Clark, T.; Spitznagel, G. W.; Klose, R.; Schleyer, P. v. R. *J. Am. Chem. Soc.* **1984**, *106*, 4412.

(64) Cremer, D.; Kraka, E. *J. Am. Chem. Soc.* **1984**, *107*, 3811.

(65) Brahms, D. L. S.; Dailey, W. P. *Chem. Rev.* **1996**, *96*, 1585-1632.

(66) Smart, B. E. In *Chemistry of Organic Fluorine Compounds II*; M. Hudlicky; A. E. Pavlath, Eds.; American Chemical Society: Washington, DC, 1995.

(67) Burton, D. J.; Hahnfeld, J. L. *Fluorine Chem. Rev.* **1977**, *8*, 119.

(68) Seyferth, D. In *Carbenes*; R. A. Moss; M. Jones, Jr., Eds.; Woley: New York, 1975; Vol. II.

(69) Boger, et al., Ciba-Geigy Corporation **1996,** USP 5,578,595.

(70) Schriewer, et al., Bayer Aktiengesellschaft **1987,** USP 4,705,788.

(71) Birchall, J. M.; Cross, G. E.; Haszeldine, R. N. *Proc. Chem. Soc.* **1960**, 81.

(72) Csuk, R.; Eversmann, L. *Tetrahedron* **1998**, *54*, 6445.

(73) Seyferth, D.; Hopper, S. P. *J. Org. Chem.* **1972**, *37*, 4070-4075.

(74) Mitsch, R. A. *Heterocyclic Chem.* **1964**, *1*, 271.

(75) Mitsch, R. A. *J. Flour. Chem.* **1966**, *3*, 245.

(76) Jonczyk, A.; Kaczmarczyk, G. *Tetrahedron Lett.* **1996**, *37*, 4085.

(77) Chen, Q. Y.; Wu, S. W. *J. Org. Chem.* **1989**, *54*, 3023-3027.

(78) Schlosser, M.; Bessard, Y. *Tetrahedron* **1990**, *46*, 5222-5229.

(79) Chen, Q. Y. *J. Flour. Chem.* **1995**, *72*, 241.

(80) Houk, K. N.; Rondan, N. G.; Mareda, J. *Tetrahedron* **1985**, *41*, 1555.

(81) Moss, R. A.; Yan, S.; Krogh-Jespersen, K. *J. Am. Chem. Soc.* **1998**, *120*, 1088-1089.

(82) Chambers, T. S.; Kistiakowsky, G. B. *J. Am. Chem. Soc.* **1934**, *56*, 399.

(83) Baldwin, J. E. In *The Chemistry of the Cyclopropyl Group*; Z. Rappoport, Ed.; John Wiley & Sons: Chichester, 1995; Vol. 2, p 469.

(84) Carpenter, B. K. In *The Chemistry of the Cyclopropyl Group, Part 2*; Z. Rappoport, Ed.; John Wiley & Sons: Chichester, 1987, p 1027.

(85) Berson, J. A. In *Rearrangements in Ground and Excited States*; P. d. Mayo, Ed.; Academic Press: New York, 1980, p 311.

(86) Borden, W. T. In *Reactive Intermediates*; M. Jones; R. A. Moss, Eds.; Wiley-Interscience: New York, 1985; Vol. 3, p 151.

(87) Gajewski, J. J. In *Hydrocarbon Thermal Isomerizations*; Academic Press: New York, 1981, p 27.

(88) Smith, F. T. *J. Chem. Phys.* **1958**, *29*, 235.

(89) Schlag, E. W.; Rabinovitch, B. S. *J. Am. Chem. Soc.* **1960**, *82*, 5996.

(90) Setser, D. W.; Rabinovitch, B. S. *J. Am. Chem. Soc.* **1964**, *86*, 564.

(91) Hoffmann, R. *J. Am. Chem. Soc.* **1968**, *90*, 1475.

(92) Pedersen, L. D.; Berson, J. A. *J. Am. Chem. Soc.* **1975**, *97*, 238.

(93) Berson, J. A.; Pedersen, L. D.; Carpenter, B. K. *J. Am. Chem. Soc.* **1976**, *98*, 122.

(94) Cianciosi, S. J.; Ragunathan, N.; Freedman, T. R.; Nafie, L. A.; Baldwin, J. E. *J. Am. Chem. Soc.* **1990**, *112*, 8204.

(95) Cianciosi, S. J.; Ragunathan, N.; Freedman, T. R.; Nafie, L. A.; Lewis, D. K.; Glenar, D. A.; Baldwin, J. E. *J. Am. Chem. Soc.* **1991**, *113*, 1864.

(96) Getty, S. J.; Davidson, E. R.; Borden, W. T. *J. Am. Chem. Soc.* **1992**, *114*, 2085.

(97) Baldwin, J. E.; Yamaguchi, Y.; Schaefer, H. F., III *J. Phy. Chem.* **1994**, *98*, 7513.

(98) Yamaguchi, Y.; Schaefer, H. F., III; Baldwin, J. E. *Chem.Phys. Lett.* **1991**, *185*, 143.

(99) Doubleday, C., Jr.; Bolton, K.; Hase, W. L. *J. Am. Chem. Soc.* **1997**, *119*, 5251.

(100) Hrovat, D. A.; Fang, S.; Borden, W. T.; Carpenter, B. K. *J. Am. Chem. Soc.* **1997**, *119*, 5253.

(101) Getty, S. J.; Hrovat, D. A.; Borden, W. T. *J. Am. Chem. Soc.* **1994**, *116*, 1521.

(102) Getty, S. J.; Hrovat, D. A.; Xu, J. D.; Barker, S. A.; Borden, W. T. *J. Chem. Soc. Faraday Trans.* **1994**, *90*, 1689.

(103) Xu, J. D.; Hrovat, D. A.; Borden, W. T. *J. Am. Chem. Soc.* **1994**, *116*, 4888.

(104) Scott, L. B. Dissertation, University of Washington, 1997.

(105) Bergman, R. G. *J. Am. Chem. Soc.* **1969**, *91*, 26.

(106) Schoffers, E.; Golebiowski, A.; Johnson, C. R. *Tetrahedron* **1996**, *52*, 3769.

(107) Taschner, M. J.; Rosen, T.; Heathcock, C. H. *Org. Syn* , *68*, 108.

(108) Tanigawa, Y.; Kanamaru, H.; Sonoda, A.; Murahashi, S. I. *J. Am. Chem. Soc.* **1977**, *99*, 2361.

(109) Seyferth, D.; Hopper, S. P.; Murphy, G. J. *J. Organmetal. Chem* **1972**, *46*, 201.

(110) Calvery, H. O. In *Organic Synthesis Collective*; 2 ed.; A. H. Blatt, Ed.; John Willey & Sons, Inc.: New York, 1941; Vol. 1, p 228.

(111) Tanigawa, Y.; Kanamaru, H.; Sonoda, A.; Murahashi, S.-I. *J. Am. Chem. Soc.* **1977**, *99*, 2361.

(112) Lindlar, H. *Helv. Chem. Acta* **1952**, 450.

(113) Barton, D. H. R. *Tetrahedron* **1991**, *47*, 8969.

(114) Bergman, R. G.; Carter, W. L. *J. Am. Chem. Soc.* **1969**, *91*, 7411.

(115) Borden, W. T. *Chem. Commun.* **1998**, 1919.

(116) Woodward, R. B.; Hoffmann, R. *Angew. Chem. Int. Ed. Engl.* **1969**, *8*, 781.

(117) Newcomb, M. *Tetrahedron* **1993**, *49*, 1151.

(118) Nonhebel, D. C. *Chem. Soc. Rev.* **1993**, 347.

(119) Martin-Esker, A. A.; Johnson, C. C.; Horner, J. H.; Newcomb, M. *J. Am. Chem. Soc.* **1994**, *116*, 9174.

(120) Newcomb, M.; Tanaka, N.; Bouvier, A.; Tronche, C.; Horner, J.; Musa, S. M.; Martinez, F. N. *J. Am. Chem. Soc.* **1996**, *118*, 8505.

(121) Newcomb, M.; Johnson, C. C.; Manek, M. B.; Varick, T. R. J. *J. Am. Chem. Soc.* **1992**, *114*, 10915.

(122) Newcomb, M.; Horner, J. H.; Emanuel, C. J. *J. Am. Chem. Soc.* **1997**, *119*, 7147.

(123) Newcomb, M.; Choi, S.-Y. *Tetrahedron Lett.* **1993**, *34*, 6363.

(124) Martinez, F. N.; Schlegel, H. B.; Newcomb, M. *J. Org. Chem.* **1996**, *61*, 8547.

(125) Martinez, F. N.; Schlegel, H. B.; Newcomb, M. *J. Org. Chem.* **1998**, *63*, 3618.

(126) Morikawa, T.; Ueijima, M.; Kobayashi, Y. *Chem. Lett.* **1988**, 1407.

(127) Morikawa, T.; Uejima, M.; Yoda, K.; Taguchi, T. *Chem. Lett.* **1990**, 467.

(128) Tian, F.; Lewis, S. B.; Bartberger, M. D.; Dolbier, W. R., Jr *J. Am. Chem. Soc.* **1998**, *120*, 6187.

(129) Hoffmann, R.; Stohrer, W. P. *J. Am. Chem. Soc.* **1971**, *93*, 6941.

(130) Gaussian 94 (Revision C. 3 ed), Frisch, M. J. ; Trucks, G. W.; Schlegel, H. B.; Gill, P. M. W.; Johnson, B. G.; Robb, M. A.; Cheeseman, J. R.; Keith, T., Petersson, G. A.; Montgomery, J. A.; Raghavachari, K; Al-Laham, M. A.; Zakrzewski, V. G.; Ortiz, J. V.; Foresman, J. B.; Cioslowski, J.; Stefanov, B. B.; Nanayakkara, A.; Challacombe, M.; Peng, C. Y.; Ayala, P. Y.; Chen, W.; Wong, M. W.; Andres, J. L.; Replogle, E. S.; Gomperts, R.; Martin, R. L.; Fox, D. J.; Binkley, J. S.; Defrees, D. J.; Baker, J.; Stewart, J. P.; Head-Gordon,, M.; Gonzalez, C.; and Pople, J. A., Gaussian Inc., . Pittsburgh PA, 1995.

(131) Gaussian 98 (Revision A.1), M. J. Frisch, G. W. Trucks, H. B. Schlegel, G. E. Scuseria, M. A. Robb, J. R. Cheeseman, V. G. Zakrzewski, J. A. Montgomery, R. E. Stratmann, J. C. Burant, S. Dapprich, J. M. Millam, A. D. Daniels, K. N. Kudin, M. C. Strain, O. Farkas, J. Tomasi, V. Barone, M. Cossi, R. Cammi, B. Mennucci, C. Pomelli, C. Adamo, S. Clifford, J. Ochterski, G. A. Petersson, P. Y.

Ayala, Q. Cui, K. Morokuma, D. K. Malick, A. D. Rabuck, K. Raghavachari, J. B. Foresman, J. Cioslowski, J. V. Ortiz, B. B. Stefanov, G. Liu, A. Liashenko, P. Piskorz, I. Komaromi, R. Gomperts, R. L. Martin, D. J. Fox, T. Keith, M. A. Al-Laham, C. Y. Peng, A. Nanayakkara, C. Gonzalez, M. Challacombe, P. M. W. Gill, B. G. Johnson, W. Chen, M. W. Wong, J. L. Andres, M. Head-Gordon, E. S. Replogle and J. A. Pople, Gaussian, Inc., Pittsburgh PA, 1998.

(132) Pople, J. A.; Nesbet, R. K. *J. Chem. Phys.* **1954**, *22*, 571.

(133) Becke, A. D. *J. Chem. Phys.* **1993**, *98*, 5648.

(134) Hariharan, P. C.; Pople, J. A. *Theor. Chim. Acta* **1973**, *28*, 213.

(135) Raghavachari, K.; Trucks, G. W. *J. Chem. Phys.* **1989**, *91*, 1062.

(136) Schlegel, H. B. *J. Chem. Phys.* **1986**, *84*, 4530.

(137) Chen, W.; Schlegel, H. B. *J. Chem. Phys.* **1994**, *101*, 5957.

(138) Smith, D. M.; Nicolaides, A.; Golding, B. T.; Radom, L. *J. Am. Chem. Soc.* **1998**, *120*, 10223.

(139) Boger, D. L.; Jenkins, T. J. *J. Am. Chem. Soc.* **1996**, *118*, 8860.

(140) Newcomb, M.; Glenn, A. G. *J. Am. Chem. Soc.* **1989**, *111*, 275.

(141) Wiberg, K. B.; Rablen, P. R. *J. Am. Chem. Soc.* **1993**, *115*, 614.

(142) Bartbrger, M. D.; Dolbier, W. R., Jr.; Lusztyk, J.; Ingold, K. U. *Tetrahedron* **1997**, *53*, 9857.

(143) Giese, B. *Radicals in Organic Synthesis: Formation of Carbon-Carbon Bonds*; Pergamon Press: Oxford, 1986.

(144) Tedder, J. M.; Walton, J. C. *Tetrahedron* **1980**, *36*, 701.

(145) Backwith, A. L.; Moad, G. J. *J. Chem.Soc., Perkin Trans. 2* **1980**, 1473.

(146) Breneman, C. M.; Wiberg, K. B. *J. Comput. Chem.* **1990**, *11*, 361.

(147) Beckwith, A. l. J.; Moad, G. *J. Chem. Soc., Perkin Trans. II* **1980**, 1473-1482.

(148) Dolbier, W. R., Jr. *Chem. Rev.* **1996**, *96*, 1557.

(149) Zhang, X.-M. *J. Org. Chem.* **1998**, *63*, 3590.

(150) Pasto, D. J.; Krasnansky, R.; Zercher, C. *J. Org. Chem.* **1987**, *52*, 3062.

(151) Bordwell, F. G.; Zhang, X.-M.; Alnajjar, M. S. *J. Am. Chem. Soc.* **1992**, *114*, 7623.

(152) Elsheimer, S.; Dolbier, W. R. J. *J. Flour. Chem.* **1988**, *40*, 119.

(153) Ellis, R. J.; Frey, H. M. *J. Chem. Soc.* **1964**, 5578.

(154) Dolbier, W. R. J.; Seller, S. F. *J. Org. Chem.* **1982**, *47*, 1.

(155) Hammond, G. S. *J. Am. Chem. Soc.* **1955**, *77*, 334.

(156) Tian, F.; Bartberger, M. D.; Dolbier, W. R., Jr. *J. Org. Chem.* **1999**, *64*, 540.

(157) Beckwith, A. L. J.; Ingold, K. U. In *Rearrangements in Ground and Excited States*; P. d. Mayo, Ed.; Academic Press: New York, 1980; Vol. 1, p 162.

(158) Friendrich, E. C.; Holmstead, R. L. *J. Org. Chem.* **1972**, *37*, 2550.

(159) Venkatesan, H.; Greenberg, M. M. *J. Org. Chem.* **1994**, *59*, 3514.

(160) Dauben, W. G.; Schutte, L.; Wolf, R. E.; Deving, E. J. *J. Org. Chem.* **1969**, *34*, 2512.

(161) Roberts, C.; Walton, J. C. *J. Chem. Soc., Perkin Trans. II* **1983**, 879.

(162) Benson, S. W. In *Thermochemical Kinetics*; 2nd ed.; Wiley: New York, 1976, p 273.

(163) Batey, R. A.; Grice, P.; Harling, J. D.; Motherwell, W. B.; Rzepa, H. S. *J. Chem. Soc., Chem. Commun* **1992**, 942.

(164) Pasto, D. J. *J. Org. Chem.* **1996**, *61*, 252.

(165) Laurie, D.; Nonhebel, D. C.; Suckling, C. J.; Walton, J. C. *Tetrahedron* **1993**, *49*, 5869.

(166) Davies, A. G.; Muggleton, B. *J. Chem. Soc., Perkin Trans. II* **1976**, 502.

(167) Krosley, K. W.; Gleicher, G. J. *J. Phy. Org. Chem.* **1993**, *6*, 228.

(168) Krishnamurthy, V.; Rawal, V. H. *J. Org. Chem.* **1997**, *62*, 1572.

(169) Dickinson, J. M.; Murphy, J. A.; Patterson, C. W.; Wooster, N. F. *J. Chem. Soc., Perkin Trans. I* **1990**, 1179.

(170) Stogryn, E. I.; Gianni, M. H. *Tetrahedron Letters*, **1970**, 3025.

(171) Murphy, J. A.; Patterson, M. H.; Wooster, N. F. *Tetrahedron Lett.* **1988**, *29*, 955.

(172) Bigot, B.; Sevin, A.; Devaquet, A. *J. Am. Chem. Soc.* **1979**, *101*, 1101.

(173) Gupta, R. R.; Kumar, M.; Gupta, V. In *Heterocyclic Chemistry* Spring, 1998.

(174) Griller, D.; Ingold, K. U. *Acc. Chem. Res.* **1980**, *13*, 317.

(175) Barton, D. H. R.; Crich, D.; Motherwell, W. B. *Tetrahedron* **1985**, *41*, 3901.

(176) Newcomb, M.; Choi, S. Y.; Horner, J. H. *J. Org. Chem.* **1999**, *64*, 1225.

(177) Chateauneuf, J.; Lusztyk, J.; Ingold, K. U. *J. Org. Chem.* **1988**, *53*, 1629.

(178) Beckwith, A. L. J.; Bowry, V. W. *J. Am. Chem. Soc.* **1994**, *116*, 2710.

(179) Beckwith, A. L. J.; Bowry, V. W.; Ingold, K. U. *J. Am. Chem. Soc.* **1992**, *114*, 4983.

(180) Bowry, V. W.; Ingold, K. U. *J. Am. Chem. Soc.* **1992**, *114*, 4992.

(181) Bartlett, P. D.; Hiatt, R. R. *J. Am. Chem. Soc.* **1958**, *68*, 1398.

(182) Taylor, K. G.; Govindan, C. K.; Kaelin, M. S. *J. Am. Chem. Soc.* **1979**, *101*, 2091.

(183) Walling, C.; Waits, H. P.; Milovanonic, J.; Pappiaonnov, C. G. *J. Am. Chem. Soc.* **1970**, *92*, 4927.

(184) Moad, G.; Rizzardo, E.; Solomon, D. H. *Tetrahedron Lett.* **1981**, *22*, 1165.

(185) Beckwith, A. L. J.; Bowry, V. W. *J. Org. Chem.* **1989**, *54*, 2681.

(186) Beckwith, A. L. J.; Bowry, V. W. *J. Org. Chem.* **1988**, *53*, 1632.

(187) Roberts, J. D.; Mazur, R. H. *J. Am. Chem. Soc.* **1951**, *73*, 2509.

(188) Roberts, J. D.; Chambers, V. C. *J. Am. Chem. Soc.* **1951**, *73*, 5034.

(189) Richey, H. G., Jr. In *Carbonium*; Olah, G. A., Schleyer, P. v. R., Eds.; Wiley-interscience: New York, 1972; Vol. III, p 1201.

(190) Wiberg, K. B.; Hess, B. A., Jr.; Ashe, A. J., III In *Carbonium*; Olah, G. A., Schleyer, P. v. R., Eds.; Wiley-Interscience: New York, 1972; Vol. III, p 1295.

(191) Olah, G. A. *Acc. Chem. Res.* **1976**, *9*, 41.

(192) Brown, H. C.; Schleyer, P. v. R. In *The nonclassical Ion Problem*; Plenum: New York, 1977, p Chapter 5.

(193) Olah, G. A.; Reddy, P. V.; Prakash, G. K. S. *Chem. Rev.* **1992**, *92*, 69.

(194) Olah, G. A.; Reddy, P.; Prakash, G. K. S. In *The Chemistry of the Cyclopropyl Group*; Rappoport, Z., Ed.; Wiley: Chichester, U. K., 1995; Vol. II, p 813.

(195) Mazur, R. H.; White, W. N.; Semenov, D. A.; Lee, C. C.; Silver, M. S.; Robters, J. D. *J. Am. Chem. Soc.* **1959**, *81*, 4390.

(196) Staral, S. J.; Yavari, I.; Roberts, J. D.; Prakash, G. K. S.; Donovan, D. J.; Olah, G. A. *J. Am. Chem. Soc.* **1978**, *100*, 8016.

(197) Saunders, M.; Laidig, K. E.; Wiberg, K. B.; Schleyer, P. v. R. *J. Am. Chem. Soc.* **1988**, *110*, 7652.

(198) Taft, R. W.; Martin, R. H.; Lampe, F. W. *J. Am. Chem. Soc.* **1965**, *87*, 2490.

(199) Hart, H.; Sandri, J. M. *J. Am. Chem. Soc.* **1959**, *81*, 320.

(200) Schleyer, P. v. R.; Dine, G. W. V. *J. Am. Chem. Soc.* **1966**, *88*, 2321.

(201) Sneen, R. A.; Lewandowski, K. W.; Taha, I. A. I.; Smith, B. R. *J. Am. Chem. Soc.* **1961**, *83*, 4843.

(202) Walborsky, H. M.; Pendleton, J. F. *J. Am. Chem. Soc.* **1960**, *82*, 1405.

(203) Newcomb, M.; Chestney, D. L. *J. Am. Chem. Soc.* **1994**, *116*, 9753.

(204) Bessard, Y.; Kuhlmann, L.; Schlosser, M. *Tetrahedorn* **1990**, *46*, 5230.

(205) Kobayashi, Y.; Morikawa, T.; Taguchi, T. *Chem. Pharm. Bull* **1983**, *31*, 2616.

(206) Reich, I. L.; Diax, A.; Winstein, S. *J. Am. Chem. Soc.* **1969**, *91*, 5635.

(207) Wiberg, K. B.; Ashe, A. J. I. *J. Am. Chem. Soc.* **1968**, *90*, 63.

BIOGRAPHICAL SKETCH

Feng Tian was born in November 29, 1967, in KaiFeng, P.R.China. In August 1985, he left his hometown for Beijing to study chemistry at Peking University and received his B.S. degree in chemistry in 1989. He then worked as a research chemist in the Science & Technology Department of the National Museum of Chinese History.

To pursue a Ph. D. degree, he arrived in United States in August 1995 and started his doctoral studies under the supervision of Professor William R. Dolbier, Jr. in the Department of Chemistry, University of Florida.

In January 2000, he will join Professor Peter G. Schultz's group as a postdoctoral research associate at the Scripps Research Institute in San Diego, California.

I certify that I have read this study and that in my opinion it conforms to acceptable standards of scholarly presentation and is fully adequate, in scope and quality, as a dissertation for the degree of Doctor of Philosophy.

William R. Dolbier

William R. Dolbier, Jr., Chairman
Professor of Chemistry

I certify that I have read this study and that in my opinion it conforms to acceptable standards of scholarly presentation and is fully adequate, in scope and quality, as a dissertation for the degree of Doctor of Philosophy.

Merle A. Battiste

Merle A. Battiste
Professor of Chemistry

I certify that I have read this study and that in my opinion it conforms to acceptable standards of scholarly presentation and is fully adequate, in scope and quality, as a dissertation for the degree of Doctor of Philosophy.

Kirk S. Sch

Kirk S. Schanze
Professor of Chemistry

I certify that I have read this study and that in my opinion it conforms to acceptable standards of scholarly presentation and is fully adequate, in scope and quality, as a dissertation for the degree of Doctor of Philosophy.

Daniel R. Talham
Associate Professor of Chemistry

I certify that I have read this study and that in my opinion it conforms to acceptable standards of scholarly presentation and is fully adequate, in scope and quality, as a dissertation for the degree of Doctor of Philosophy.

Hai-Ping Cheng

Hai-Ping Cheng
Associate Professor of Physics

This dissertation was submitted to the Graduate Faculty of the Department of Chemistry in the College of Liberal Arts and Sciences and to the Graduate School and was accepted as partial fulfillment of the requirements for the degree of Doctor of Philosophy.

December 1999

Dean, Graduate School

LD
1780
1999
T551

UNIVERSITY OF FLORIDA
3 1262 08555 1389